On the Dynamic Spectrum Access for Next Generation Wireless Communication Systems

Tang Pak Kay

(B.Eng. (Hons.), NUS)

A THESIS SUBMITTED

FOR THE DEGREE OF DOCTOR OF PHILOSOPHY

NUS GRADUATE SCHOOL FOR INTEGRATIVE SCIENCES AND ENGINEERING

NATIONAL UNIVERSITY OF SINGAPORE

Acknowledgement

I would like to take this opportunity to express my heartfelt gratitude to all those who have contributed in one way or another to the completion of this thesis.

Firstly, I gratefully acknowledge the support provided by the Agency of Science, Technology and Research (A*STAR). The completion of this thesis is possible due to the generous funding provided by the A*STAR Graduate Scholarship (AGS). Through their commitment and enthusiasm, the A*STAR Graduate Academy staff have greatly helped to provide and maintain a healthy research environment.

Special thanks to my supervisors, Dr. Yong Huat CHEW and Dr. Michael ONG, who are both from the Institute for Infocomm Research (I^2R). I am especially indebted to them for their supervision and guidance throughout the candidature, without which, the completion of this thesis would not have been possible. I have benefitted tremendously from them in terms of research knowledge and also in choosing research as a future career. I also greatly appreciate the meticulous effort put in by Dr. Chew in going through and refining my writings, as well as the enthusiasm shown during in-depth discussions which sometimes extend beyond office hours.

I would also like to acknowledge the great support provided by the staff of the NUS Graduate School of Integrative Sciences and Engineering (NGS), which ensured the smooth and prompt execution of administrative matters. In particular, many thanks to A/Prof. Justine Burley for her tremendous effort put in to make the courses GS 5001 and GS 5002 so interesting and interactive.

I would also like to thank friends and colleagues from I^2R for their support and help rendered during the candidature. In particular, I would like to thank Wai Leong YEOW for sharing with us his knowledge on Markov decision processes. Last but not least to my family members for their kind understanding and support. Their encouragements and sacrifices are greatly appreciated.

Table of Contents

Summary

New spectrum management techniques with greater flexible spectrum usage rights have been called for to address the apparent spectrum scarcity problem. Dynamic spectrum access (DSA), which represents a paradigm shift away from the current static spectrum allocation approach, has been identified as a promising approach in the near future.

In this thesis, the possible new spectrum access models are broadly classified into three categories, namely, the public commons model, the private commons model, and the coordinated access model. The public commons model refers to the coexistence of wireless networks in a given spectrum band where a typical example is given by the existing unlicensed bands. Opportunistic spectrum access (OSA) is an example of the private commons model, where secondary usage of spectrum aims to enhance the spectrum utilization efficiency in a licensed band. The coordinated access model involves sharing spectrum among multiple radio systems in either an agreed manner or through a spectrum agent. Complete spectrum sharing and virtual spectrum partitioning are two possible sharing schemes under this model.

The OSA, complete spectrum sharing and virtual spectrum partitioning models are the main focus of this thesis. These models offer different levels of spectrum access flexibilities and impose new and unique design challenges. The main objective of this thesis is to develop analytical platforms for each of these spectrum access models so that the service capacity of the radio systems under prescribed Grade-of-Service (GoS) guarantees can be computed. From the results obtained, we design and propose appropriate spectrum admission control (SAC) policies and study the achievable improvement in the spectrum utilization efficiency.

For OSA, we studied the impact of the PR activities on the SR transmission opportunity time. The theoretical probability density function (p.d.f.) of the opportunity time under a given PR traffic model is derived. In addition, the theoretical p.d.f. of the duration where SR transmission is not possible, due to PR transmission in all the frequency bins, is also derived.

We next examined the virtual spectrum partitioning model whereby two proprietary radio systems with GoS guarantees can access each others' excess spectrum to support additional traffic demands. The SAC problem can be formulated using four dimensional Markov chain models. FCFS, RES and random discard (RD) SAC policies were developed to study the service capacity and the incurred tradeoffs.

The complete spectrum sharing model in which two radio systems completely share a spectrum band with their access being coordinated through a spectrum manager is also examined. We consider two possible scenarios under this model. In the first scenario, we analyze and compare the maximum service capacity of the radio systems while still satisfying their respective GoS requirements based on RES and RD SAC policies, as well as a policy developed based on constrained Markov decision process (CMDP). In the second scenario, we include the services' pricing in the utility function. The SAC problem is formulated as a CMDP and solved analytically to derive the optimal policy which results in maximum revenue for the spectrum manager.

List of Figures

List of Tables

List of Abbreviations

CMDP	Constrained Markov Decision Process
CR	Cognitive Radio
CTMC	Continuous Time Markov Chain
DSA	Dynamic Spectrum Access
FCFS	First-Come-First-Served
GoS	Grade-of-Service
MAC	Medium Access Control
OSA	Opportunistic Spectrum Access
p.d.f	Probability Density Function
PAN	Personal Area Network
PR	Primary Radio
QoS	Quality-of-Service
RAT	Radio Access Technology
RD Policy	Random Discard Policy
RES Policy	Reservation Policy
RVI Algorithm	Relative Value Iteration Algorithm
SDR	Software-Defined Radio
SR	Secondary Radio
UWB	Ultra-Wideband
WRAN	Wireless Regional Area Network

Chapter 1
Introduction

The current spectrum management policy adopts static assignment and exclusive access of spectrum to different service providers. For example, in the United States, the frequencies from 54 MHz to 890 MHz are segmented into smaller bands which are assigned exclusively for over the air television broadcasting services [1]. This spectrum management model is effective in mitigating interference between co-located radio systems and has been adopted by the wireless telecommunication industry for many years.

Driven by consumer demand for different services, the development and emergence of new wireless communication systems in recent years have grown tremendously. Correspondingly, the demands for radio spectrum have also increased significantly and the current spectrum management model shows its limitations. Firstly, the rigid and bureaucratic nature of the spectrum allocation process has shown to be incapable of reallocating spectrum on a sufficiently dynamic basis to accommodate the demands of new and emerging radio systems. Secondly, tenure for the exclusive access rights run up to many years in most cases. As a result, the amount of vacant radio spectrum available for static assignment diminishes quickly with the rapid emergence of more wireless radio systems. A survey of the US frequency allocation chart from 3 kHz up to 300 GHz reveals that vacant frequency band is available only from 3 kHz to 9 kHz [2], while the remaining bands are highly cluttered with various designated services and applications. As a result, spectrum scarcity poses an imminent problem for the development of future wireless communication systems.

The Federal Communications Commission (FCC) established the Spectrum Policy Task Force (SPTF) in 2002 to identify, recommend and evaluate changes to the current spectrum management policy. Field measured results by the SPTF as well as various interested agencies showed that *actual* usage of scarce spectrum resources can be highly inefficient [3-5]. Recently, measured spectrum activity results by the spectrum governing agencies in Singapore also arrived at similar conclusions [6].

The above findings revealed that the apparent spectrum scarcity is more appropriately addressed as a *spectrum access problem*. At any time and location, spectrum activities in most frequency bands occupy only a small fraction of time. However, because the frequency band is already allocated exclusively to a proprietary radio system, other radio systems within the same geographical area do not have access rights even when it has been left fallow for a period of time. Thus result in the low spectrum utilization efficiency observed. Given the high economic value of radio spectrum, a new paradigm shift in spectrum management is of paramount importance. The development of novel management concepts and access models are necessary to increase the spectrum utilization efficiency, and also to spur the development of more innovative radio access technologies (RAT).

Following the recommendations put forward by the SPTF, the FCC has taken significant steps to remove rigid regulatory barriers. DSA is the new paradigm in spectrum management and its definition and available approaches are still evolving. However, the spectrum management policies can be broadly classified into three main categories, namely the public commons model, the private commons model, and the coordinated access model. The spectrum management policies are categorized and shown in Figure 1.1. It is envisioned that with the establishment of these novel spectrum management models, network operators will have more flexibility in

defining their operation models and as a result, innovative market structures and business concepts can flourish.

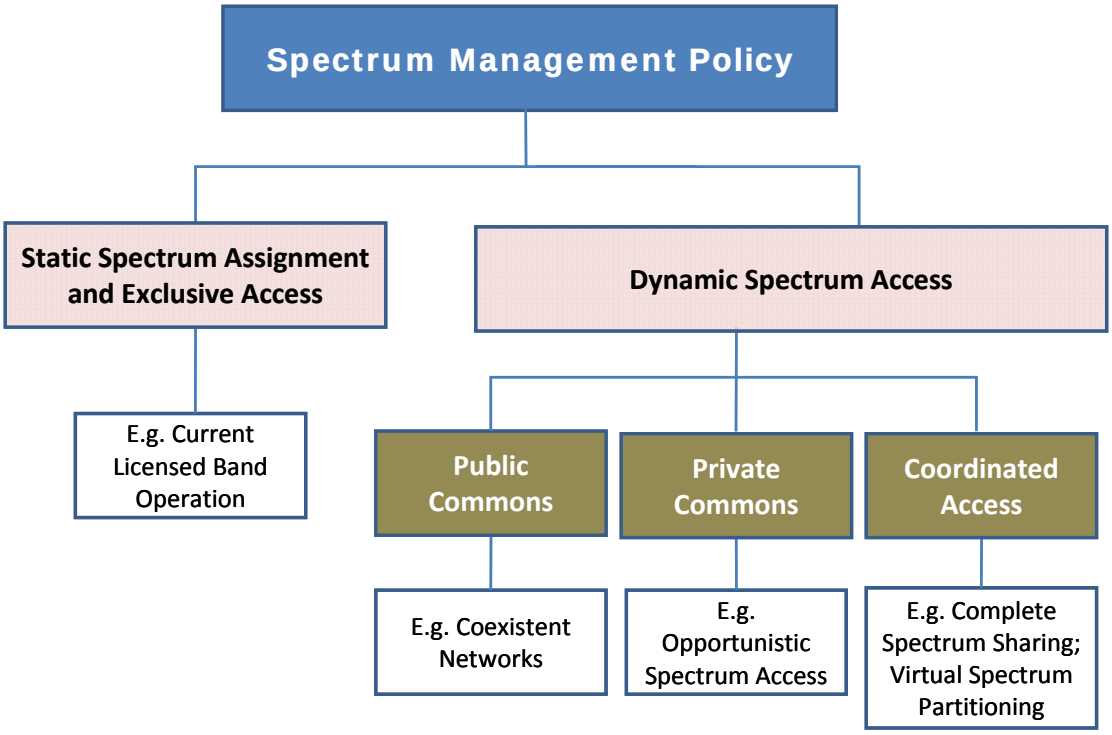

Fig. 1.1 Classification of spectrum management policies and access models.

In the following sections, we give a brief introduction to these models and present some of the practical scenarios under each framework.

1.1 Public Commons Model

Under this framework, exclusive access rights are abolished and radio systems are free to access any portion of the stipulated spectrum band. The current spectrum access model adopted in the unlicensed ISM band (2.4 GHz) is a pre-cursor to this model where current systems such as Bluetooth, Zigbee, WiFi (IEEE 802.11b/g) and WiMAX systems operate and coexist in this band [7]. Radio systems operating in the unlicensed bands are required to comply with certain technical regulations, such as the

transmission power level. For example, the measured equivalent isotropically radiated power (EIRP) for UWB transmissions from 3.1 GHz to 10.6 GHz is specified not to exceed -41.3dBm per megahertz of bandwidth. The imposed spectrum mask is to ensure the amount of interference generated can be tolerated by the other coexistent radio systems. In addition, the radio systems normally also adopt various etiquettes for medium access control (MAC) to mitigate interference. For example, the carrier sense multiple access/collision avoidance (CSMA/CA) protocol is implemented in WLAN devices, while Bluetooth devices adopt frequency hopping spread spectrum technology.

However, the quality-of-service (QoS) may be degraded due to inter-system interference and the problem is aggravated when unlicensed devices become more pervasive in the future. For example, Figure 1.2 illustrates a possible scenario in which multiple unlicensed radio systems are co-located in the same geographical region and their operations are overlapped in frequency. Without proper designed precautions, all the coexistent systems may finally fail to perform satisfactorily, particularly when all the systems are heavily loaded.

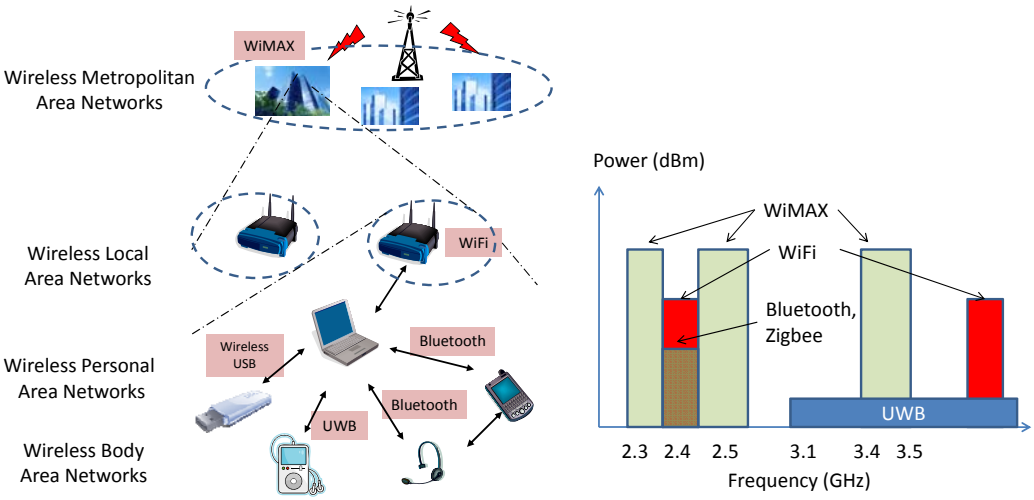

Fig. 1.2 Co-located radio systems which operate in the unlicensed band.

The future challenge for radio systems operating under this framework is to adopt more intelligent and advanced interference mitigation techniques such as multi-channel CSMA/CA [8] and adaptive transmit power control (TPC) schemes [9]. More recently, cognitive technologies have been introduced and their continued development will enable adaptive interference mitigation techniques through channel sensing and intelligent collision avoidance algorithms [10-13], thus ensuring the operational reliability of coexistent radio systems.

1.2 Private Commons Model

Under this model, the licensee has exclusive access rights to the allocated spectrum within a specified geographic area, and can also transfer the access rights to other radio systems. In the literature, the licensed radio system is commonly referred to as the primary radio (PR) system. When a frequency band which is assigned to a PR system is not being utilized at a particular time and geographic location, a spectrum hole or 'white space' [14] is said to exist. A secondary radio (SR) system can dynamically access the temporally available spectrum holes for transmission. The SR is said to have *opportunistic* access to the spectrum.

To avoid causing excessive interference to the PR system, SRs are granted lower access priority and the secondary transmission is required to backoff when a PR transmission is detected on the same frequency. Figure 1.3 shows an example of an OSA scheme. In this example, the SRs are referred to as spectral agile radios [15, 16] which can dynamically switch among the idle channels and access the spectrum holes available in the time and frequency domains. Initially only Channels 2, 3 and 4 are accessible by the SRs. At time T_0, a PR transmission is detected in Channel 4. Hence, the SR transmitting on that channel must backoff. The transmission opportunity time

[17] given by this example is denoted by the continuous periods in which spectrum holes are available to the SRs. The duration of the 'black space' [17] is indicated by the period in which all the channels are occupied by the PRs. OSA imposes many technical challenges and cognitive radio (CR) technology has been identified as a promising platform to develop devices for OSA. More details on CR technology will be reviewed in Chapter 2.

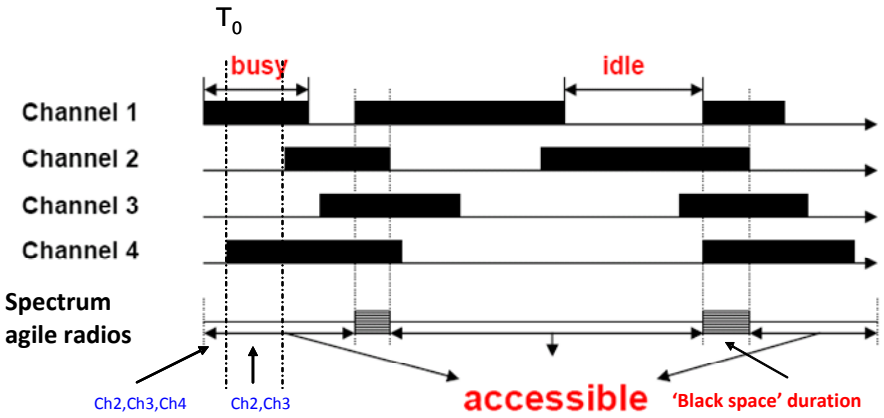

Fig. 1.3 OSA by spectrum agile radios, adapted from [16].

Secondary spectrum access could be mandated by spectrum governing authorities who seek to improve the spectrum utilization efficiency in certain spectrum bands. On the other hand, the SR system may also obtain spectrum access by leasing unused spectrum from the PR system in a secondary spectrum market [18]. With such added flexibility, this access model provides greater incentive (in terms of revenue generated by granting secondary access to other radio systems) for the spectrum licensee to improve its utilization efficiency.

A practical example of an adaptive radio system that senses and shares the usage of spectrum with a PR system on a secondary basis has been developed by the next-generation (XG) program [19] under the Defense Advanced Research Projects

Agency (DARPA). The developed radio system has since been demonstrated to be capable of accessing the available spectrum holes over a wide range of frequencies.

In general, the SRs may operate based on centralized or distributed architecture. Figure 1.4 illustrates a possible scenario in which the SR system adopts centralized architecture and we present two possible cases under this scenario.

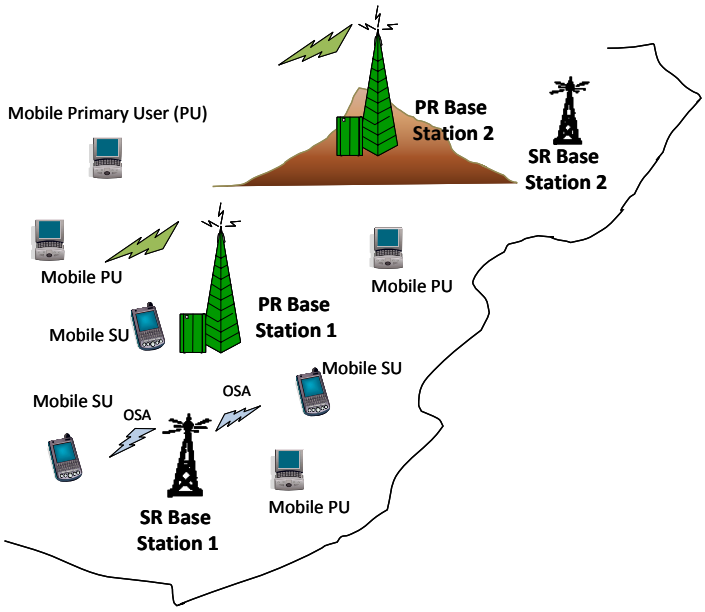

a) Non-cooperative

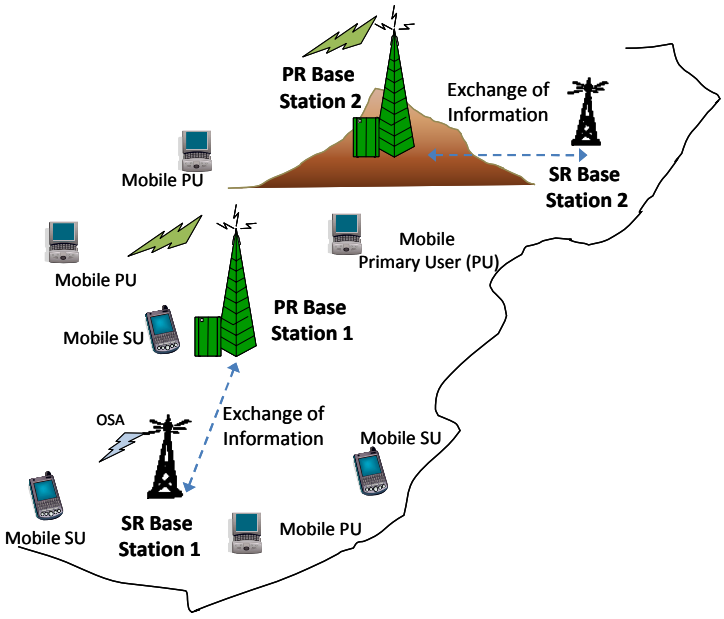

b) Cooperative

Fig. 1.4 Centralized SR system architecture.

In the first case which is illustrated in Fig. 1.4(a), the operation of the PR system is unaffected by the introduction of the SR system. The SRs have to perform spectrum sensing and detection of spectrum holes, and feedback the information to the SR system controller (or base station) through a common control channel. Medium access control (MAC) is performed by the SR system controller which will allocate the available communication channels to the requesting SRs. The system model adopted in the IEEE 802.22 Wireless Regional Area Networks (WRAN) [20] standard for OSA in the UHF/VHF television bands is a practical example of centralized architecture.

In an alternative scenario which is shown in Fig. 1.4(b), the SR and PR systems may exchange information for cooperative OSA. In this scenario, the PR system assists the SR system to determine secondary spectrum access opportunities in the time and frequency domains. Such a concept is aligned with recent interest to study primary operator assisted OSA [21]. The shortcoming of this approach is that the PR system needs to implement additional functionalities to communicate with the SR system. Such a situation is more likely if improvements in spectrum utilization efficiency are significant (over the non-cooperative scenario).

On the other hand, in the distributed architecture illustrated in Figure 1.5, the SR system operates without a centralized controller. To realize the secondary access for a distributed network is technically challenging. In practice, a separate fixed sensor network may be used to sense and detect the spectrum holes. In such a scenario, the SRs are not required to perform spectrum sensing but rely on the information from the sensor network for secondary access. Such a similar concept was also proposed and described in [22].

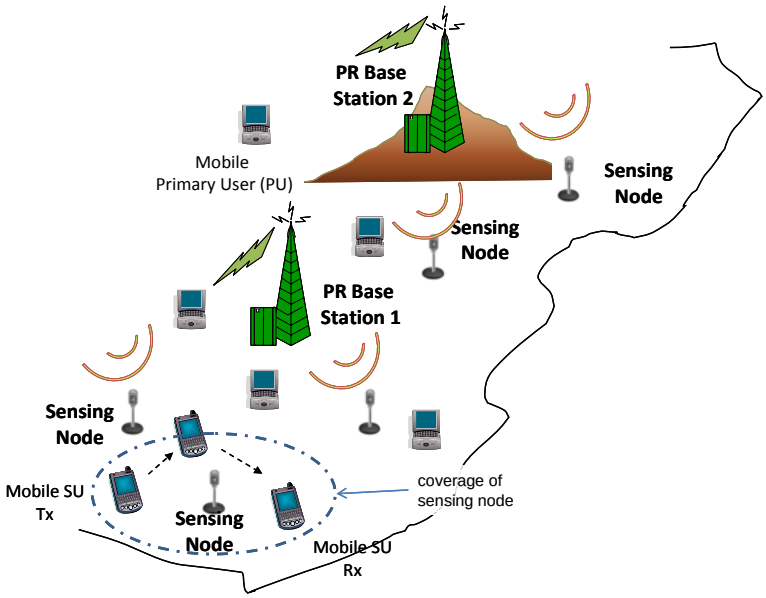

Fig. 1.5 Distributed secondary radio system.

In Fig. 1.5, the wireless coverage of each sensor node is assumed to be small compared to that of the PR and hence the detected spectrum holes within its coverage can be assumed to be identical. For example, the SRs could be part of a body area network (BAN) or personal area network (PAN) operating within the wireless coverage of the sensor node. Initially, all the SRs are in idle mode and listen for secondary transmission. When a SR wishes to transmit to another SR, it first requests the sensor network to sense and detect for available spectrum holes. Based on the results, the sensor network may deny the SR spectrum access when secondary transmission opportunities are unavailable. On the other hand, if a frequency band is detected to be unused, the sensor network will return with an acknowledgement and the SR may transmit to other nearby SRs on that frequency. The information may be transmitted to the destination node directly or via multiple hops.

It is important to note that the system architectures for OSA are still evolving, which give rise to many proposed interesting and innovative architectures. The architectures described in this section are just some of the possible OSA scenarios.

1.3 Coordinated Access Model

Under this framework, exclusive access rights to the frequency bands of a common spectrum are dynamically allocated and possibly traded among multiple radio systems. In addition, access to the spectrum resources is coordinated through a centralized system controller. Due to improved trunking efficiency, better spectrum utilization is achievable (compared to the static partition approach) when multiple radio systems share the aggregated spectrum in a coordinated manner. We present two possible scenarios under this model. The first scenario represents a virtual spectrum partitioning model and is illustrated in Figure 1.6. The second scenario represents a complete spectrum sharing model and is shown in Figure 1.7.

In Fig. 1.6, it is assumed that Radio A (R_A) and Radio B (R_B) are proprietary radio systems that provide different services. The two radio systems are assumed to form a heterogeneous multi-radio network through an additional adaptation layer in their protocol stack to facilitate the sharing of spectrum resources. Assuming that a large increase in service requests causes the traffic demand to exceed the maximum capacity of R_A, then R_B may support R_As' traffic demands using its excess spectrum. Spectrum negotiations are performed between R_A and R_B via the common link and in this case, user A_5 is able to obtain wireless access using the excess spectrum from R_B. The tradeoff is the need to perform vertical handoff and dynamic reconfiguration of the transmission parameters. A practical example of a similar dynamic spectrum sharing scenario is being studied and developed under the IEEE P1900.4 standards [23] where multiple radio systems share their spectrum resources in a coordinated manner through a Network Resource Manager (NRM).

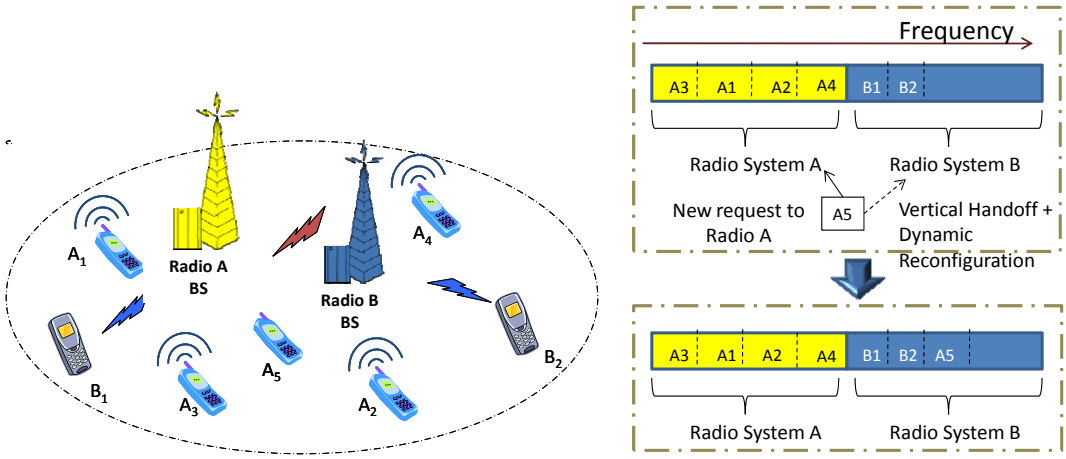

Fig. 1.6 Virtual spectrum partition in a heterogeneous multi-radio network.

In the previous scenario, the admission of User A_5 is performed jointly by the two radio systems. In the second scenario which is depicted in Fig. 1.7, the traffic demands are aggregated at the spectrum manager which performs dynamic allocation of spectrum to multiple radio systems. This could be representative of a scenario whereby a licensee performs short duration lease of spectrum to several radio systems.

In Fig. 1.7, it is assumed that two radio systems denoted by R_A and R_B completely share the spectrum band, and provide different wireless services over a geographical region. The respective base station performs spectrum requests to the spectrum manager. It is assumed that each radio system has its own control channels and requests only a portion of the spectrum for transmission. An exclusive access right to a frequency band is allocated to the admitted request for transmission. However, tenure of the access right is valid only for a short duration (in comparison to that in static spectrum allocation). An example of such a spectrum access model is being studied under the DIMSUMnet project [24].

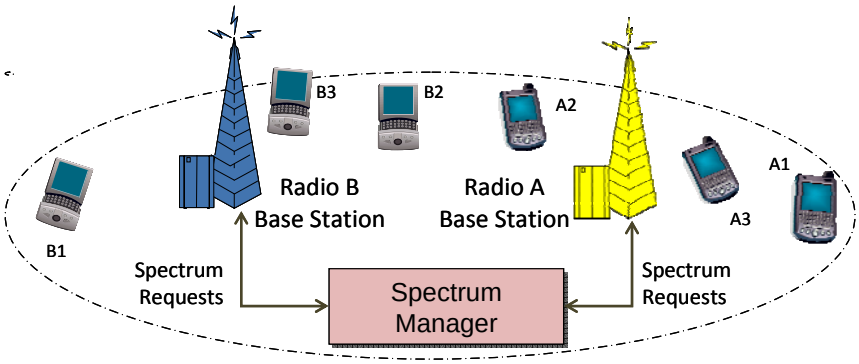

Fig. 1.7 Complete spectrum sharing in a multi-radio network.

1.4 Research Motivation

Spectrum scarcity poses an imminent problem for the development of future wireless communication systems. DSA will revolutionize the design of future wireless communication systems and the manner in which the radios operate.

One of the challenges for DSA involves efficiently allocating limited spectrum resources to multiple radio systems. This brings about the concept of spectrum admission control (SAC). SAC in a multiple radio system environment is analogous to the call admission control (CAC) in a single radio system which offers multiclass services. Both CAC and SAC aim to achieve better spectrum utilization efficiency. However, there are differences in their objectives and the adopted approach. CAC is performed at the call level, and generally caters to the admission of multiclass services while still fulfilling their respective Quality-of-Service (QoS) requirements [25]. On the other hand, SAC is performed at the radio access level and caters to the Grade-of-Service (GoS) constraints such as the blocked service probability of individual radio systems. Figure 1.8 illustrates an example of the hierarchal differences between CAC and SAC.

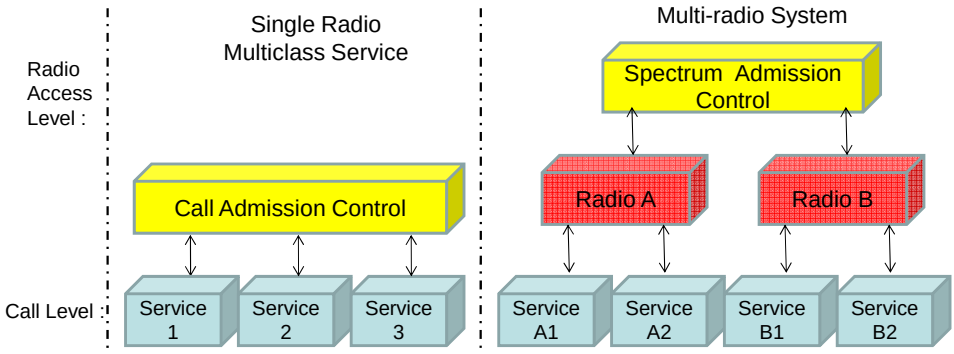

Fig. 1.8 Example of the hierarchal differences between CAC and SAC.

This thesis focuses primarily on the opportunistic and coordinated spectrum access models. The motivation for this research derives from the fact that while these novel spectrum access models described in the above sections can significantly improve the current spectrum utilization efficiency, however, they also impose new and unique design challenges that need to be overcome in order to take advantage of the new flexibilities introduced. In addition, most existing works in the literature consider only best effort service connection for the DSA radios. As continued efforts to enhance user satisfaction, it is expected that there will be a need to provision for GoS guarantee for all the radio systems. The design of SAC policies becomes more challenging when heterogeneous radio systems incorporate different levels of GoS guarantee.

In this thesis, the main objective is to develop analytical platforms so as to study and analyze the service capacity of the radio systems under the framework of these newly proposed spectrum access models. From the results obtained, we further enhance the service capacities through the proposal and development of various SAC policies so that the limited spectrum resources can be utilized more efficiently to support higher traffic demands and yet fulfill the GoS guarantee of each radio system.

OSA is a novel spectrum access concept, and since SR transmissions rely on spectrum holes, the PRs' activities therefore have very significant impact on the SR transmission opportunity time which in turn affects the dropped service probability. A fundamental research challenge at the PHY layer involves identifying and modeling the statistics of the spectrum holes which are sporadically distributed in the time and frequency domains. The motivation for modeling the durations of both the opportunity time and duration of the 'black spaces' (Fig. 1.3) derives from the fact that better understanding of their statistics has important practical implications which can be explained as follows.

Most existing works in the literature [26, 27] are developed based on statistical distribution fitting methods and the statistics are limited to one channel only. However, the PR activities may change at different rates. In the future, SRs are more likely to dynamically switch between the available spectrum holes over multiple frequency bands (such as the case depicted in Fig. 1.3). Therefore, these statistics provide better insight on the relationship between the PR activities and the opportunity time, and also the duration of 'black spaces'.

Under the coordinated access model, most of the related works in the literature [28, 29] pertaining to the virtual spectrum partition model study only the increase in the service capacity through computer simulation. To enhance the sharing of spectrum resources in a multi-radio network, it is necessary to develop analytical platforms which enable the study of both the increase in the service capacity as well as the incurred performance tradeoffs such as the probability of vertical handoffs for this model.

On the other hand in the complete spectrum sharing model, the spectrum band is shared completely among multiple radio systems. In general, the radio systems have

different system parameters such as transmission bandwidth, GoS guarantees and traffic demands. The need to design adaptable and robust SAC policies so as to share the limited spectrum resources efficiently and still fulfill the respective radio systems' requirements thus provides an interesting and challenging research motivation.

The research issues pertaining to DSA not only span the technological frontiers but the problems also involve the economic interests of industry stakeholders and regulatory policy issues. On one hand, the FCC has acknowledged the limitations of the current spectrum management policy, and has actively encouraged the investigation and study of DSA models [30]. In response to their initiatives, some of the recent major works on OSA include the standardization work performed by the IEEE 802.22 workgroup. On the other hand, there are also emerging works which study possible business models for spectrum trading [31] and spectrum pricing [32, 33] for coordinated DSA. The vibrancy of on-going research works demonstrates the great interest to adopt DSA for future wireless communication systems. These observations provide additional motivation for undertaking these research problems.

1.5 Thesis Organization

The remaining of this thesis is organized as follows. In Chapter 2, we review the related works in the literature. SDR and CR technologies are identified as the enabling technologies which provide the required platform for the development and implementation of these DSA models. Our belief in the relationship between SDR, CR and DSA is explicitly presented and recent research developments in SDR and CR technologies are covered. In addition, related works pertaining to the public commons, private commons, and coordinated access models are reviewed. We also present some works on the development of on-body communications.

In Chapter 3, we study the impact of the PR activities on the SR transmission opportunity time, as well as the duration of the 'black spaces'. We present the derivation of the theoretical p.d.f. of the opportunity time for a small number of frequency bands. The analytical approach to obtain the theoretical p.d.f. is then generalized to an arbitrary number of frequency bands. We further postulate and show that the theoretical p.d.f. of the opportunity time can be closely approximated using lesser number of terms. In addition, the derivation of theoretical p.d.f. for the 'black spaces' is also presented.

In Chapter 4, the virtual spectrum partitioning model depicted in Fig 1.6 is examined. Based on a simple FCFS SAC policy, we first develop a four-dimensional Markov chain model, from which the steady-state solution enables concurrent computation of the service capacity under given GoS constraints as well as the corresponding amount of incurred tradeoffs. We then design a RES and a RD SAC policy to further enhance the service capacity of the multi-radio network. The Markov chain models for the RES and RD SAC policies are also presented. The performances of the RES and RD policies are compared against the FCFS policy.

In Chapter 5, we study the complete spectrum sharing model described in Fig. 1.7 and examined two possible cases. For the first case, we developed analytical platforms to compute the maximum service capacity of the multi-radio network given by RD and RES SAC policies as well as a SAC policy formulated based on discrete-time constrained Markov decision process. The analytical solution to each of these SAC policies is presented and the maximum service capacities of the radio systems under given GoS constraints are compared. For the second case, we assume the offered services incur different service charges and incorporate their pricing in the objective function of the problem. The SAC is formulated as a maximization problem

in which the objective of the spectrum manager is to maximize the average revenue obtained from servicing the traffic demands, and at the same time fulfill the GoS constraints of the individual radio systems.

Finally, we conclude the thesis with the presentation of the thesis contributions and the discussion on possible future works in Chapter 6.

Chapter 2

Literature Review

In this chapter, we give an introduction to software-defined radio (SDR) and cognitive radio (CR) technologies, and explain why they are the enabling technologies for dynamic spectrum access (DSA). A review of the related works on opportunistic spectrum access (OSA), virtual spectrum partitioning and complete spectrum sharing is presented. We also review the developments to incorporate CR technologies in radio systems developed under the public commons spectrum model.

2.1 Technology for Next Generation Radios and DSA

Current spectrum management adopts static spectrum assignment policy. In contrast, future wireless communication systems are likely to adopt DSA with the objective to improve the spectrum utilization efficiency. Both, SDR and CR technologies have emerged as promising technical platforms to develop such capabilities.

A SDR can be described as one in which the functions, operation modes, and applications can be configured and reconfigured using various software control [34]. This means that transmission parameters such as the signal bandwidth, carrier frequency, modulation, and even the adopted protocols can be flexibly changed through software control. With such flexibilities, SDR technology is capable of providing seamless inter-connectivity in a diverse world of radio access technologies and standards. However, with growing trends to develop multi-function devices and coupled with increasing interests to provide context-aware services, communication

devices require more intelligence and autonomy in decision making. Hence, the concept of CR was conceived.

CR technology has emerged to equip radio devices with cognitive capabilities through sensing, learning, awareness and reasoning. The definition of CR varies according to the described context. As such, researchers and academics still argue over its exact definition. However, it is widely acknowledged that SDR technology is a key enabler to realize CRs, which can be generally described as a SDR that additionally senses its environment, tracks changes, and reacts upon its findings so as to optimize the radio performance [35].

There are two general class of CRs, namely technology centric CRs and user centric CRs [36]. Technology-centric cognitivity comprises of the intelligence to provide most appropriate radio resources for the needs of the radio devices, for example, the identification of spectrum opportunities for OSA. User-centric cognitivity comprises of user support functions and together with technology-centric cognitivity, they provide the user with context aware services.

The definition and functionalities of CR, SDR and DSA are still evolving. However, in a more general sense, we classify their relationship by the Venn diagram in Figure 2.1. In Fig. 2.1, both CRs and DSA are enabled by SDR technology. However, as previously mentioned, a SDR could simply be a device that is based on software controlled architecture, and equipped with multi-mode connection capability. A user-centric CR could be developed upon SDR technology and include a cognitive engine [35] to recognize user behavior and interests, and therefore provide context-aware services to the user. In a possible scenario, a user could purchase movie tickets through his mobile phone [37] and the CR device recognizes the interests of the user

through progressive learning. It would then inform the user of subsequent new movie releases that is deemed to suit his/her interests.

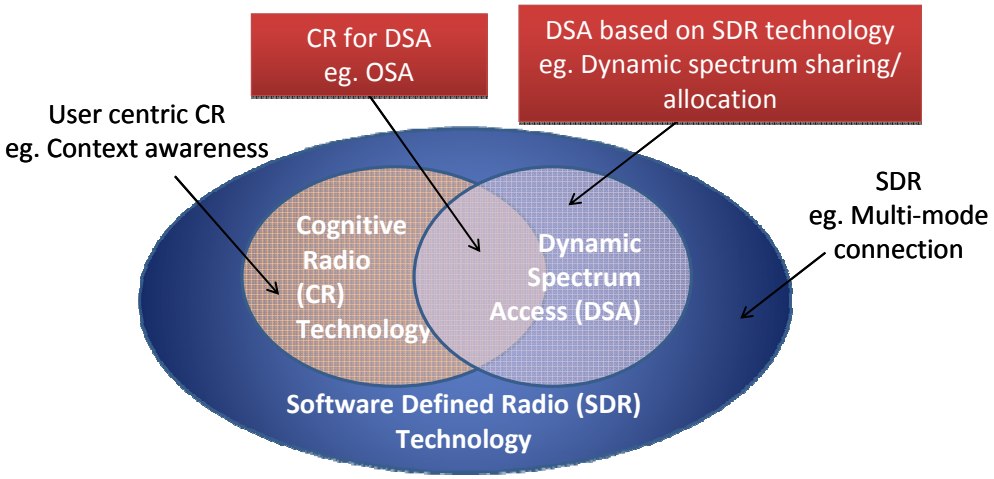

Fig. 2.1 Relationship between SDR, CR and DSA.

The area of concern in this thesis is highlighted in red in Fig. 2.1. OSA (Figs. 1.4 and 1.5) would require technology centric CRs that could sense and track the availability of spectrum holes, and identify suitable opportunities for secondary transmission. Although we do not rule out the future use of CRs, as an initial development, we believe that SDR technology is sufficient to support the virtual spectrum partitioning and complete spectrum sharing models (Figs. 1.6 and 1.7, respectively). This is because these access models generally do not require radio systems to sense for spectrum holes.

2.2 Software-Defined Radio and Cognitive Radio Technology

2.2.1 Introduction to SDR

Traditional hardware based radio devices have limited support for multi-mode connection and cross-functionality, and may only be modified through physical

hardware changes. This results in limited connectivity in the plethora of waveforms and wireless standards which exist today. In 1999, Joseph Mitola introduced the idea of SDRs [38]. A SDR has most of its functions implemented through modifiable software or firmware operating on programmable processing technologies [39]. These programmable processors include field programmable gate arrays (FPGA), digital signal processors (DSP), programmable System on Chip (SoC), General Purpose Processors (GPP), etc. Figure 2.2 shows the general architecture of a SDR transceiver.

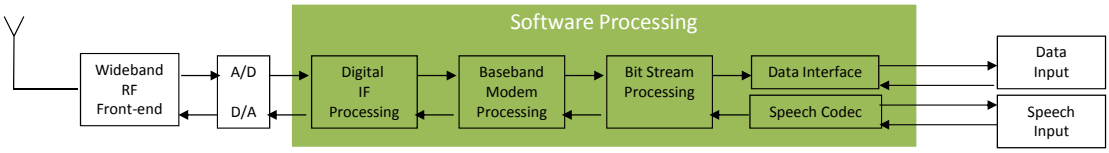

Fig. 2.2 General transceiver architecture for SDR, adopted from [40].

Referring to Fig. 2.2, the architecture incorporates a wideband RF front-end for transmission over wide ranges of frequencies and is supported by software controlled digital backend processing. The RF signals are passed into an analog-to-digital converter (ADC) and the quantized baseband signal is then processed. Through software implementation, the generation of signal waveforms (for example, OFDM, spread-spectrum, etc), and modulation schemes can be reconfigured dynamically. The use of software to control the operations of the backend processes makes the device dynamically reconfigurable, thus being able to adopt and communicate using different radio access technologies flexibly in the virtual spectrum partitioning and complete spectrum sharing models.

Currently, the most standard receiver architectures are the super heterodyne and homodyne receivers (zero-intermediate-frequency). With the development of fast data-converters (ADCs/DACs) and high speed programmable processors, these well-

known structures can be modified to work as a SDR receiver [41]. The key technologies within a transceiver for a SDR include:

- wideband antennas and programmable filters [42, 43],
- wideband low-noise-amplifiers (LNA) and most importantly,
- wideband ADCs [44].

The bandwidth and linearity of each of these stages will determine the dynamic range of operations and signal distortion in the various stages.

In the literature, there are three general methods for SDRs to obtain software updates/upgrades. They are namely static, pseudo-static and dynamic software downloading [40]:

Static download

This refers to the situation whereby the communication device is pre-programmed with a few common communication standards like GSM, 3G, WiFi, etc. From the devices' database, the user/device is able to select the standard most suitable for communications. The internal states of the device are then configured to that standard. It is evident that this method has limited flexibility.

Pseudo-static download

Pseudo-static downloads allows over the air reconfiguration of protocols and applications or updates of software programs. The contents may be programmed by the network operator or radio device manufacturer and transmitted wirelessly to the mobile device. This option offers greater flexibility compared to static downloading.

Dynamic download

Dynamic download further allows over the air reconfiguration during a transmission. Over-the-air or other remote reprogramming updates/upgrades, reduces the time and costs required for operation and maintenance.

2.2.2 Introduction to CR

In 2000, Mitola further developed the SDR concept and coined the term cognitive radio (CR) in [45]. From the definition given in Section 2.1, there are two main characteristics of CR, namely reconfigurability and cognitivity.

Reconfigurability is enabled by SDR technology and a possible relationship between SDR and CR which is illustrated in [35], is reproduced in Figure 2.3. In the model, the combination of the cognitive engine, SDR and various sensing mechanisms constitute a CR. The cognitive engine takes information from external sensing (radio environment) and processes it to optimize the desired objective based on its internal hardware capabilities. It is also responsible for learning traits relevant to its objective function. The cognitive engine also controls the parameters of the SDR so as to change its functionalities.

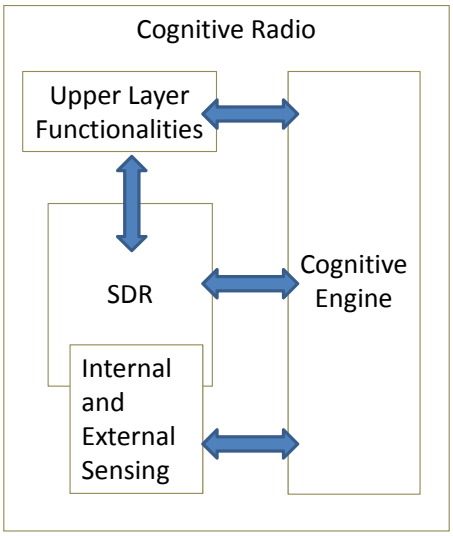

Fig. 2.3 Illustration of the relationship between SDR and CR [35].

On the other hand, cognitivity refers to the capability to sense and process relevant information from the radio environment, learn and adapt to the changes.

These traits are captured in the cognition cycle [46] which comprises of numerous key processes: Observe, Orient, Plan, Learn, Decide and Act.

The cognition cycle described in [46] is generic to user and technology centric CRs. We present a possible simplified cognition cycle in Figure 2.4 for OSA. The three main functionalities in this cycle consist of spectrum sensing, spectrum analysis, and transmission decision. Drawing a parallel with the generic cognition cycle, these functionalities are analogous to Observe, Learn, Decide and Act processes, respectively. These functionalities can be described as follows:

3 *Spectrum Sensing* of the radio environment may encompass the following:

- Sensing for spectrum holes and channel state information which include the estimation of interference levels.

4 *Spectrum Analysis* process may encompass the following:

4.1 Processing of channel state information;

4.2 Prediction of channel capacity;

5 The *Transmission Decision* process may encompass the following:

5.1 Decision to transmit/ wait for another spectrum opportunity;

5.2 Reconfiguration of flexible PHY layer, e.g. Modulation, carrier frequency, power control, beamforming and etc for adaptive transmission;

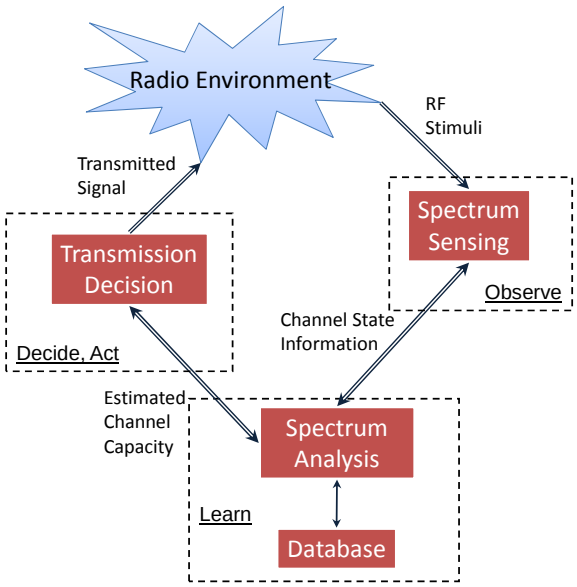

Fig. 2.4 A possible simplified version of the cognition cycle for OSA.

2.3 Opportunistic Spectrum Access

In this section, an overview on the related works pertaining to OSA is first presented. The challenges and methodologies when performing spectrum sensing and primary radio detection to realize opportunistic access are discussed.

2.3.1 Some Recent Research on OSA

The basic concept of OSA is to open licensed radio spectrum to secondary usage while limiting the interference on the PR system. It is commonly acknowledged that a concept similar to OSA was first introduced in [47] under the concept of *spectrum pooling*, which is a resource sharing strategy that organizes and groups available unused spectrum into a common pool and spectrum resources are allocated dynamically to requesting SR systems. Subsequently, spectrum pooling algorithms based on an OFDMA scheme was further developed in [48].

The neXt-Generation (XG) program from the Defense Advanced Research Projects Agency (DARPA) developed a XG radio system with the focus on intelligent policy-based negotiations and radio etiquettes so as to sense and share the usage of spectrum [49, 50]. Similarly, the CORVUS project [51] aims to use spectrum in a nonintrusive manner so as not to impede the access rights of the licensed users. The IEEE 802.22 WRAN [20] standardization workgroup was formed to study issues pertaining to secondary access in the television broadcasting frequency bands in the United States. More recently, the concept of CRs was extended to Cognitive Wireless Networks (CWN) [52].

2.3.2 Sensing, Detection and Modeling of Spectrum Holes

The statistics of the PR activity in each channel has significant impact on the SR transmission. The sensing, detection and hence the modeling of these activities are important considerations that can significantly influence the performance of SR systems. This section summarizes the progress in these areas and some of the challenges in the implementation of OSA radio systems.

In a multi-user, multi-path environment with fluctuating noise levels and varying RF power being received at the antenna, one of the main technical challenges is to enable reliable and robust detection of spectrum holes as well as active PR transmissions. The hidden PR [22] problem must also be adequately addressed. This problem will be illustrated and discussed in more details subsequently.

As it is not practical to continuously sense the spectrum, spectrum sensing is normally performed on a periodic basis. Therefore, the sensing rate has important practical implications on the performance of both the PR and SR systems. These issues are represented in Figure 2.5.

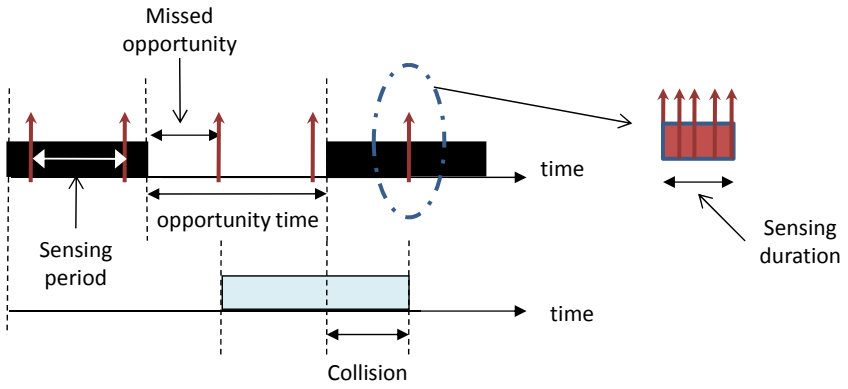

a) Slow sensing rate

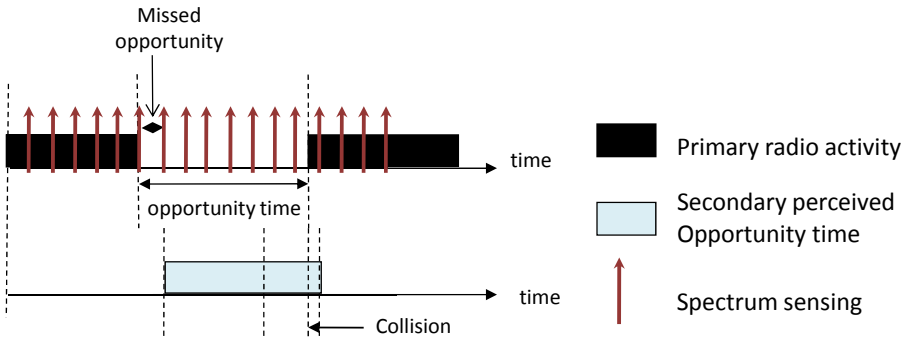

b) Fast sensing rate

Fig. 2.5 Effect of sensing rate on the opportunity time and collision with PR.

In Fig. 2.5(a), a slow sensing rate is used in the detection of secondary access opportunities. Given the slow sensing rate, there is higher probability of missing out on available secondary transmission opportunities. In addition, collisions with a PR transmission are more likely to occur if the sensing rate is too slow. On the other hand, the sensing rate is faster in Fig. 2.5(b). Although the missed opportunities may be reduced, it may not be cost effective because a faster sensing rate consumes more energy and reduces the secondary transmission time. The performance tradeoff for the described problem was investigated in [53] and other related works.

Spectrum Sensing Algorithms

In the literature, there are a few methods under investigation for spectrum sensing, which include wideband and narrowband, as well as cooperative sensing.

Narrowband spectrum sensing usually involves individually sensing and detection of the spectrum activity in each sub-band of a larger frequency band. The problem was analyzed in [53], where an analytical framework to derive an adaptive sensing period for each sub-band was developed. The objective is to maximize the discovery of spectrum opportunities and at the same time minimize the delay in finding an available channel. Similarly, in [54] the authors formulated a periodic sensing scheme for each sub-band as a finite horizon partially observable Markov decision process and derived the sensing period using linear programming techniques. However, the analysis was restricted to PR and SR systems which adopt slotted access models. The study was subsequently extended to consider continuous time access model in [55].

The sensing duration shown in Fig. 2.5 is also an important design parameter as it affects how quickly the SR is able to backoff when an active PR transmission reappears in the frequency band. A multi-resolution spectrum sensing [56] technique which first coarsely senses the entire frequency band, followed by finer resolution sensing of small frequency ranges was proposed. As it avoids sensing the entire frequency band at maximum resolution, this technique is found to significantly reduce the sensing duration.

On the other hand, wideband spectrum sensing is usually performed over a much wider frequency range altogether which possibly consist of multiple sub-bands [57]. Recently there are increasing interests to investigate the performance of wideband spectrum sensing. References [57-61] explore innovative techniques to

perform wideband spectrum sensing using wavelet transform methods. The investigations in [61] showed that by adopting wideband sensing, the detection of spectrum opportunities and PR transmissions in fading environments can be improved significantly, but at the expense of higher computational complexity.

Problem of Hidden Nodes

Assuming an omni-directional PR transmission, the hidden node problem can be explained using Figure 2.6. A SR, S_1, wishes to communicate with S_2. Due to its location and technical limitations, S_1 perceives that frequency channel F_1 is available and transmits. Unknown to S_1, a PR, denoted by P_1, is receiving on the same frequency and its reception is interfered.

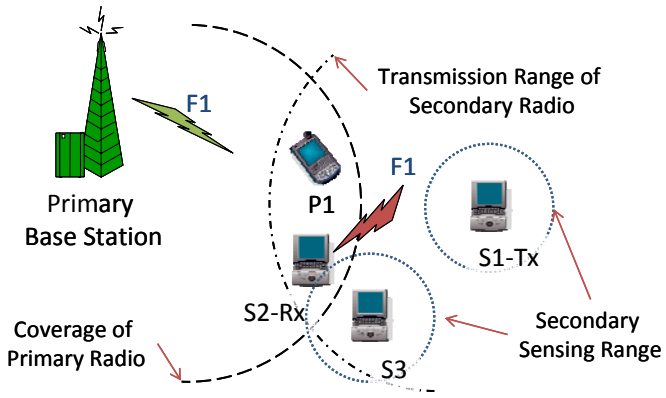

Fig. 2.6 Hidden PR situation.

Cooperative spectrum sensing [62, 63] involves multiple terminals concurrently sensing for spectrum opportunities at different geographical locations and centralizes the detection results for decision making. By exploiting spatial diversity, recent research results [64 - 66] indicate that the hidden node problem can be alleviated through cooperative sensing. For the scenario depicted in Fig. 2.6, channel F_1 will be detected as unavailable by both S_2 and S_3, and thus S_1 would be

denied transmission on F_1. However due to the aggregation of sensing results for joint decision making, the improved accuracy comes at the cost of additional communication overheads [67].

Detection Techniques

A few detection techniques have been extensively explored in the literature, namely, matched filter detection, energy detection and cyclostationary feature detection. The pros and cons of each technique are discussed and their performances were evaluated in [68]. In summary, matched filter detection is able to achieve better detection than energy detection for the same given SNR. However, as a coherent detection technique, it requires time synchronization with the primary signal and would require a different receiver for different classes of PR systems. On the other hand, energy detection can be easily implemented using simple Fast Fourier Transform (FFT) circuits, but may encounter a 'SNR wall' in some situations [69]. In addition, the detection threshold is highly susceptible to noise level uncertainties. Hence, energy detection is not suitable for detection of spectrum holes in which the PR system adopts spread spectrum transmission techniques.

Cyclostationary feature detection [70] utilizes periodic statistics of the mean and autocorrelation functions of the transmitted signals for detection. Random noise does not exhibit cyclostationarity and the periodic signature of each modulation scheme is unique. Therefore in the presence of random noise, the PR transmission could still be identified under certain SNR. Although this technique is more robust than matched filter and energy detection, its complexity increases by N^2 due to the computation of the cross-correlation multiplications from the N-point FFT [69]. A block diagram for a cyclostationary feature detector is shown in Figure 2.7.

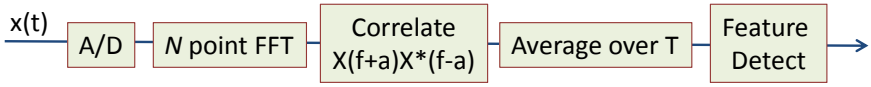

Fig. 2.7 Block diagram of cyclostationary feature detector, reproduced from [69].

Modeling of Spectrum Holes

Comparatively, limited work has been performed on the modeling of spectrum holes in the literature which can be found in [26, 27, and 71].

In [26], the authors modeled the duration of white spaces for numerous individual WLAN channels in the 2.4 GHz ISM band and found that the hyper-Erlang p.d.f. can best describe the duration of white spaces for each individual channel. On the other hand, by adopting a simplistic slotted access model for the SR, the authors described the duration of white spaces for a channel in terms of the number of timeslots which are unoccupied by PR traffic [27]. The duration of white spaces for each channel in this case is approximated by a geometric distribution. The results of the measurements performed by the Dutch Radio Regulatory Body over twelve cities in the Netherlands were presented in [71]. The measurements were performed in steps of 100 kHz from 400 MHz to 1 GHz and the measurements were taken at 10s interval over a 24-hour period for each frequency range. It was found that the PR activities in each frequency bin can be approximately modeled as an exponential on/off process.

2.3.3 Secondary Access

Distributed and Centralized Secondary Access

In general, the SR system architecture may be distributed (Fig. 1.4) or centralized (Fig. 1.5). Without a common MAC protocol, the competition for spectrum access opportunities among SRs or systems in a distributed DSA scenario

can be analyzed based on game theories [72, 73]. In this case, each radio will apply appropriate strategies in a distributive manner so as to maximize its desired utility function [74]. In [75], game theory methodologies were investigated with the objective to develop adaptive waveform schemes for interference avoidance in distributed spectrum sharing networks. A distributed cognitive MAC protocol for a SR system with energy constraints is presented in [75]. The objective is to maximize the expected throughput, while limiting the interference caused to the PR system.

On the other hand, some examples of recent OSA approaches adopting centralized system architecture include the CORVUS project by the University of California at Berkeley, as well as the IEEE 802.22 standardization work on WRAN. The development of spectrum pooling in [48] also adopts a centralized architecture. In these works, contention of spectrum access opportunities among multiple users is usually resolved through a centralized system controller. In addition, a dedicated control channel is available for the exchange of control messages and spectrum sensing information.

Some works also adopt cross-layer approaches which incorporate spectrum sensing in the design of secondary access schemes. In [77] the authors presented a MAC protocol for OSA in multi-channel cognitive wireless networks which include the consideration of channel sensing errors. In [78], cross-layer opportunistic MAC protocols which integrate spectrum sensing with packet scheduling for wireless ad hoc networks were studied and analyzed.

Other Secondary Access Methodologies

The main concern in OSA is to avoid causing excessive interference to PRs. In the literature, some research works has shown the effectiveness of the OFDMA approach for interference avoidance [78, 79]. In addition, OFDMA is also an

attractive access scheme due to its inherent flexibility of simultaneously using multiple noncontiguous frequency bands for transmission [80]. In this case, when primary transmissions are detected in one or multiple sub-carriers, the secondary transmission may still be possible using non-contiguous sub-carriers. Spectrum pooling using OFDMA is illustrated in Figure 2.8. In this case, a SR transmission requires a minimum of four OFDM sub-carriers.

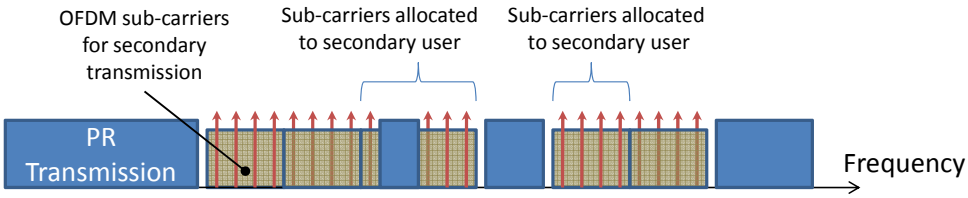

Fig. 2.8 Spectrum pooling based on OFDMA.

In contrast to the strict backoff policy which is adopted in most works in the literature, in some cases the SR may still be allowed to transmit even when a primary transmission is detected in the same channel. This is possible as long as the interference level at the primary receiver is below a specified acceptable threshold [81]. Such an access concept is based on an interference model which is proposed by the FCC [82]. The interference model ensures a specified PR performance by imposing a limit on the received interference power at the primary receiver. The limit is represented by the maximum amount of interference the primary receiver could tolerate in a certain channel, beyond which new or existing secondary transmissions should not access that channel. The interference model is illustrated in Figure 2.9.

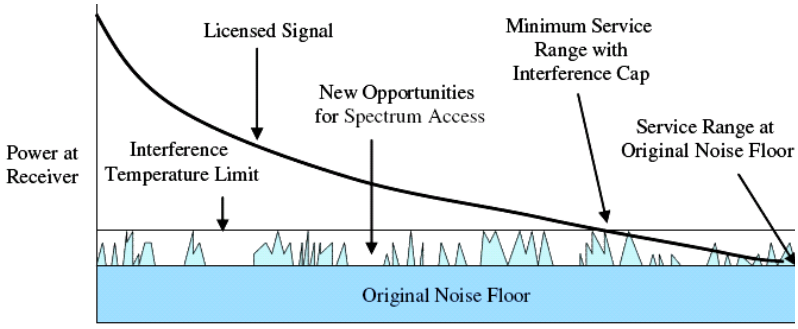

Fig. 2.9 Interference Model [82].

2.4 Coordinated Spectrum Access

As shown in Fig. 1.1, another aspect of DSA involves spectrum sharing among multiple radio systems in which their access is coordinated. In this section, we review some of the standardization work as well as other research efforts on coordinated dynamic spectrum access. In particular, we review the spectrum sharing models proposed in the literature and studies on the auction of spectrum via a spectrum manager.

2.4.1 Heterogeneous Multi-Radio Networks

As an overview, the IEEE SCC41/ P1900 [23] workgroup investigates and standardizes new methods of interference management, coordination and information sharing between different RATs for dynamic spectrum sharing in networks comprising of heterogeneous systems. The tasks are distributed among four main standardization bodies, namely: IEEE P1900.1, IEEE P1900.2, IEEE P1900.3 and IEEE P1900.4. The role of P1900.1 workgroup is to provide technically precise definitions and explanations of key concepts in spectrum management, CR, SDR and related technologies. It is also responsible for identification, investigation and creation

of new capabilities of these technologies. The P1900.2 workgroup recommends and provide technical guidelines for analyzing potential coexistence and/ or interference management methodologies. The P1900.3 workgroup is responsible for developing specific analysis techniques for compliance testing and evaluation of radio systems with DSA capability. Of related interest are the research efforts by the P1900.4 workgroup, which is responsible for defining building blocks for optimization of radio resource usage among different radio access networks and performance of spectrum access control in heterogeneous wireless networks. Two new workgroups were proposed recently, namely P1900.5 and P1900.6, which respectively focuses on the development of policy language and RF sensing algorithms to support radio systems with cognitive capability.

There are numerous European projects which examined advanced spectrum sharing methodologies for various applications. For example, the European IST project on Transparently Reconfigurable UbiquitouS Terminal (TRUST) [83] concerns the development of advanced spectrum sharing techniques through the use of SDR technology. In particular, the project studies the impact and potential benefits of the various spectrum sharing scenarios.

The projects on Dynamic Radio for IP-Services in Vehicular Environments (DRiVE) and Spectrum Efficient Uni and Multicast Services over Dynamic multi-Radio Networks in Vehicular Environments (OverDRiVE) studied methods for sharing spectrum resources between DVB-T, UMTS and GSM standards in a common frequency range via coordinated dynamic spectrum allocation in both temporal and spatial domains [84]. On the other hand, part of the European IST FP6 project WINNER [85] involves the development of system architectures that enables

B3G (Beyond 3G) systems to take advantage of flexible spectrum usage enabled by both intra and inter-system spectrum sharing concepts.

The European IST End to End Reconfigurability II (E^2R II) project [86] studies the development of common platforms so as to facilitate the optimization of resource usage among different radio access networks (RANs) through the use of reconfigurable and cognitive system architectures. Through these common platforms, users can experience seamless ubiquitous communications where and when needed in the future. The E^2R architectural framework is shown in Figure 2.10.

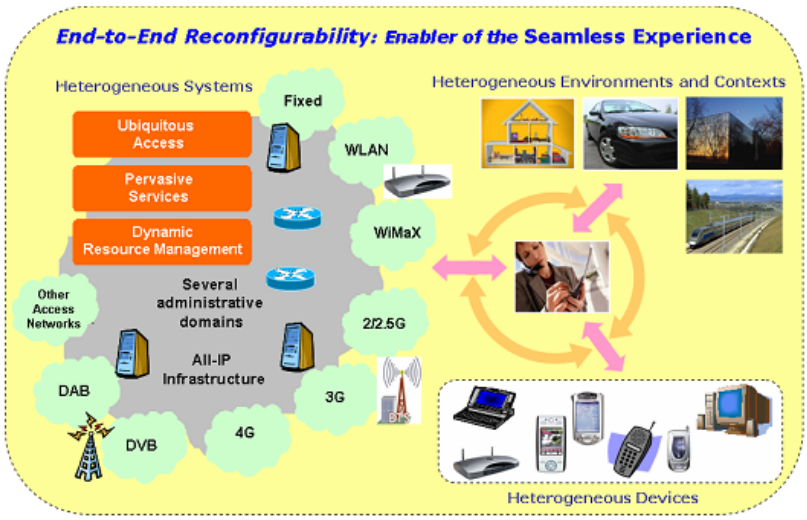

Fig. 2.10 Architectural framework of E^2R project [86].

2.4.2 Dynamic Spectrum Sharing Models

The European IST project on Transparently Reconfigurable Ubiquitous Terminal (TRUST) identified a few possible spectrum sharing models [29, 87] which are illustrated in Figure 2.11.

In Fig. 2.11(a), each radio system is a licensed radio and has exclusive access to an allocated frequency band. However, there also exists a shared frequency band

whereby the radio systems share the resource in a non-overlapping manner. The radio systems may only access the shared frequency band when they have depleted their own resources.

Figure 2.11(b) represents a virtual spectrum partition model whereby each radio system is assigned a licensed frequency band, and when its resources are depleted, the radio system may lease and utilize excess resources from the other radio system. This scenario corresponds to that described in Fig. 1.6, where two different radio systems share their excess bandwidth to support higher traffic demands.

In Fig. 2.11(c), the radio systems completely share the entire frequency band in a non-overlapping manner in which the wireless access for users from the different radio systems is coordinated. This model represents complete spectrum sharing which is similar to that illustrated in Fig. 1.7. OFDMA has been identified as a suitable scheme for this spectrum sharing model due to its inherent flexibility of simultaneously using multiple noncontiguous sub-carriers for transmission and was analyzed in [88] to support frequency spectrum sharing in both contiguous and fragmented scenarios.

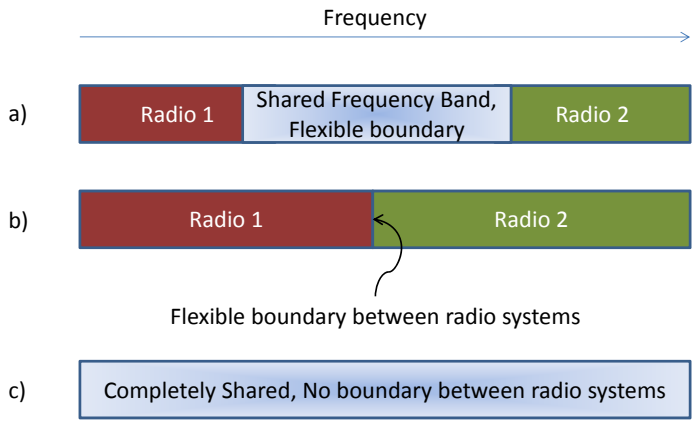

Fig. 2.11 Envisioned spectrum sharing models under IST TRUST project [29].

The spectrum sharing models shown in Fig. 2.11 were also adopted by various other research projects. For example, the models shown in Fig. 2.11(a) and (c) were further studied in the DRiVE and OverDRiVE projects. In [29], the system performance given by inter-operator spectrum sharing adopting the models shown in Fig. 2.11(a) and (b) were examined. In [28], the service capacity given by a static spectrum allocation model was compared with that using the spectrum sharing model in Fig. 2.11(c).

The model in Fig. 2.11(b) was further extended in the IEEE P1900.4 standardization works to include spectrum sharing between multiple operators. The scenario assumes different frequency bands are allocated to several operators who all have the flexibility of sharing their spectrum resource. Each operator manages its own spectrum usage through an Operator Spectrum Manager (OSM). Furthermore, a Network Reconfiguration Manager (NRM), which is developed in the P1900.4 standard, resides in the system architecture of each operator. The NRMs facilitate the exchange of information so as to negotiate and perform coordinated dynamic spectrum access. An example is illustrated in Figure 2.12 [89].

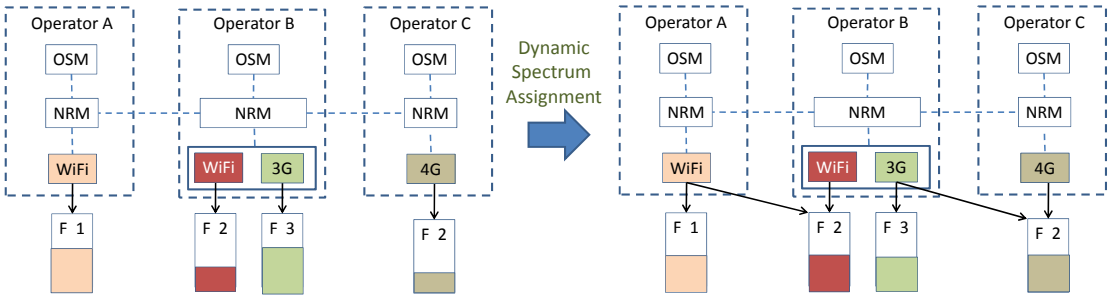

Fig. 2.12 Dynamic spectrum assignment between multiple operators [89].

Three operators A, B, and C provide different services in different frequency bands. The initial situation is depicted by the scenario on the left, whereby the WiFi

network of Operator A and the 3G network of Operator B experiences high usage. On the other hand, Operator Bs' WiFi network and Operator Cs' 4G network experience relatively lighter usage. Inter-operator negotiations and spectrum assignments are performed by the respective NRMs which after load balancing, the usage and traffic assignments are depicted by the scenario on the right. Through inter-operator spectrum sharing, the networks can support higher traffic demands. The P1900.4 workgroup also studies dynamic spectrum assignment between multiple networks which are owned by a single operator.

2.4.3 Spectrum Auctioning via a Spectrum Manager

Auctioning of exclusive spectrum access rights to radio systems via a spectrum manager has also been studied in the literature. For example, the DIMSUMnet [24] project describes the development of a coordinated spectrum access model via a regional spectrum broker. This concept is based on a centralized system architecture in which the spectrum broker manages a large portion of the spectrum band and dynamically assigns smaller portions of it to individual RANs. The RANs are required to bid for the required amount of spectrum resource to serve immediate traffic demands. Alternatively, the RANs could in anticipation of higher traffic, place an advanced reservation to the spectrum broker for a certain amount of spectrum. When the bid is successful, the RAN has exclusive access to the resources in which the lease is valid for a fixed duration and after the lease expires it must be renewed.

In the literature, there are also various lease based dynamic spectrum allocation algorithms. The tenure for the access rights in these models is much shorter compared to the static spectrum assignment approach. For example, [90] describes a centralized protocol known as Dynamic Spectrum Access Protocol (DSAP) for

managing spectrum resources through coordinated spectrum access among multiple radio systems. In [91], the authors proposed an algorithm to dimension the priority between network operators as well as the relative priorities between multi-class services into a spectrum sharing metric when allocating spectrum to multiple network operators.

In [92], a system architecture which incorporates joint radio resource management and spectrum auctioning in a heterogeneous network environment is presented. The analysis of spectrum auctioning among a group of radios subjected to an interference constraint is presented in [93]. To enable fair spectrum pricing, a model for computing the price per Hertz of spectrum with a certain level of interference was established in [94]. In a similar work, the combination of spectrum pricing and allocation algorithms so as to react dynamically to the market demands is proposed in [95].

2.5 Public Commons

Radio systems operating under this model may freely access the stipulated spectrum band and their operations may overlap in the frequency domain. However, the potential improvement in spectrum utilization efficiency provides the incentive for network operators to adopt more advanced interference mitigation techniques.

2.5.1 Cognitive UWB

In [96], the authors introduced cognitive UWB radio, which is a radio system based on UWB transmission with the capability of self-adapting to the characteristics of the surrounding radio environment. There are many interests to develop cognitive

UWB radio [97 - 99] because UWB radios span over a very large frequency range in which many other wireless systems operate. Hence there is great incentive to leverage on CR technology and develop adaptive interference mitigation techniques.

Adaptive Waveform

For pulse based UWB radio, a possible method for interference mitigation is through the use of adaptive waveforms for transmission. In [100], an adaptive waveform generation technique is presented which senses and adapts to the radio environment. Coexistence with other radio systems is also investigated using bit error rate as the metric for performance evaluation. In [101], a flexible waveform generation technique which shows improved interference suppression to and from narrowband signals is discussed.

Multi-band OFDM

On the other hand, there are also research efforts on cognitive UWB radio systems adopting multi-band OFDM transmission. For example, techniques for detecting interfering signals and shaping the spectral waveform for interference mitigation for a UWB radio using multi-band OFDM transmission technique is analyzed and demonstrated in [102]. In [103], the author discusses general methods for eliminating and reducing interference. In addition, the coexistence between multi-band OFDM based UWB radio and WiMax were explored in [10].

To maintain low spectral leakage between non-contiguous sub-carriers, a cosine modulated filter-bank technique was proposed in [104]. In [105], an adaptive multi-band OFDM waveform generation technique was designed based on Prolate

Spheroidal Wave Functions, in which the authors found to be effective in producing the desired spectral nulls for interference mitigation.

2.5.2 Other Research Efforts

The enhancement in system throughput from employing a cognitive based adaptive frequency hopping operation for Bluetooth transmission (2.4 GHz) in the presence of WLAN (IEEE 802.11b) signals was analyzed in [26]. In [106], it is proposed to use game theoretical models to analyze the network performances of cognitive UWB radio.

2.6 Conclusion

In this chapter, we have provided a review of the related works in the literature. From the review, there are many on-going research efforts studying various scenarios of DSA, which include OSA, complete spectrum sharing and virtual spectrum partitioning models. We also reviewed some recent developments under the public commons policy. Radio systems under this policy stand to gain from better throughput by incorporating interference mitigation techniques enabled by CR technology.

Chapter 3

Distribution of Opportunity Time and 'Black Spaces'

As a result of different PR on/off statistics [4], spectrum holes are sporadically distributed in the time and frequency domains. In this chapter, we present an analytical platform to derive the theoretical p.d.f of the opportunity time as well as the 'black spaces' for a SR system which span *N* frequency bins. This work provides a better insight on the relationship between the PR on/off activities and the statistics of these parameters. Some related works in the literature can be found in [26, 27].

This chapter is organized as follows. The system model is presented in Section 3.1. From a continuous time Markov chain (CTMC) model of the PR activities, we derive the lumped irreducible Markov chain model in Section 3.2. The derivation for the p.d.f. of the opportunity time is presented in Section 3.3. In Section 3.4, we present our simulation setup and results. This chapter is concluded in Section 3.5.

3.1 System Model and Assumptions

The radio spectrum under consideration is partitioned into *N* frequency bins, which are numbered as $F_1, F_2, ..., F_N$. SRs can utilize the available spectrum holes in one or more of the frequency bins for transmission. The bandwidth of each frequency bin can be chosen so that it matches to the PR occupying that frequency band. Each PR is assumed to utilize the full bandwidth of the frequency bin for transmission. Therefore, frequency bins do not necessary have the same bandwidth and the PR activities between any two frequency bins can be assumed to be independent.

Primary radio transmissions have priority over SR transmissions; hence, SRs may access the spectrum only if at least one unused frequency bin is available. However, to limit the interference on PR transmissions, a strict backoff policy is imposed on the SRs which must cease transmission upon detecting an incumbent PR transmission in the frequency bin. Figure 3.1 shows the OSA model with $N = 4$.

At a given referenced time, we let a_i denote the observed PR activity in the i^{th} frequency bin, i.e.,

$$a_i = \begin{cases} 1, & \text{if bin } i \text{ is in use,} \\ 0, & \text{if bin } i \text{ is unused.} \end{cases} \tag{3.1}$$

for $i = 1, 2, ...N$. The continuous random variable, $T_{0,1,0,1}$, denotes the time in which frequency bins 1 and 3 are unused while frequency bins 2 and 4 are being utilized by the PR. The opportunity time, is defined as the duration between the instances when an unused frequency bin is first available over the spectrum band to the instance when all frequency bins just become unavailable to the SR. This is denoted by τ as shown in Fig. 3.1. Secondary access is denied when primary transmissions occupy all the frequency bins. This duration is referred to as the 'black spaces' and is indicated by $T_{1,1,1,1}$ in Fig. 3.1.

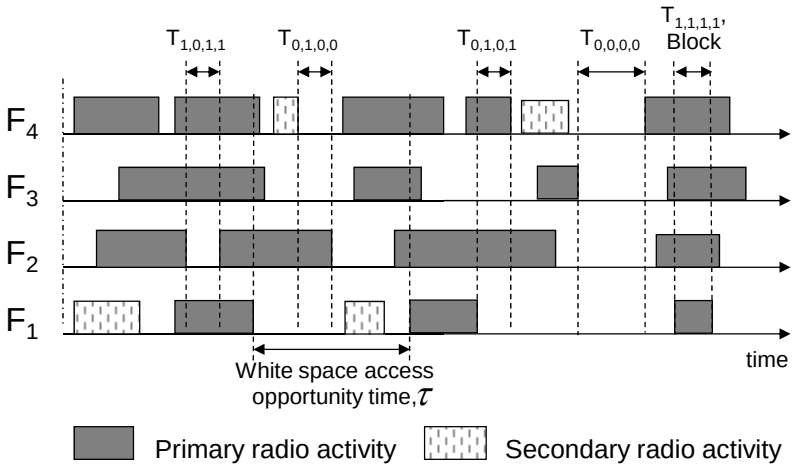

Fig. 3.1 System model with $N = 4$.

Extensive measurement performed by the Dutch Radio Regulatory Body [71] over twelve cities in the Netherlands showed that the PR activities can be approximately modeled by an exponential on/off process. Following this finding, the PR activity in each frequency bin is also modeled as an exponential on/off process, where the on state $(a_i = 1)$ corresponds to a PR is transmitting and the off state $(a_i = 0)$ corresponds to the frequency bin is unused. Although the exponential on/off model may not fully describe the activities for all PR systems, as a start, we assume that such a distribution is sufficient since it is analytically manageable. The transition rate from the on state to the off state and vice versa for the i^{th} frequency bin are $\mu_{\text{on},i}$ and $\mu_{\text{off},i}$, respectively. Each unique combination of PR activities, denoted by $(a_1, a_2, ...a_N)$, defines a *state* in the CTMC model. Hence, there are 2^N independent and distinct states in the model for *N* frequency bins.

We denote the sojourn time for the system to remain in the state $(a_1, a_2, ...a_N)$ by $T_{a_1,a_2,...a_N}$. We show in Appendix A that the random variable $T_{a_1,a_2,...a_N}$ is exponentially distributed with p.d.f. $f_{a_1,a_2,...a_N}(t)$ given by:

$$f_{a_1,a_2,...a_N}(t) = \left[\prod_{i=1}^{N} e^{-t\left[a_i\mu_{\text{on},i} + (1-a_i)\mu_{\text{off},i}\right]}\right] \sum_{i=1}^{N} \left[a_i\mu_{\text{on},i} + (1-a_i)\mu_{\text{off},i}\right], \quad t \geq 0. \tag{3.2}$$

For example, the p.d.f. of $T_{0,1,0,1}$ is given by $f_{0,1,0,1}(t) = \mu_{0,1,0,1} e^{-\mu_{0,1,0,1} t}$ for $t \geq 0$, where $\mu_{0,1,0,1} = \mu_{\text{off},1} + \mu_{\text{on},2} + \mu_{\text{off},3} + \mu_{\text{on},4}$. Since it is reasonable to assume that radio activities in all the frequency bins are independent to each other, the steady state probability of a given state $(a_1, a_2, ...a_N)$, denoted by $\pi_{(a_1,a_2,...a_N)}$, can be expressed as

$$\pi_{(a_1,a_2,...a_N)} = \prod_{i=1}^{N} P_{a_i} = \prod_{i=1}^{N} \left(\frac{a_i\mu_{\text{off},i}}{\mu_{\text{on},i} + \mu_{\text{off},i}} + \frac{(1-a_i)\mu_{\text{on},i}}{\mu_{\text{on},i} + \mu_{\text{off},i}} \right), \tag{3.3}$$

where P_{a_i} denotes the steady-state probability for activity a_i of the i^{th} frequency bin. Note that $1/\mu_{\text{on},i}$ and $1/\mu_{\text{off},i}$ respectively denote the mean sojourn time in the on state and off state of the i^{th} frequency bin. Note that $\mu_{\text{on},i}$ and $\mu_{\text{off},i}$ represent the transition rates of the i^{th} frequency bin and they all have the unit of min^{-1}.

3.2 Derivations Using Lumped Irreducible Markov Chain Model

Direct derivation of the distribution of the opportunity time using the above-mentioned CTMC model would be very complex especially when N is large. To simplify the analysis, we developed a lumped irreducible Markov chain model. We derive the lumped state transition probabilities and sojourn time for this model and use the results in the subsequent sections to derive the p.d.f. of the opportunity time.

We illustrate the derivation of the lumped Marko chain model using $N = 2$ as an example. Figure 3.2 shows the CTMC model, its equivalent irreducible Markov chain, and the *lumped irreducible Markov chain* [107] which lumped together those states having identical number of unused frequency bins.

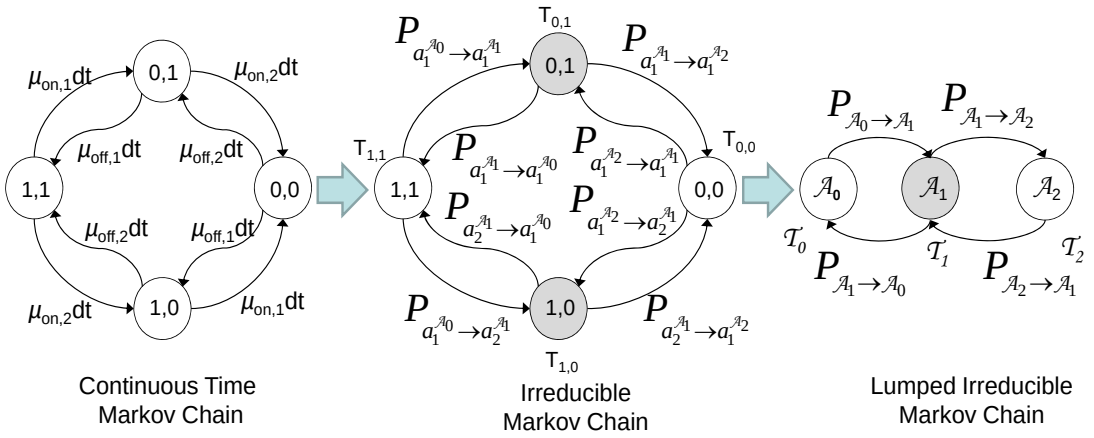

Fig. 3.2 Markov chain representation for $N = 2$.

In the CTMC model, the possible states are (0,0), (0,1), (1,0) and (1,1). The transitions from (0,1) to (1,0) or vice versa are not taken into consideration since the probability that radio activities in two or more frequency bins changing concurrently is negligible. In the lumped irreducible Markov chain, the *lumped states* are denoted as $\mathcal{A}_0 = \{(1,1)\}$, $\mathcal{A}_1 = \{(0,1),(1,0)\}$ and $\mathcal{A}_2 = \{(0,0)\}$. The lumped state $\mathcal{A}_1$ consists of two states denoted by $a_1^{\mathcal{A}_1} = (0,1)$ and $a_2^{\mathcal{A}_1} = (1,0)$, and these two states both represent only one unused frequency bin.

In general, for *N* frequency bins, there are $N+1$ unique lumped states, namely $\mathcal{A}_0, \mathcal{A}_1, ..., \mathcal{A}_N$, compared to 2^N states in the irreducible Markov chain. The number of states in a general lumped state $\mathcal{A}_m$, $(0 \le m \le N)$ is given by the binomial coefficient C_m^N, and we denote the i^{th} state in $\mathcal{A}_m$ as $a_i^{\mathcal{A}_m}$, $i = 1, 2, ...C_m^N$. Transitions between any states in a lumped state are not considered.

3.2.1 Deriving the Lumped Transition Probabilities

Let $q_{a_i \to a_j}$ denote the one-step transition rate from $a_i \in \mathcal{A}_m$ to $a_j \in \mathcal{A}_{(m-1)}$ in the continuous-time Markov chain. The probability that the system makes a transition from the state $a_i \in \mathcal{A}_m$ to the state $a_j \in \mathcal{A}_{(m-1)}$ is denoted by $P_{a_i \to a_j}$, and it can be expressed as:

$$P_{a_i \to a_j} = q_{a_i \to a_j} \Big/ \sum_{k \ne i, a_k \in \mathcal{A}_k} q_{a_i \to a_k} . \tag{3.4}$$

From the state transition probabilities of the irreducible Markov chain, we now derive an expression to evaluate the *lumped transition probabilities*, $P_{\mathcal{A}_m \to \mathcal{A}_{(m-1)}}$. Let π_{a_i} denote the steady-state probability of the state $a_i \in \mathcal{A}_m$, which can be obtained

from (3.3). The weight, w_{a_i}, is defined as the steady-state probability of the state $a_i^{\mathcal{A}m}$ normalized by the lumped steady-state probability, $\sum_{a_i \in \mathcal{A}_m} \pi_{a_i}$, i.e.

$$w_{a_i} = \pi_{a_i} \Big/ \sum_{a_i \in \mathcal{A}_m} \pi_{a_i} . \tag{3.5}$$

For a general lumped state $\mathcal{A}_m$, where $0 \le m \le N$, the total outward *lumped transition probability* must sum to one. For the lumped states $\mathcal{A}_0$ and $\mathcal{A}_N$, since there is only one possible outward transition to their respective adjacent lumped state, hence $P_{\mathcal{A}_0 \to \mathcal{A}_1} = 1$ and $P_{\mathcal{A}_N \to \mathcal{A}_{(N-1)}} = 1$. In addition, for each state in $\mathcal{A}_m$ (i.e., $a_i^{\mathcal{A}m}$, $i = 1, 2, ...C_m^N$), any one of the *m* available frequency bins could become unavailable after the next transition, hence each state can possibly transit to *m* states in $\mathcal{A}_{(m-1)}$. In general, since the states $a_i^{\mathcal{A}m}$ have different occurrence probability, $P_{\mathcal{A}_m \to \mathcal{A}_{(m-1)}}$ is computed as a summation of the state transition probabilities, $P_{a_i^{\mathcal{A}m} \to a_j^{\mathcal{A}(m-1)}}$, weighted by w_{a_i}. Thus we have the following equations for the lumped transition probabilities:

$$P_{\mathcal{A}_m \to \mathcal{A}_{(m-1)}} = \sum_{a_i \in \mathcal{A}_m, a_j \in \mathcal{A}_{(m-1)}} w_{a_i} P_{a_i \to a_j} , \tag{3.6}$$

and

$$P_{\mathcal{A}_m \to \mathcal{A}_{(m+1)}} + P_{\mathcal{A}_m \to \mathcal{A}_{(m-1)}} = 1 . \tag{3.7}$$

In (3.6), we perform a weighted sum based on the steady state probability of the individual states (in the lumped state) so as to ensure the steady state behavior of the lumped Markov chain remains identical to the irreducible Markov chain [107].

In particular, when the primary on/off statistics is identical for all the frequency bins, $\mu_{\text{on},i} = \mu_{\text{on}}$ and $\mu_{\text{off},i} = \mu_{\text{off}}$ for $i = 1, 2, ..N$. The lumped transition probability can be simplified to:

$$P_{\mathcal{A}_m \to \mathcal{A}_{(m-1)}} = m\mu_{\text{off}} \Big/ \left[m\mu_{\text{off}} + \left(N - m \right) \mu_{\text{on}} \right]. \tag{3.8}$$

3.2.2 Sojourn Time

Next, we present how the p.d.f. of the *sojourn time* for each lumped state can be derived. Since $\mathcal{A}_0$ and $\mathcal{A}_N$ comprises of only one state, their sojourn times denoted respectively by the random variables $\mathcal{T}_0$ $(=T_{1,1,\cdots,1})$ and $\mathcal{T}_N$ $(=T_{0,0,\cdots,0})$, are exponentially distributed and can be obtained from (3.2). For $\mathcal{A}_m$, where $1 \le m \le (N-1)$, there are altogether C_m^N states (with different occurrence probability in general) which contribute to the lumped sojourn time. Therefore, the random variable $\mathcal{T}_m$, which denotes the lumped sojourn time for $\mathcal{A}_m$, is a mixture of the sojourn time from each state and takes the form of a hyper-exponential distribution. The p.d.f. of $\mathcal{T}_m$ can be expressed as:

$$f\left(\mathcal{T}_m\right) = \sum_{a_i \in \mathcal{A}_m} w_{a_i} f_{a_i^{\mathcal{A}_m}}\left(t\right),\ t \ge 0. \tag{3.9}$$

where $\sum_{a_i \in \mathcal{A}_m} w_{a_i} = 1$ are real coefficients and is obtained from (3.5), $f_{a_i^{\mathcal{A}_m}}\left(t\right)$ is the p.d.f. of the sojourn time of the i^{th} state in $\mathcal{A}_m$ and can be obtained from (3.2) directly.

When the primary on/off statistics in each frequency bin is identical, we can deduce that the sojourn time is identically distributed for each state within a lumped state, and is given in (3.2). Furthermore, it can also be deduced that w_{a_i} are equal for $a_i \in \mathcal{A}_m$. Therefore, $\mathcal{T}_m$ is exponentially distributed and its p.d.f. can be derived from (3.2) directly. For example, when $N = 2$, $\mu_{\text{on}} = 2$ and $\mu_{\text{off}} = 5$, $f\left(\mathcal{T}_1\right)$ is given as $f\left(\mathcal{T}_1\right) = 7e^{-7t}$, $t \ge 0$. We present an example to illustrate the evaluation.

Example: To evaluate $f(\mathcal{T}_1)$ and lumped transition probabilities for $N=2$.

We let $N=2$ and assume that $\mu_{\text{on},1}=10/3$, $\mu_{\text{off},1}=2.5$, $\mu_{\text{on},2}=2$ and $\mu_{\text{off},2}=5$. Assuming $a_1^{\mathcal{A}_1}=(0,1)$ and using (3.3), the steady-state probability is computed as $\pi_{a_1^{\mathcal{A}_1}}=\mu_{\text{on},1}\mu_{\text{off},2}/[(\mu_{\text{on},1}+\mu_{\text{off},1})(\mu_{\text{off},2}+\mu_{\text{on},2})]=0.408$. Similarly, the steady-state probability of $a_2^{\mathcal{A}_1}=(1,0)$ is $\pi_{a_2^{\mathcal{A}_1}}=0.122$. The weight of each state can be computed using (3.5) and are given as $w_{a_1^{\mathcal{A}_1}}=0.769$ and $w_{a_2^{\mathcal{A}_1}}=0.231$. For $N=2$, $f(\mathcal{T}_1)$ is expressed as $f(\mathcal{T}_1)=w_{a_1^{\mathcal{A}_1}}f_{a_1^{\mathcal{A}_1}}(t)+w_{a_2^{\mathcal{A}_1}}f_{a_2^{\mathcal{A}_1}}(t)$. In this case, we obtain:

$$f(\mathcal{T}_1)=3.461e^{-4.5\mathcal{T}_1}+1.923e^{-8.33\mathcal{T}_1},\ \mathcal{T}_1\geq 0. \tag{3.10}$$

With reference to Fig. 3.2 and from (3.4), we obtain $P_{a_1^{\mathcal{A}_1}\to a_1^{\mathcal{A}_0}}=\mu_{\text{off},1}/(\mu_{\text{off},1}+\mu_{\text{on},2})$, $P_{a_2^{\mathcal{A}_1}\to a_1^{\mathcal{A}_0}}=\mu_{\text{off},2}/(\mu_{\text{on},1}+\mu_{\text{off},2})$. Using (3.6), we therefore obtain $P_{\mathcal{A}_1\to\mathcal{A}_0}=0.566$ and $P_{\mathcal{A}_1\to\mathcal{A}_2}=0.434$. Note that in this example, each state in $\mathcal{A}_1$ only transits to only one state in $\mathcal{A}_0$ or $\mathcal{A}_2$. ■

3.3 Deriving the P.D.F. of the Opportunity Time

In this section, we present the procedure to derive the p.d.f. of the opportunity time. The opportunity time τ is defined as the continuous time elapsed when the system just transits out from $\mathcal{A}_0$ to the time it first returns back to $\mathcal{A}_0$. We shall refer the sequence of states visited during this time interval as a *path*. As theoretically there are infinite possible paths and each path has an associated occurrence probability, τ should be described by a p.d.f. We derive an expression for τ in terms of the state

sojourn time by first using $N = 2$ and $N = 3$ as examples before generalizing the procedure to *N* frequency bins.

3.3.1 Deriving the Expression for τ

Consider $N = 2$ where there are a total of three lumped states in the lumped irreducible Markov chain as shown in Figure 3.3.

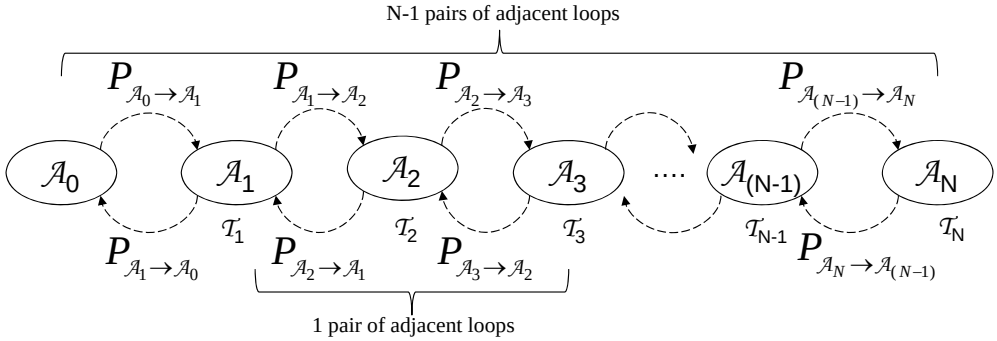

Fig. 3.3 Markov chain representation for general *N*.

The path $\mathcal{A}_0 \to \mathcal{A}_1 \to \mathcal{A}_0$ represents the system starts at $\mathcal{A}_0$, transits to $\mathcal{A}_1$ and then returns to $\mathcal{A}_0$. This path occurs with a probability given by $P_{\mathcal{A}_0 \to \mathcal{A}_1} P_{\mathcal{A}_1 \to \mathcal{A}_0}$, and the associated opportunity time is the sojourn time of $\mathcal{A}_1$ which is denoted by the random variable $\mathcal{T}_1$. Multiple visits between two adjacent lumped states constitute to *loops* in the path. For example, when the system transits from $\mathcal{A}_1$ to $\mathcal{A}_2$ and then back to $\mathcal{A}_1$, one complete loop occurs between $\mathcal{A}_1$ and $\mathcal{A}_2$. However, for each possible path, the loop between the lumped states $\mathcal{A}_0$ and $\mathcal{A}_1$ can only be performed once. This is because by definition, the opportunity time for that path terminates when the system first returns to $\mathcal{A}_0$.

Many loops can be performed between two adjacent lumped states if the two states are visited multiple times. Let l_1 be the number of loops performed

between $\mathcal{A}_1$ and $\mathcal{A}_2$. When $l_1 = 1$, the path $\mathcal{A}_0 \to \mathcal{A}_1 \to \mathcal{A}_2 \to \mathcal{A}_1 \to \mathcal{A}_0$ is obtained. The occurrence probability of this path is $P_{\mathcal{A}_0 \to \mathcal{A}_1} P_{\mathcal{A}_1 \to \mathcal{A}_2} P_{\mathcal{A}_2 \to \mathcal{A}_1} P_{\mathcal{A}_1 \to \mathcal{A}_0}$ and the opportunity time is given by the random variable $\mathcal{T}_1^{(0)} + \mathcal{T}_2^{(0)} + \mathcal{T}_1^{(1)}$, where the superscript $^{(l_1)}$ is to denote the sojourn time when $\mathcal{A}_1$ is revisited for the $l_1{}^{\text{th}}$ time. For all l_1, the random variables $\mathcal{T}_1^{(l_1)}$ are independent and identically distributed. Similarly when $l_1 = 2$, two loops are performed between $\mathcal{A}_1$ and $\mathcal{A}_2$, the path $\mathcal{A}_0 \to \mathcal{A}_1 \to \mathcal{A}_2 \to \mathcal{A}_1 \to \mathcal{A}_2 \to \mathcal{A}_1 \to \mathcal{A}_0$ is obtained with the opportunity time given by the random variable $\mathcal{T}_1^{(0)} + \mathcal{T}_2^{(0)} + \mathcal{T}_1^{(1)} + \mathcal{T}_2^{(1)} + \mathcal{T}_1^{(2)}$. In general, the opportunity time increases by $\left(\mathcal{T}_1 + \mathcal{T}_2\right)$ for each additional loop performed between $\mathcal{A}_1$ and $\mathcal{A}_2$; however, the occurrence probability decreases by the factor $\left(P_{\mathcal{A}_1 \to \mathcal{A}_2} P_{\mathcal{A}_2 \to \mathcal{A}_1}\right)$.

From the illustration above, the occurrence probability of a given path can be evaluated from the product of the transition probabilities of the respective states visited in the path. Hence for $N = 2$ and evaluating over all possible paths, τ is expressed as a summation of the random variables $\mathcal{T}_1$ and $\mathcal{T}_2$:

$$\tau = P_{\mathcal{A}_0 \to \mathcal{A}_1} P_{\mathcal{A}_1 \to \mathcal{A}_0} \sum_{l_1=0}^{\infty} \left[\left(P_{\mathcal{A}_1 \to \mathcal{A}_2} P_{\mathcal{A}_2 \to \mathcal{A}_1} \right)^{l_1} \right] \times \left[\sum_{r_1=0}^{l_1} \left(\mathcal{T}_1^{(r_1)} \right) + \sum_{r_2=0}^{l_1-1} \left(\mathcal{T}_2^{(r_2)} \right) \right], \tag{3.11}$$

where the summation over l_1 represents l_1 loops are performed between $\mathcal{A}_1$ and $\mathcal{A}_2$ before returning to $\mathcal{A}_0$. Note that the summation over r_1 is from zero to l_1, while the summation over r_2 is from zero to $l_1 - 1$. This is because the state $\mathcal{A}_1$ is visited $l_1 + 1$ times, hence the random variable $\mathcal{T}_1$ is summed $l_1 + 1$ times.

For $N = 2$, multiple loops can exist only between the pair of adjacent states $\mathcal{A}_1$ and $\mathcal{A}_2$. Consider the case where $N = 3$. In this case, loops can exist between $\mathcal{A}_1$ and $\mathcal{A}_2$, and also between $\mathcal{A}_2$ and $\mathcal{A}_3$. In general, when there are multiple pairs of

adjacent lumped states in the lumped Markov chain, there exist different paths which will statistically give the same opportunity time. For example, for $N = 3$, let l_1 and l_2 denote the number of loops performed between $\mathcal{A}_1$ and $\mathcal{A}_2$ and between $\mathcal{A}_2$ and $\mathcal{A}_3$, respectively. For $l_1 = 2$ and $l_2 = 1$, there are two possible paths given by $\mathcal{A}_0 \to \mathcal{A}_1 \to \mathcal{A}_2 \to \mathcal{A}_1 \to \mathcal{A}_2 \to \mathcal{A}_3 \to \mathcal{A}_2 \to \mathcal{A}_1 \to \mathcal{A}_0$ and $\mathcal{A}_0 \to \mathcal{A}_1 \to \mathcal{A}_2 \to \mathcal{A}_3 \to \mathcal{A}_2 \to \mathcal{A}_1 \to \mathcal{A}_2 \to \mathcal{A}_1 \to \mathcal{A}_0$. These two paths have identical number of visits to the same states and differ only in the order in which the states are visited. The occurrence probabilities for these two paths are identical and are both given by $P_{\mathcal{A}_0 \to \mathcal{A}_1} P_{\mathcal{A}_1 \to \mathcal{A}_2} P_{\mathcal{A}_2 \to \mathcal{A}_1} P_{\mathcal{A}_1 \to \mathcal{A}_2} \times P_{\mathcal{A}_2 \to \mathcal{A}_3} P_{\mathcal{A}_3 \to \mathcal{A}_2} P_{\mathcal{A}_2 \to \mathcal{A}_1} P_{\mathcal{A}_1 \to \mathcal{A}_0}$. Similarly, the random variable for the two *conditional* (on $l_1 = 2$ and $l_2 = 1$) opportunity times are both given by $\mathcal{T}_1^{(0)} + \mathcal{T}_2^{(0)} + \mathcal{T}_1^{(1)} + \mathcal{T}_2^{(1)} + \mathcal{T}_3^{(0)} + \mathcal{T}_2^{(2)} + \mathcal{T}_1^{(2)}$.

By definition, the loop between $\mathcal{A}_0$ and $\mathcal{A}_1$ can only be performed once. There is therefore only one possible path to complete the required number of loops between the adjacent pairs of lumped states $\mathcal{A}_0$ and $\mathcal{A}_1$, $\mathcal{A}_1$ and $\mathcal{A}_2$. However in general, if l_m and $l_{(m+1)}$ are the desired number of loops to be performed between the two pairs of adjacent lumped states $\mathcal{A}_m$ and $\mathcal{A}_{(m+1)}$, $\mathcal{A}_{(m+1)}$ and $\mathcal{A}_{(m+2)}$, $1 \le m \le (N-2)$, respectively, the number of different paths such that $\mathcal{A}_m$ is visited $(l_m + 1)$ times, $\mathcal{A}_{(m+1)}$ is visited $(l_m + l_{(m+1)})$ times and $\mathcal{A}_{(m+2)}$ is visited $l_{(m+1)}$ times is given by $C_{l_{(m+1)}}^{l_m + l_{(m+1)} - 1}$. The detailed derivation of this expression is presented in Appendix B. Hence for $N = 3$ and evaluating the number of possible arrangements between $\mathcal{A}_2$ and $\mathcal{A}_3$, τ, which averages over all ensembles of l_1 and l_2, is given by

$$\tau = P_{\mathcal{A}_0\to\mathcal{A}_1}P_{\mathcal{A}_1\to\mathcal{A}_0}\sum_{l_1=0}^{\infty}\left\{\left(P_{\mathcal{A}_1\to\mathcal{A}_2}P_{\mathcal{A}_2\to\mathcal{A}_1}\right)^{l_1}\sum_{l_2=0}^{\infty}\left\{C_{l_2}^{l_1+l_2-1}\left(P_{\mathcal{A}_2\to\mathcal{A}_3}P_{\mathcal{A}_3\to\mathcal{A}_2}\right)^{l_2}\times \left[\sum_{r_1=0}^{l_1}\left(\mathcal{T}_1^{(r_1)}\right)+\sum_{r_2=0}^{l_1+l_2-1}\left(\mathcal{T}_2^{(r_2)}\right)+\sum_{r_3=0}^{l_2-1}\left(\mathcal{T}_3^{(r_3)}\right)\right]\right\}\right\}. \tag{3.12}$$

Note that, if $l_1 = 0$, i.e. the path is $\mathcal{A}_0 \to \mathcal{A}_1 \to \mathcal{A}_0$, then $l_1 + l_2 - 1 < l_2$. By definition, $C_{l_2}^{l_1+l_2-1} = 0$ for all values of $l_2 \neq 0$ and $l_1 + l_2 - 1 < l_2$. Hence the terms in (3.12) are automatically reduced to zero and this ensures the loop $\mathcal{A}_0 \to \mathcal{A}_1 \to \mathcal{A}_0$ must be performed at least once in order to perform non-zero number of $\mathcal{A}_2 \to \mathcal{A}_3 \to \mathcal{A}_2$ loops, i.e. if $l_2 > 0$, then $l_1 \neq 0$.

In general, for *N* frequency bins, the random variable τ is obtained by evaluating the opportunity time for each path over all possible paths. With reference to Fig. 3.3, since there are $(N-1)$ pairs of adjacent loops, there are $(N-1)$ summation terms. In addition, as each lumped state $\mathcal{A}_m$, $(1 \le m \le N)$, can theoretically be visited infinite times, hence there are *N* summation terms (r_1 to r_N) corresponding to the random variables representing the respective state sojourn times. In general for *N* frequency bins, τ can be expressed as:

$$\tau = \underbrace{P_{\mathcal{A}_0\to\mathcal{A}_1}P_{\mathcal{A}_1\to\mathcal{A}_0}}_{\text{1 loop between } \mathcal{A}_0 \text{ and } \mathcal{A}_1}\underbrace{\sum_{l_1=0}^{\infty}\left\{\left(P_{\mathcal{A}_1\to\mathcal{A}_2}P_{\mathcal{A}_2\to\mathcal{A}_1}\right)^{l_1}}_{l_1 \text{ loops between } \mathcal{A}_1 \text{ and } \mathcal{A}_2}\underbrace{\sum_{l_2=0}^{\infty}\left\{C_{l_2}^{l_1+l_2-1}\left(P_{\mathcal{A}_2\to\mathcal{A}_3}P_{\mathcal{A}_3\to\mathcal{A}_2}\right)^{l_2}}_{l_2 \text{ loops between } \mathcal{A}_2 \text{ and } \mathcal{A}_3}\ldots$$

$$\underbrace{\sum_{l_{N-1}=0}^{\infty}\left\{C_{l_{N-1}}^{l_{N-2}+l_{N-1}-1}\left(P_{\mathcal{A}_{(N-1)}\to\mathcal{A}_N}P_{\mathcal{A}_N\to\mathcal{A}_{(N-1)}}\right)^{l_{N-1}}}_{l_{N-1} \text{ loops between } \mathcal{A}_{(N-1)} \text{ and } \mathcal{A}_N}\times\left[\underbrace{\sum_{r_1=0}^{l_1}\left(\mathcal{T}_1^{(r_1)}\right)}_{\mathcal{T}_1 \text{ is summed } (l_1+1) \text{ times}}+\underbrace{\sum_{r_2=0}^{l_1+l_2-1}\left(\mathcal{T}_2^{(r_2)}\right)}_{\mathcal{T}_2 \text{ is summed } (l_1+l_2) \text{ times}}+\ldots\right.$$

$$\left.\ldots+\sum_{r_{(N-1)}=0}^{l_{N-2}+l_{N-1}-1}\left(\mathcal{T}_{N-1}^{(r_{(N-1)})}\right)+\underbrace{\sum_{r_N=0}^{l_{N-1}-1}\left(\mathcal{T}_N^{(r_N)}\right)}_{\mathcal{T}_N \text{ is summed } l_{N-1} \text{ times}}\right]\ldots\Bigg\}\Bigg\}. \tag{3.13}$$

Generalizing the explanation given for (3.12), the above formulation also ensures that

l_m $(1 \le m \le N)$ can only be non-zero provided that all the previous loops are performed at least once. We note that (3.13) can be simplified by taking the moment generating function (MGF) of the p.d.f. of the random variables, $\mathcal{T}_1, \mathcal{T}_2, ...\mathcal{T}_N$. We demonstrate the approach for the case when the primary on/off activities are statistically identical and also when they are statistically non-identical.

3.3.2 Statistically Identical Primary On/Off Activity

In general, the exponential distribution expressed as $f(x) = \lambda e^{-\lambda x},\ x \ge 0$, has expectation given by $1/\lambda$ and the corresponding MGF is given as $\lambda/(\lambda - s),\ s < \lambda$. For the case where the primary on/off statistics is identical in all the *N* frequency bins, the MGF of (3.13) is:

$$\begin{aligned} \mathcal{G}_\tau(s) = \frac{\lambda_1}{\lambda_1 - s} P_{\mathcal{A}_0 \to \mathcal{A}_1} P_{\mathcal{A}_1 \to \mathcal{A}_0} \sum_{l_1=0}^{\infty} \Bigg\{ \left(P_{\mathcal{A}_1 \to \mathcal{A}_2} P_{\mathcal{A}_2 \to \mathcal{A}_1} \frac{\lambda_1}{\lambda_1 - s_1} \frac{\lambda_2}{\lambda_2 - s} \right)^{l_1} \\ \times \sum_{l_2=0}^{\infty} \Bigg\{ C_{l_2}^{l_1 + l_2 - 1} \left(P_{\mathcal{A}_2 \to \mathcal{A}_3} P_{\mathcal{A}_3 \to \mathcal{A}_2} \frac{\lambda_2}{\lambda_2 - s} \frac{\lambda_3}{\lambda_3 - s} \right)^{l_2} ... \times \\ \sum_{l_{N-1}=0}^{\infty} \Bigg\{ C_{l_{N-1}}^{l_{N-2} + l_{N-1} - 1} \left(P_{\mathcal{A}_{N-1} \to \mathcal{A}_N} P_{\mathcal{A}_N \to \mathcal{A}_{N-1}} \frac{\lambda_{N-1}}{\lambda_{N-1} - s} \frac{\lambda_N}{\lambda_N - s} \right)^{l_{N-1}} \Bigg\} ... \Bigg\}, \end{aligned} \tag{3.14}$$

where $1/\lambda_m = \left[(N-m)\mu_{\text{on}} + m\mu_{\text{off}} \right]^{-1}$ denote the expectation of $\mathcal{T}_m$.

Example: To evaluate $f(\tau)$ for $N = 2$ (identical on/off statistics).

From (3.11), since the random variables $\mathcal{T}_1^{(r_1)}$ and $\mathcal{T}_2^{(r_2 - 1)}$ are independent to each other, the MGF is given as:

$$\mathcal{G}_\tau(s) = \frac{\lambda_1}{\lambda_1 - s} P_{\mathcal{A}_0 \to \mathcal{A}_1} P_{\mathcal{A}_1 \to \mathcal{A}_0} \times \sum_{l_1=0}^{\infty} \left(P_{\mathcal{A}_1 \to \mathcal{A}_2} P_{\mathcal{A}_2 \to \mathcal{A}_1} \frac{\lambda_1}{\lambda_1 - s} \frac{\lambda_2}{\lambda_2 - s} \right)^{l_1}, \tag{3.15}$$

where $\mathcal{G}_\tau(s)$ denotes the MGF of τ. $1/\lambda_1 = (\mu_{\text{on}} + \mu_{\text{off}})^{-1}$ and $1/\lambda_2 = (2\mu_{\text{off}})^{-1}$ denote the expectation of the random variables $\mathcal{T}_1$ and $\mathcal{T}_2$, respectively. Eq. (3.15) is a convergent infinite geometric series; hence it can be expressed as

$$\begin{aligned}\mathcal{G}_\tau(s) &= \frac{\lambda_1}{\lambda_1 - s} P_{\mathcal{A}_0 \to \mathcal{A}_1} P_{\mathcal{A}_1 \to \mathcal{A}_0} \sum_{l_1=0}^{\infty} \left(P_{\mathcal{A}_1 \to \mathcal{A}_2} P_{\mathcal{A}_2 \to \mathcal{A}_1} \frac{\lambda_1}{\lambda_1 - s} \frac{\lambda_2}{\lambda_2 - s} \right)^{l_1} \\ &= \frac{\lambda_1 P_{\mathcal{A}_1 \to \mathcal{A}_0} (\lambda_2 - s)}{s^2 - s(\lambda_1 + \lambda_2) + P_{\mathcal{A}_1 \to \mathcal{A}_0} \lambda_1 \lambda_2}.\end{aligned} \tag{3.16}$$

We have used (3.7) to simplify the transition probabilities in (3.16). Since (3.16) is a real and proper rational function in *s*, by the Fundamental Theorem of Algebra [108], it can be shown that (3.16) can be expressed in terms of partial fractions. After some algebraic simplification, the discriminant of the quadratic polynomial in the denominator is given by $\mathcal{D} = 4P_{\mathcal{A}_1 \to \mathcal{A}_0} \times (1 - P_{\mathcal{A}_1 \to \mathcal{A}_0}) + [\lambda_1 + \lambda_2 (1 - 2P_{\mathcal{A}_1 \to \mathcal{A}_0})]^2$. Since $\mathcal{D}$ is positive for real values of λ_1 and λ_2, $\mathcal{G}_\tau(s)$ can be expressed as a partial fraction with two linear distinct real roots, i.e.

$$\mathcal{G}_\tau(s) \equiv c_1 / (s + \beta_1) + c_2 / (s + \beta_2). \tag{3.17}$$

Eq. (3.17) shows that the p.d.f. of τ should take the form of a hyper-exponential distribution with two exponential terms. The exponent of the individual terms are respectively given by $\beta_1 = -0.5(\mu_{\text{on}} + 3\mu_{\text{off}} + \theta)$ and $\beta_2 = -0.5(\mu_{\text{on}} + 3\mu_{\text{off}} - \theta)$. In addition, $c_1 = \mathcal{G}_\tau(s)(s + \beta_1)\big|_{s=-\beta_1}$, $c_2 = \mathcal{G}_\tau(s)(s + \beta_2)\big|_{s=-\beta_2}$ and $\theta^2 = (\mu_{\text{on}} + 3\mu_{\text{off}})^2 - 8P_{\mathcal{A}_1 \to \mathcal{A}_0} \mu_{\text{off}} (\mu_{\text{on}} + \mu_{\text{off}})$. By taking the inverse transform of (3.16), the general p.d.f. of τ for $N = 2$ is:

$$\begin{aligned}f(\tau) = 0.5(\mu_{\text{on}} + \mu_{\text{off}}) P_{\mathcal{A}_1 \to \mathcal{A}_0} \Big\{ &\left[\theta + 2\mu_{\text{off}} (\mu_{\text{on}} - \mu_{\text{off}}) \right] e^{\beta_1 \tau} \\ &+ \left[\theta - 2\mu_{\text{off}} (\mu_{\text{on}} - \mu_{\text{off}}) \right] e^{\beta_2 \tau} \Big\}, \ \tau \geq 0.\end{aligned} \tag{3.18}$$

■

In general, the MGF for larger values of *N* contain many terms. Nevertheless, it can be simplified by using the identity (Proof is presented in Appendix C):

$$\sum_{i=0}^{\infty} C_i^{i+j-1}\zeta^i = (1-\zeta)^{-j}. \tag{3.19}$$

where $0<\zeta<1$. Using (3.19) and starting with the summation over l_{N-1}, the summation terms in (3.14) can be recursively simplified. Note the summation over l_1 represents a convergent infinite geometric progression and (3.14) can therefore be simplified into a real and proper polynomial in terms of *s*. We illustrate the simplification with an example using $N=4$ where the details given in Appendix D.

Example: To evaluate $f(\tau)$ for $N=4$ (identical on/off statistics) using (3.19).

From (3.14) and (3.19), and after some algebraic simplification, the random variable $G_\tau(s)$ for $N=4$ is given by

$$G_\tau(s) = X_0(1-X_2-X_3)/(1-X_1-X_2-X_3+X_1X_3), \tag{3.20}$$

where $1/\lambda_1=(\mu_{\text{off}}+3\mu_{\text{on}})^{-1}$, $1/\lambda_2=(2\mu_{\text{off}}+2\mu_{\text{on}})^{-1}$, $1/\lambda_3=(3\mu_{\text{off}}+\mu_{\text{on}})^{-1}$ and $1/\lambda_4=(4\mu_{\text{off}})^{-1}$ are the expectation of the random variables $\mathcal{T}_1$, $\mathcal{T}_2$, $\mathcal{T}_3$ and $\mathcal{T}_4$, respectively. In addition, $X_0=P_{\mathcal{A}_0\to\mathcal{A}_1}P_{\mathcal{A}_1\to\mathcal{A}_0}\,\lambda_1/(\lambda_1-s)$,

$X_1=P_{\mathcal{A}_1\to\mathcal{A}_2}P_{\mathcal{A}_2\to\mathcal{A}_1}\,\lambda_2\lambda_1/\left[(\lambda_2-s)(\lambda_1-s)\right]$, $X_2=P_{\mathcal{A}_2\to\mathcal{A}_3}P_{\mathcal{A}_3\to\mathcal{A}_2}\,\lambda_2\lambda_3/\left[(\lambda_2-s)(\lambda_3-s)\right]$,

$X_3=P_{\mathcal{A}_3\to\mathcal{A}_4}P_{\mathcal{A}_4\to\mathcal{A}_3}\,\lambda_3\lambda_4/\left[(\lambda_3-s)(\lambda_4-s)\right]$.

Substituting $\mu_{\text{on}}=2$ and $\mu_{\text{off}}=5$, we obtain

$$f(\tau)=0.26e^{-27.9\tau}+1.09e^{-20.2\tau}+1.89e^{-11.6\tau}+1.78e^{-2.3\tau},\ \tau\ge 0. \tag{3.21}$$

The expectation and variance are 0.355 and 0.17, respectively. ■

3.3.3 Statistically Non-Identical Primary On/Off Activity

For this case, we can also write down $\mathcal{G}_\tau(s)$ for *N* frequency bins. The expression is in terms of the MGF of the distribution of the sojourn times for the states in the lumped irreducible Markov chain. This is given as:

$$\begin{aligned}\mathcal{G}_\tau(s) = P_{\mathcal{A}_0\to\mathcal{A}_1}P_{\mathcal{A}_1\to\mathcal{A}_0}\mathcal{T}_1(s)\sum_{l_1=0}^{\infty}\left[\left(P_{\mathcal{A}_1\to\mathcal{A}_2}P_{\mathcal{A}_2\to\mathcal{A}_1}\mathcal{T}_1(s)\mathcal{T}_2(s)\right)^{l_1}\right]\times \\ \sum_{l_2=0}^{\infty}\left[C_{l_2}^{l_1+l_2-1}\left(P_{\mathcal{A}_2\to\mathcal{A}_3}P_{\mathcal{A}_3\to\mathcal{A}_2}\mathcal{T}_2(s)\mathcal{T}_3(s)\right)^{l_2}\right]\times\ldots \\ \sum_{l_{N-1}=0}^{\infty}\left[C_{l_{N-1}}^{l_{N-2}+l_{N-1}-1}\left(P_{\mathcal{A}_{N-1}\to\mathcal{A}_N}P_{\mathcal{A}_N\to\mathcal{A}_{N-1}}\mathcal{T}_N(s)\mathcal{T}_{N-1}(s)\right)^{l_{N-1}}\right],\end{aligned} \tag{3.22}$$

where $\mathcal{T}_m(s)$ denotes the MGF of the p.d.f. of $\mathcal{T}_m$. When *N* is large, performing direct inverse transform on (3.22) may be computationally intensive. By applying (3.19) recursively through a computer program and subsequently expressing the resultant polynomial (in *s*) into partial fractions, the exact p.d.f. can be easily obtained by performing an inverse transform on the partial fractions as shown in (3.17).

Example: To evaluate $f(\tau)$ using $N=3$ (non-identical on/off statistics).

From (3.12) and taking its MGF, we obtain

$$\begin{aligned}\mathcal{G}_\tau(s) &= P_{\mathcal{A}_0\to\mathcal{A}_1}P_{\mathcal{A}_1\to\mathcal{A}_0}\mathcal{T}_1(s)\sum_{l_1=0}^{\infty}\left\{\left[\left(P_{\mathcal{A}_1\to\mathcal{A}_2}P_{\mathcal{A}_2\to\mathcal{A}_1}\right)\mathcal{T}_1(s)\mathcal{T}_2(s)\right]^{l_1}\right\} \\ &\quad\times\sum_{l_2=0}^{\infty}\left\{C_{l_2}^{l_1+l_2-1}\left[\left(P_{\mathcal{A}_2\to\mathcal{A}_3}P_{\mathcal{A}_3\to\mathcal{A}_2}\right)\mathcal{T}_2(s)\mathcal{T}_3(s)\right]^{l_2}\right\} \\ &= \frac{P_{\mathcal{A}_0\to\mathcal{A}_1}P_{\mathcal{A}_1\to\mathcal{A}_0}\mathcal{T}_1(s)\left[\left(P_{\mathcal{A}_2\to\mathcal{A}_3}P_{\mathcal{A}_3\to\mathcal{A}_2}\right)\mathcal{T}_2(s)\mathcal{T}_3(s)-1\right]}{\left[\left(P_{\mathcal{A}_1\to\mathcal{A}_2}P_{\mathcal{A}_2\to\mathcal{A}_1}\right)\mathcal{T}_1(s)\mathcal{T}_2(s)+\left(P_{\mathcal{A}_2\to\mathcal{A}_3}P_{\mathcal{A}_3\to\mathcal{A}_2}\right)\mathcal{T}_2(s)\mathcal{T}_3(s)-1\right]},\end{aligned} \tag{3.23}$$

where $\mathcal{T}_m(s)$ denotes the MGF of the p.d.f. of the random variable $\mathcal{T}_m$. If we denote $1/\lambda_{0,0,1}$, $1/\lambda_{0,1,0}$, $1/\lambda_{1,0,0}$, $1/\lambda_{0,1,1}$, $1/\lambda_{1,0,1}$, $1/\lambda_{1,1,0}$ and $1/\lambda_{0,0,0}$ as the expectation of the random variables $T_{0,0,1}$, $T_{0,1,0}$, $T_{1,0,0}$, $T_{0,1,1}$, $T_{1,0,1}$, $T_{1,1,0}$ and $T_{0,0,0}$, respectively, and

$$\mathcal{T}_1(s) = w_{a_1^{\mathcal{A}_1}} \frac{\lambda_{0,1,1}}{\lambda_{0,1,1}-s} + w_{a_2^{\mathcal{A}_1}} \frac{\lambda_{1,0,1}}{\lambda_{1,0,1}-s} + w_{a_3^{\mathcal{A}_1}} \frac{\lambda_{1,1,0}}{\lambda_{1,1,0}-s},$$

$$\mathcal{T}_2(s) = w_{a_1^{\mathcal{A}_2}} \frac{\lambda_{0,0,1}}{\lambda_{0,0,1}-s} + w_{a_2^{\mathcal{A}_2}} \frac{\lambda_{0,1,0}}{\lambda_{0,1,0}-s} + w_{a_3^{\mathcal{A}_2}} \frac{\lambda_{1,0,0}}{\lambda_{1,0,0}-s}, \ \mathcal{T}_3(s) = \lambda_{0,0,0}/(\lambda_{0,0,0}-s).$$

Note that we have used (3.19) to obtain the expression in (3.23). Substituting the values $\mu_{\text{on},1} = 2.5$, $\mu_{\text{off},1} = 10/3$, $\mu_{\text{on},2} = 2$, $\mu_{\text{off},2} = 5$, $\mu_{\text{on},3} = 20/11$ and $\mu_{\text{off},3} = 20/3$, the p.d.f. for τ is expressed as

$$\begin{aligned} f(\tau) = {} & 0.56e^{-20.68\tau} + 0.06e^{-13.64\tau} + 1.46e^{-12.58\tau} + 0.096e^{-11.1\tau} + 0.16e^{-10.29\tau} \\ & + 0.01e^{-8.23\tau} + 2.01e^{-2.44\tau}, \ \tau \geq 0. \end{aligned} \tag{3.24}$$

The expectation and variance are 0.35 and 0.16, respectively. ■

Note that there are seven exponential terms in (3.24) and this can be explained as follows. For *N* frequency bins with pair-wise distinct on/off PR activity, excluding the state denoted by $\mathcal{A}_0$, the system can be modeled by $(2^N - 1)$ states. The p.d.f. of τ therefore has $(2^N - 1)$ exponential terms. However, given all the possible paths and transition probabilities, $f(\tau)$ is a mixture of the sojourn time of each state.

3.4 Simulations and Results

A simulation program using MATLAB was performed to verify the correctness of the derived theoretical p.d.f. We would like to emphasize that the simulation was developed and performed separately from the theoretical p.d.f. The simulation is developed based on the on/off statistics of each frequency bin. We generate five hundred thousand PR activities for each frequency bin with on/off duration following independent exponential distributions. We then checked through the activities in all the frequency bins to identify the continuous duration of the

available white spaces defined in Fig. 3.1. The time elapsed when a white space just becomes available to when it becomes unavailable again constitutes a sample of τ. Many values of τ are collected and the simulated p.d.f. can be easily obtained from the simulation data. Similarly, the simulated p.d.f. for the 'black spaces' can be obtained as well.

3.4.1 Verification of Analytical Results

Figure 3.4 shows the semi-log plot for the p.d.f. of $\mathcal{T}_1$ with different on/off rates when $N = 2$. In the first case, we plot the p.d.f. for the values $\mu_{\text{on},1} = 10/3$, $\mu_{\text{off},1} = 2.5$, $\mu_{\text{on},2} = 2$ and $\mu_{\text{off},2} = 5$. In the second case, only the off rate for frequency bin 1 is decreased to 1.25 while the other rates remain unchanged. From Fig. 3.4, the theoretical p.d.f. and the simulated p.d.f. tallies very well except at its lower tail due to insufficient samples of τ are collected from the simulation. For the second case, the probability that $\mathcal{T}_1$ has a value lesser than 0.25min is lower but the probability that $\mathcal{T}_1$ has a value larger than 0.25min is higher when compared to the first case. This is because statistically frequency bin 1 has more radio activity when $\mu_{\text{off},1}$ is larger (case 1), hence in the second case, a SR tends to have a higher probability of detecting a longer duration of white space for that frequency bin. This can also be seen from (3.2) that the statistics for the sojourn time of $a_2^{\mathcal{A}_1} = (1,0)$ remains unchanged, and the mean sojourn time for the state $a_1^{\mathcal{A}_1} = (0,1)$ is statistically increased compared to the first case.

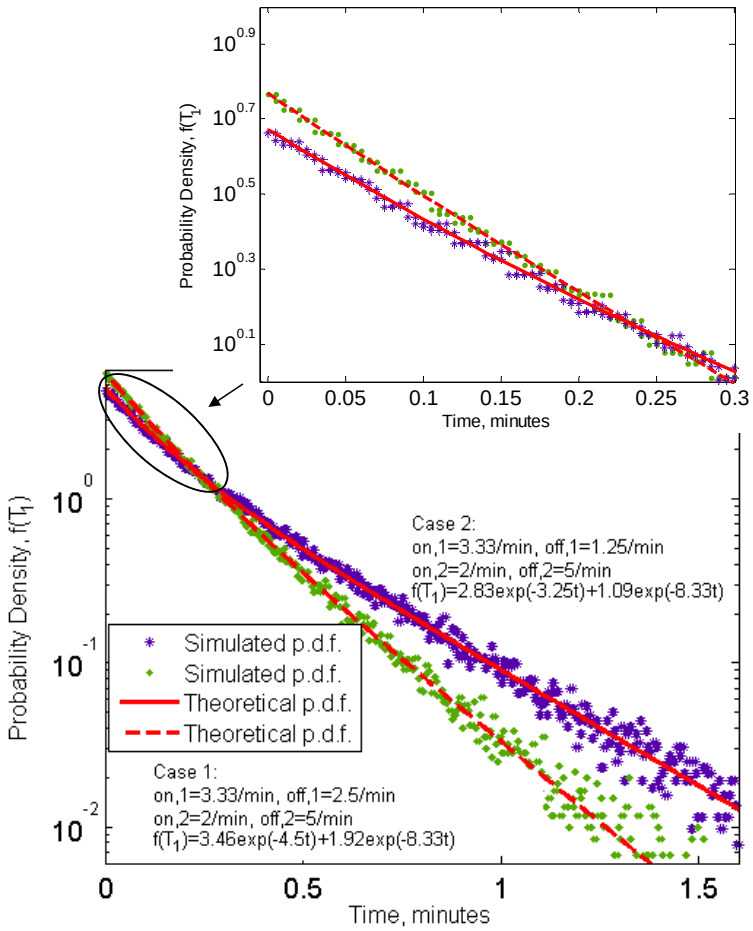

Fig. 3.4 p.d.f. of $f(\mathcal{T}_1)$ for N=2 with different on/off activities.

In Figure 3.5, we plot the p.d.f. of τ for $N=3$ and $N=4$ with identical on/off statistics. For these results, the parameters are $\mu_{\text{on}}=2$ and $\mu_{\text{off}}=5$. The theoretical p.d.f. of τ for $N=4$ is given in (3.21). In addition, we also plot the p.d.f. of τ for $N=2$ and $N=3$ with non-identical on/off statistics. For non-identical on/off statistics and $N=2$, the evaluation parameters are $\mu_{\text{on},1}=2.5$, $\mu_{\text{off},1}=10/3$, $\mu_{\text{on},2}=2$ and $\mu_{\text{off},2}=5$. We retain these values and add an additional frequency bin with activity factors given by $\mu_{\text{on},3}=20/3$ and $\mu_{\text{off},3}=20/11$ in the case with $N=3$. From these results, it is observed that all things being equal, in general, having an additional frequency bin increases the probability of having a longer access opportunity time.

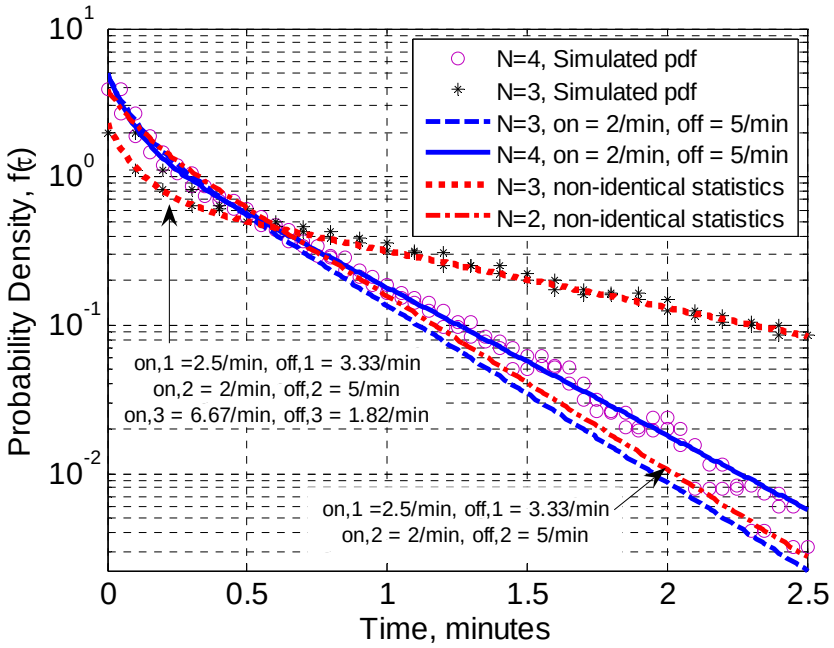

Fig. 3.5 p.d.f. of τ for N=3 and N=4 (identical on/off statistics); and for N=2 and N=3 (non-identical on/off statistics).

Figure 3.6 shows the theoretical cumulative density function (c.d.f.) of τ and also for the duration of 'black space' (i.e., no available frequency bin for SR transmission) when the primary on/off activities are identical for $N = 2$. The c.d.f. of the duration of 'black space' can be derived from (3.2) by substituting $a_i = 1,\ \forall i$. We compare the c.d.f. of τ for the sets of values given by (a) $\mu_{\text{on}} = 2$ and $\mu_{\text{off}} = 2.5$, (b) $\mu_{\text{on}} = 2$ and $\mu_{\text{off}} = 5/3$, (c) $\mu_{\text{on}} = 10/3$ and $\mu_{\text{off}} = 2.5$, (d) $\mu_{\text{on}} = 10/3$, $\mu_{\text{off}} = 5/3$. Comparing between (a) and (c), and between (a) and (b), we can observe that the change in μ_{on} has statistically lesser impact on the duration of τ compared to the change in μ_{off}, i.e. a statistically longer opportunity time can be achieved by reducing μ_{off} than by increasing μ_{on}. However, changing μ_{on} has a greater impact on the statistics of $T_{1,1}$, i.e. the duration of black space. When μ_{on} is increased, the duration of the 'black space' is statistically shorter. A similar observation can be derived when comparing (c) and (d), and between (c) and (a).

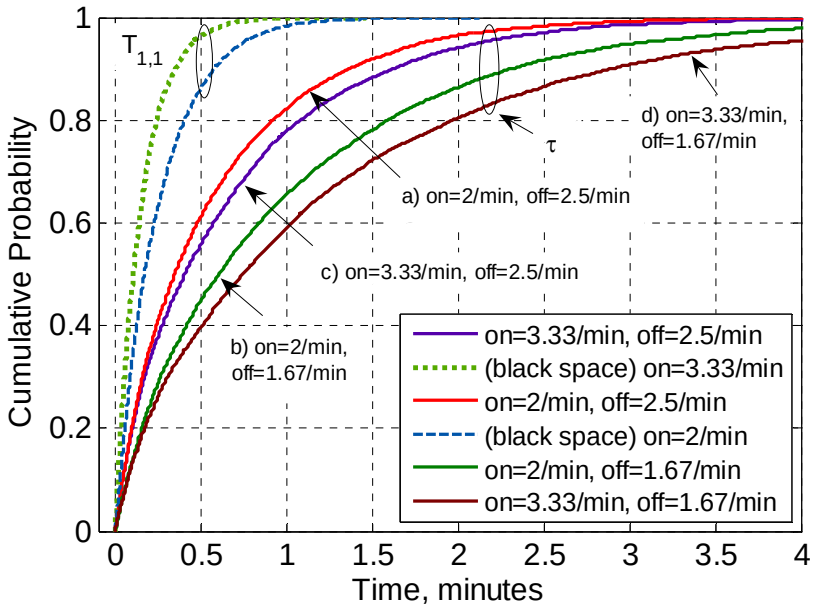

Fig. 3.6 C.D.F of τ for different values of μ_{on} and μ_{off} for $N = 2$.

In addition, for a given cumulative probability α, the threshold duration, τ_α, can be determined from the c.d.f. of τ. The physical meaning of τ_α can be interpreted as follow. If there is only one secondary request and its service time is less than or equals to τ_α, and supposing the system is able to sense the beginning of white spaces (in practice this is limited by the channel sensing rate), the probability that a secondary request will be successfully served without being forced to drop is guaranteed to be better than 1-α. For example, if $\alpha = 0.6$, we obtain $\tau_\alpha = 1\,\text{min}$ for d). In this case, the probability in which a secondary request can be completely served without being forced to drop (due no available frequency bin), is less than 0.4 if its service time is less than 1 min.

3.4.2 Statistical Fitting with Simulated Results

From (3.21), the theoretical p.d.f. has four terms. Alternatively, we perform curve fitting for the simulated results by using the hyper-exponential distribution with

four terms. The fitting is performed using a commercial software package, TOMLAB™. The estimated p.d.f. is

$$f\left(\hat{\tau}\right) = 0.223e^{-24.05\hat{\tau}} + 0.97e^{-19.33\hat{\tau}} + 1.82e^{-10.31\hat{\tau}} + 1.77e^{-2.29\hat{\tau}},\ \hat{\tau} \geq 0. \tag{3.28}$$

The mean squared error (MSE) between the theoretical p.d.f. and fitted p.d.f. is about 0.0022. Similarly, we perform similar curve fitting using a hyper-exponential function with seven terms on the simulated data for the p.d.f. given in (3.26). The distribution of the statistical fit is given as:

$$\begin{aligned} f\left(\hat{\tau}\right) = {} & 0.58e^{-22.92\hat{\tau}} + 0.09e^{-14.01\hat{\tau}} + 1.43e^{-12.85\hat{\tau}} + 0.088e^{-11.37\hat{\tau}} \\ & + 0.163e^{-10.12\hat{\tau}} + 0.011e^{-8.2\hat{\tau}} + 2.03e^{-2.44\hat{\tau}},\ \hat{\tau} \geq 0. \end{aligned} \tag{3.29}$$

The simulated, fitted and theoretical p.d.f. are plotted in semi-log scale and is shown in Figure 3.7. The MSE between the fitted and the theoretical p.d.f. is about 0.002.

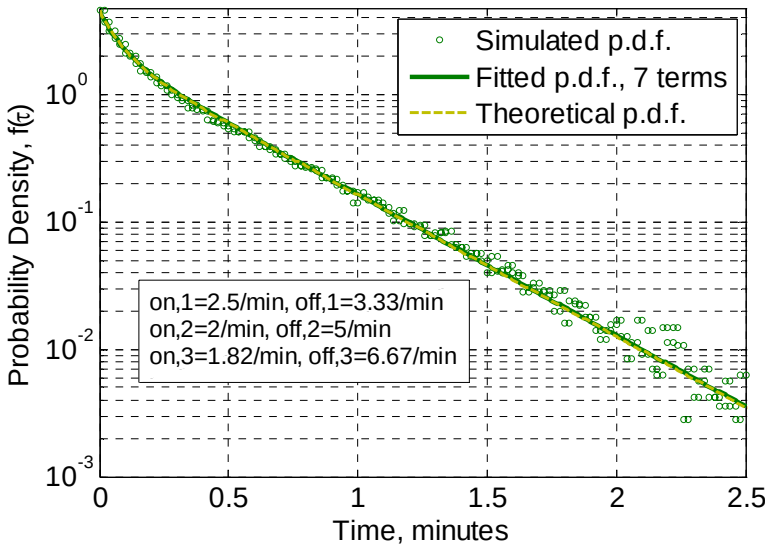

Fig. 3.7 Simulated, statistically fitted and analytical p.d.f. of τ, $N = 3$.

Comparing (3.29) with (3.26), and (3.28) with (3.21), the statistical fit to simulated data gives a good approximation to the theoretical expression. Hence, we can obtain a good approximation to the theoretical expression by performing a statistical fit to simulated data.

3.4.3 Extension to More Frequency Bins

From the theoretical p.d.f., we note that some of the terms have less significant effect on the overall distribution. For example, in (3.26), the terms $0.06e^{-13.64\tau}$, $0.01e^{-8.23\tau}$ have relatively much smaller impact on the p.d.f. This makes us speculate that perhaps we can best fit the p.d.f. by only a few exponential terms and achieve reasonably good approximation to the theoretical expression. We perform curve fitting to simulated data for various values of *N*, using a hyper-exponential distribution with two to five terms and compare the MSE between the simulated p.d.f. and statistically fitted p.d.f. The results are tabulated in Table 3.1. For statistically non-identical on/off activities, the mean on/off rates in the frequency bins are chosen from 10 to 0.91. For statistically identical on/off activities, the values $\mu_{\text{on}} = 2$ and $\mu_{\text{off}} = 5$ are used.

From the results, it is evident that a hyper-exponential distribution with two terms is an inadequate fit as the MSE is too large. With three or more exponent terms, a closer fit is obtained. Since the difference in the MSE when three or more terms are used is small, this suggests that for practical purposes, a hyper-exponential distribution with three exponent terms gives sufficiently good approximation to the theoretical p.d.f. Both Figure 3.8 and Figure 3.9 further confirm this. Fig. 3.8 shows the curve fitting using two to four exponent terms for $N = 9$ in which frequency bins have statistically non-identical radio activities. Fig. 3.9 shows the case for $N = 6$ where the radio activities of frequency bins are statistically identical.

TABLE 3.1 COMPARISON OF MSE FOR VARIOUS N.

	Non-identical Statistics				*Identical Statistics*			
N	***2 terms***	***3 terms***	***4 terms***	***5 terms***	***2 terms***	***3 terms***	***4 terms***	***5 terms***
3	0.021	0.0043	0.0032	0.0027	0.024	0.0023	0.0023	0.0023
4	0.033	0.0054	0.0047	0.0040	0.031	0.0025	0.0022	0.0022
5	0.035	0.0050	0.0039	0.0030	0.033	0.0034	0.0029	0.0027
6	0.034	0.0044	0.0038	0.0035	0.036	0.0033	0.0030	0.0029
7	0.042	0.0034	0.0027	0.0022	0.037	0.0039	0.0030	0.0028
8	0.037	0.0032	0.0025	0.0025	0.033	0.0036	0.0028	0.0026
9	0.044	0.0040	0.0038	0.0038	0.043	0.0040	0.0034	0.0033
10	0.042	0.0036	0.0035	0.0035	0.040	0.0042	0.0035	0.0035

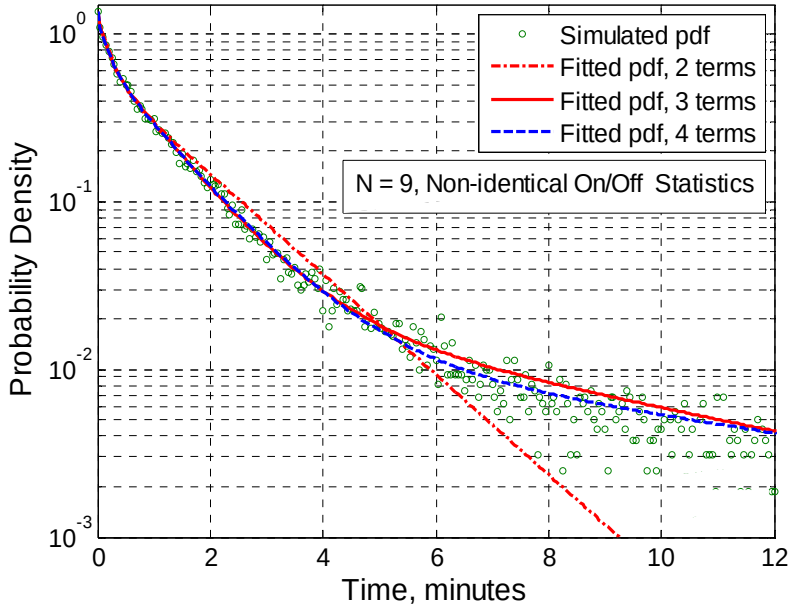

Fig. 3.8 Simulated p.d.f. and statistically fitted p.d.f. for τ, N=9.

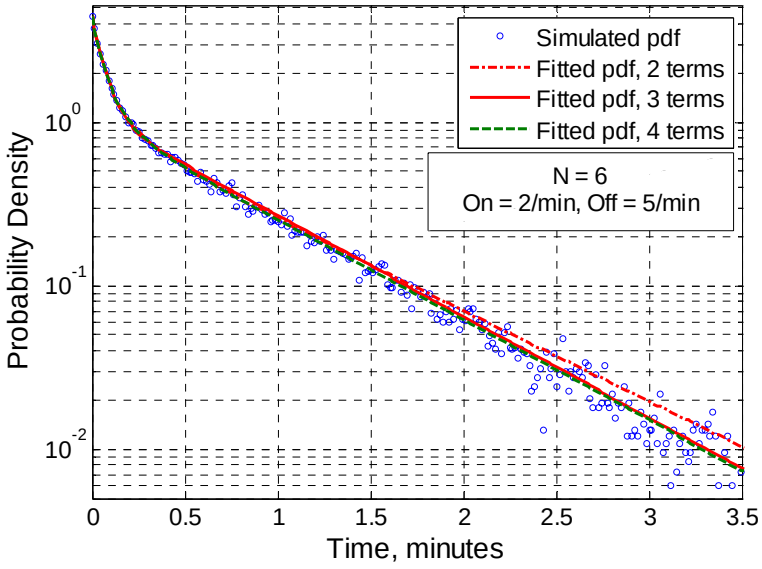

Fig. 3.9 Simulated p.d.f. and statistically fitted p.d.f. for τ , N=6.

3.5 Conclusion

In this chapter, we presented the analytical platform to derive the theoretical distribution of the opportunity time as well as the duration of the 'black spaces' for a SR system spanning N frequency bins. Between any two frequency bins, the PR activities are assumed to be independent, and the activities in each frequency bin follow an exponential on/off process. Using a lump irreducible Markov chain, we modeled and analyzed the cases when the PR on/off activities in the frequency bins are statistically non-identical and also when they are identical. The analytical approach (which can be performed systematically with a computer) to obtain the theoretical p.d.f. of the opportunity time is presented. The theoretical p.d.f for the 'black spaces' for N frequency bins is also derived.

The results show the p.d.f. of the opportunity time follows a hyper-exponential distribution with $(2^N - 1)$ terms when the PR on/off activities in the frequency bins are pair-wise distinct, while having N terms if the activities are statistically identical.

In practice, especially if N is large, having many terms in the expression may be cumbersome. We showed using simulated data and statistical distribution fitting with commercial software that for the range of parameters evaluated, a hyper-exponential distribution with three exponential terms may be sufficient to approximate the theoretical p.d.f. reasonably well. The opportunity time in this research gives a measure of the continuous SR transmission time (where the SR transmission is not forcibly terminated by onset of PR transmission in all the channels). The duration of the ‘black spaces’ gives a measure of the duration in which SR transmissions are not possible due to no available spectrum holes.

Chapter 4

Virtual Spectrum Partitioning Multi-radio Network

In the future, spectrum utilization efficiency can also be improved through the use of reconfigurable technology. By leveraging on the different system requirements, higher trunking efficiency is achievable through appropriately designed spectrum admission control (SAC) policies. This leads to higher overall spectrum utilization efficiency compared to the aggregated performances of the standalone systems. In this chapter, we study the virtual spectrum partitioning model depicted in Fig. 1.6. In the multi-radio network, individual proprietary radio systems generally have different system parameters, such as service bandwidth and GoS guarantees for example.

Some related works in the literature can be found in [85, 86, 88 and 109]. In most of these works, the enhancement in service capacity is evaluated through computer simulations. In addition, the incurred tradeoffs, i.e. performance of vertical handoffs when a service request accesses resources owned by another radio system, has not been quantified. In this work, we develop analytical platforms to compute the service capacity and the incurred tradeoffs concurrently. We also develop appropriate SAC policies to further enhance the service capacity of the multi-radio network.

This chapter is organized as follows. In Section 4.1, we discuss the system model and in Section 4.2, we present a novel four-dimensional Markov chain model based on the FCFS admission policy. In Section 4.3, we discuss the computer simulation setup, and present results for the FCFS policy in Section 4.4. We present and analyze the performance given by the RES and RD policies in Section 4.5 and Section 4.6, respectively. The comparisons of the performance of the three policies are presented in Section 4.7. The chapter is concluded in Section 4.8.

4.1 System Model and Assumptions

Our system model assumes a service provider owns two separate radio systems, namely, R_A and R_B, which adopt the same RAT but provide different services to the same geographical area. By default, R_A provides Type 1 service and R_B provides Type 2 service. For ease of analysis, we assume the two radio systems have the same wireless coverage and together form a multi-radio network through an additional reconfigurable layer in their protocol stack. Spectrum admissions are performed between R_A and R_B via the common link. The functionality of the system model is explicitly described in Section 1.3 and also illustrated in Fig. 1.6.

We assume that users will first attempt to access its default radio system. Service requests are vertically handed off and the devices are required to be dynamically reconfigured only when the default radio system is unable to support the new user. In this case, a Type 1 service is reconfigured to transmit using the resources owned of R_B, and vice versa. To avoid performing more vertical handoffs and device reconfiguration the vertically handoff service is served using the resources from the cooperating radio system for the entire duration of its transmission. We further assume there is negligible delay when a vertical handoff is performed. When a request is unable to be served by both systems, a blocked service for that service type occurs and we assume that all blocked services are cleared immediately. The blocked service probability gives an indication of the GoS for that service type.

For ease of comparison and analysis, we assume R_A and R_B can be normalized into having N_A and N_B units of spectrum resources, respectively. U_A and U_B denote the units of bandwidth required for a Type 1 and Type 2 service, respectively, and $U_B > U_A$. For simplicity and without loss of generality, we assume that the same

service require identical units of bandwidth when served by either of the radio systems. The arrival of Type 1 and Type 2 service requests are assumed to follow a Poisson process with mean rates λ_1 and λ_2 respectively. Their service times are assumed to follow a negative exponential distribution with mean rates $1/\mu_1$ and $1/\mu_2$, respectively. The Poisson arrival and negative exponentially distributed traffic models may not fully describe the traffic patterns of some radio systems; however, as a start, we assume that such a distribution is sufficient since it is analytically manageable.

4.2 Markov Chain Model for FCFS Policy

In this section, we present the modeling of a simple FCFS SAC policy using a Markov chain. The possible states of occupancy for the multi-radio network can be modeled using a four-dimensional Markov chain. The states are denoted as (w, x, y, z), where *w* represents the number of Type 2 vertical handoff services in R_A; *x* represents the number of Type 1 vertical handoff services in R_B. *y* represents the number of Type 2 services in R_B; *z* represents the number of Type 1 services in R_A. Therefore, the state $(1,2,3,4)$ represents one Type 2 vertical handoff service and four Type 1 services in R_A, two Type 1 vertical handoff services and three Type 2 services in R_B.

For this policy, we let $y_{\max} = N_B/U_B$, $z_{\max} = N_A/U_A$, $x_{\max} = \lfloor N_B/U_A \rfloor$ and $w_{\max} = \lfloor N_A/U_B \rfloor$. The notation $\lfloor \chi \rfloor$ denotes the largest integer value less than or equals to χ. As an example, Figure 4.1 shows the Markov chain model for the FCFS policy with $N_A = 3$, $U_A = 1$, $N_B = 4$, $U_B = 2$, $w = 0$, $x_{\max} = 4$, $y_{\max} = 2$ and $z_{\max} = 3$.

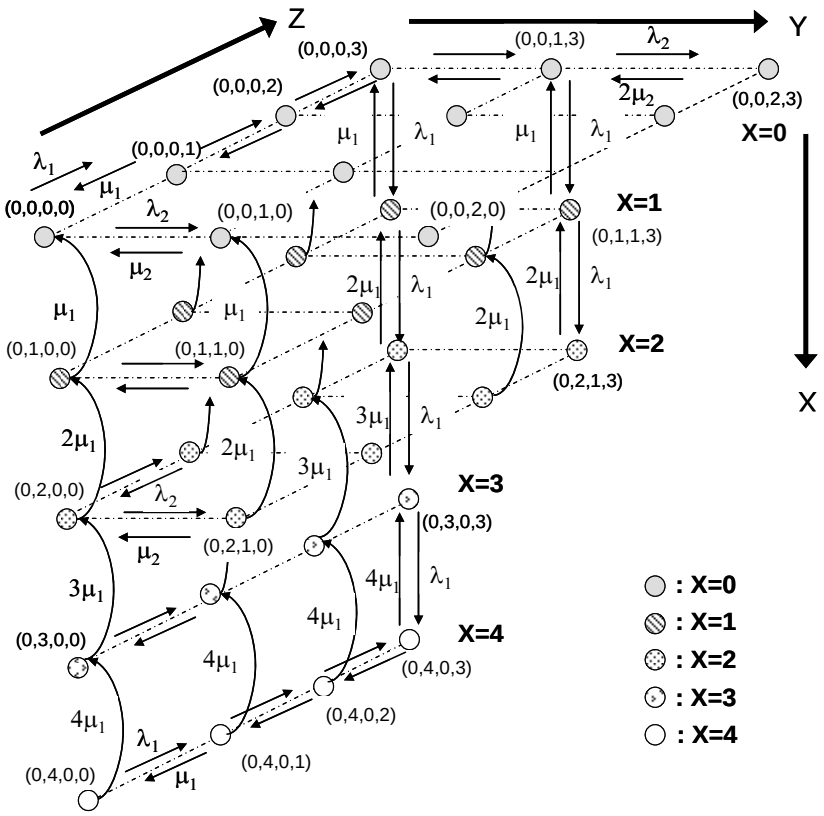

Fig. 4.1 Markov chain model for FCFS policy. $w=0,\ x_{\max}=4,\ y_{\max}=2,\ z_{\max}=3$.

At the arrival of a new Type 1 service request, if the system state is at $(0,x,y,z_{\max})$ and a handoff to R_B is possible i.e. $(x+1)U_A+yU_B\le N_B$, a vertical handoff is performed and the system transits to $(0,x+1,y,z_{\max})$. However, if there is a new Type 1 or Type 2 service request and the system is currently at $(0,0,y_{\max},z_{\max})$, the respective request will be blocked.

At each state transition, we assume only one service may be admitted or terminated and the state transitions are governed by the transition equations as follow:

- Increase in the number of Type 1 services being served by R_A, i.e. $(0,0,y,z)\to(0,0,y,z+1)$ with rate λ_1 for $0\le z\le z_{\max}-1$ and $0\le y\le y_{\max}$. (4.1)

- Increase in the number of Type 2 services being served by R_B, i.e. $(0,0,y,z) \rightarrow (0,0,y+1,z)$ with rate λ_2 for $0 \le y \le y_{\max} - 1$ and $0 \le z \le z_{\max}$. (4.2)

- Increase in the number of Type 1 vertical handoff services, i.e. $(0,x,y,z_{\max}) \rightarrow (0,x+1,y,z_{\max})$ with rate λ_1 for $z = z_{\max}$ and $(x+1)U_A + yU_B \le N_B$. (4.3)

- Increase in the number of Type 2 vertical handoff services, i.e. $(w,0,y_{\max},z) \rightarrow (w+1,0,y_{\max},z)$ with rate λ_2 for $y = y_{\max}$ and $(w+1)U_B + zU_A \le N_A$. (4.4)

- Increase in the number of Type 1 vertical handoff services, i.e. $(w,x,y,z) \rightarrow (w,x+1,y,z)$ with rate λ_1 for $(z+1)U_A + wU_B > N_A$ and $(x+1)U_A + yU_B \le N_B$. (4.5)

- Increase in the number of Type 2 vertical handoff services, i.e. $(w,x,y,z) \rightarrow (w+1,x,y,z)$ with rate λ_2 for $xU_A + (y+1)U_B > N_B$ and $(w+1)U_B + zU_A \le N_A$. (4.6)

- Increase in the number of Type 1 services being served by R_A, i.e. $(w,x,y,z) \rightarrow (w,x,y,z+1)$ with rate λ_1 for $(z+1)U_A + wU_B \le N_A$ and $xU_A + yU_B \le N_B$. (4.7)

- Increase in the number of Type 2 services being served by R_B i.e. $(w,x,y,z) \rightarrow (w,x,y+1,z)$ with rate λ_2 for $(y+1)U_B + xU_A \le N_B$ and $zU_A + wU_B \le N_A$. (4.8)

- Decrease in the number of Type 1 services being served by R_A, i.e. $(0,0,y,z) \rightarrow (0,0,y,z-1)$ with rate $z\mu_1$ for $1 \le z \le z_{\max}$ and $0 \le y \le y_{\max}$. (4.9)

- Decrease in the number of Type 2 services being served by R_B, i.e. $(0,0,y,z) \rightarrow (0,0,y-1,z)$ with rate $y\mu_2$ for $1 \le y \le y_{\max}$ and $0 \le z \le z_{\max}$. (4.10)

- Decrease in the number of Type 1 vertical handoff services i.e. $(0,x,y,z) \rightarrow (0,x-1,y,z)$ with rate $x\mu_1$ for $0 \le z \le z_{\max}$, $xU_A + yU_B \le N_B$ and $x \ge 1$. (4.11)

- Decrease in the number of Type 2 vertical handoff services i.e. $(w,0,y,z) \rightarrow (w-1,0,y,z)$ with rate $w\mu_2$ for $0 \le y \le y_{\max}$, $(w+1)U_B + zU_A \le N_A$ and $w \ge 1$. (4.12)

- Decrease in the number of Type 1 vertical handoff services i.e. $(w,x,y,z) \rightarrow (w,x-1,y,z)$ with rate $x\mu_1$ for $zU_A + wU_B \le N_A$, $xU_A + yU_B \le N_B$ and $x \ge 1$. (4.13)

- Decrease in the number of Type 2 vertical handoff services i.e. $(w,x,y,z) \rightarrow (w-1,x,y,z)$ with rate $w\mu_2$ for $xU_A + yU_B \le N_B$, $wU_B + zU_A \le N_A$ and $w \ge 1$. (4.14)

- Decrease in the number of Type 1 services being served by R_A i.e. $(w,x,y,z) \rightarrow (w,x,y,z-1)$ with rate $z\mu_1$ for $zU_A + wU_B \le N_A$, $xU_A + yU_B \le N_B$ and $z \ge 1$. (4.15)

- Decrease in the number of Type 2 services being served by R_B i.e. $(w,x,y,z)\rightarrow(w,x,y-1,z)$ with rate $y\mu_2$ for $yU_B+xU_A\le N_B$, $zU_A+wU_B\le N_A$ and $y\ge 1$. (4.16)

Finally, for the normalization of the state probabilities:

$$\sum_{h=0}^{w_{\max}}\sum_{i=0}^{x_{\max}}\sum_{j=0}^{y_{\max}}\sum_{k=0}^{z_{\max}}P(h,i,j,k)=1, \tag{4.17}$$

such that $jU_B+iU_A\le N_B$ and $kU_A+hU_B\le N_A$. Expressing the above transition equations in a matrix, we can easily solve for the steady-state probabilities.

A blocked Type 1 service occurs under the condition that the admission of the new service request causes the total traffic to exceed the capacity of R_A and R_B. The Type 1 blocked service probability is given as:

$$P_{block^1}=P\left\{\left[\left(wU_B+(z+1)U_A>N_A\right)\cap\left(yU_B+(x+1)U_A>N_B\right)\right]|\,\lambda_1\right\}. \tag{4.18}$$

Similarly, the Type 2 blocked service probability is given as:

$$P_{block^2}=P\left\{\left[\left(zU_A+(w+1)U_B>N_A\right)\cap\left(xU_A+(y+1)U_B>N_B\right)\right]|\,\lambda_2\right\}. \tag{4.19}$$

The admission of Type 1 vertical handoff service is possible under the condition that the new service request causes the total traffic to exceed the given capacity of R_A but not that of R_B. The Type 1 vertical handoff probability is given as:

$$P_{VHO^1}=P\left\{\left[\left(wU_B+(z+1)U_A>N_A\right)\cap\left(yU_B+(x+1)U_A\le N_B\right)\right]|\,\lambda_1\right\}. \tag{4.20}$$

Similarly, the Type 2 vertical handoff probability is given as:

$$P_{VHO^2}=P\left\{\left[\left(xU_A+(y+1)U_B>N_B\right)\cap\left(zU_A+(w+1)U_B\le N_A\right)\right]|\,\lambda_2\right\}. \tag{4.21}$$

In the FCFS scheme, the offered capacity for each service type under a given initial load is given by the maximum arrival rate such that the GoS requirements of *both* services are fulfilled concurrently. This may be expressed as

$$C_i = \min\left\{\lambda_i \middle| P_{block^1} < p_{b^1}, \lambda_i \middle| P_{block^2} < p_{b^2}\right\},\ i = 1,2\,. \tag{4.22}$$

The notation $\lambda_1 \middle| P_{block^1 < p_{b^1}}$ denotes the arrival rate of Type 1 service conditioned on the blocked Type 1 service probability being satisfied.

4.3 Simulation Setup

A simulation program using MATLAB was developed to validate the analytical results. We generated ten thousand service requests for each service type. Each service request follows a Poisson arrival process and has exponentially distributed service times. In the simulation program, separate counters are used to record the number of blocked requests and vertical handoffs for each service type. The appropriate counter is incremented when a service is blocked or when a service vertical handoff is performed. The blocked service and vertical handoff probabilities for that particular service type can therefore be obtained. Identical parameters for the traffic demands are used for the simulation as well as the mathematical analysis, and the simulated and analytical results are plotted together. The graphs show the correctness of both the analysis and the developed Markov chain model.

4.4 Results for FCFS Policy

We evaluate the service capacity for the multi-radio network under a FCFS SAC policy and compare it against the aggregated service capacity of the two radio systems when they operate independently. In the following, we let $N_A = 5$, $U_A = 1$, $N_B = 6$ and $U_B = 2$. We assume that a 3% blocked service probability for both services is the prescribed GoS guarantee. The mean service times for Type 1 and

Type 2 service are arbitrary set at $\mu_1 = 0.4$ and $\mu_2 = 0.5$, respectively. We fix the average arrival rate of Type 2 service requests at $\lambda_2 = 0.3575$ and vary the arrival rate of Type 1 service requests. Given these traffic parameters, this means that when the two radio systems operate independently, the blocked Type 2 service probability is 3% (i.e. R_B is at its maximum capacity); and the maximum Type 1 service arrival rate is $\lambda_1 = 0.752$. Figures 4.2 and 4.3 show the blocked service probabilities for Type 1 and Type 2 services for the multi-radio network, respectively. Figure 4.4 shows the vertical handoff probability of Type 1 service.

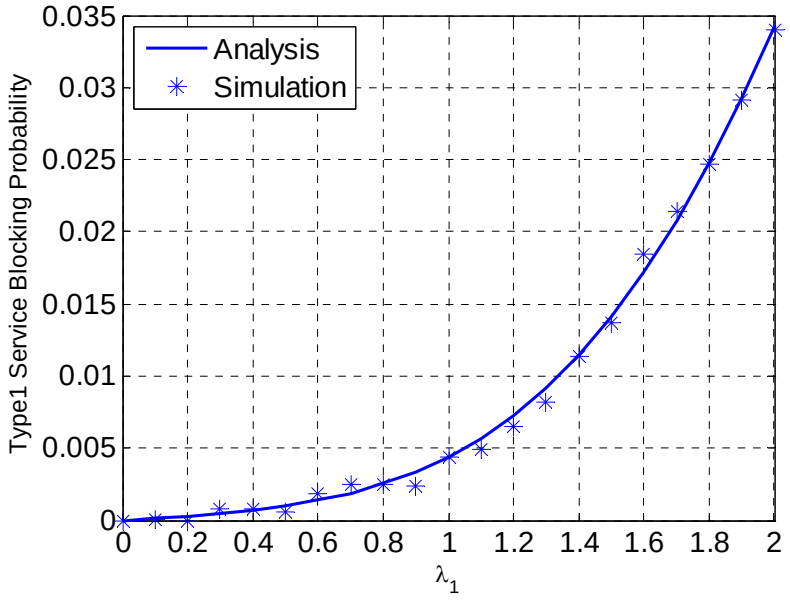

Fig. 4.2 Blocked Type 1 service probability for multi-radio network.

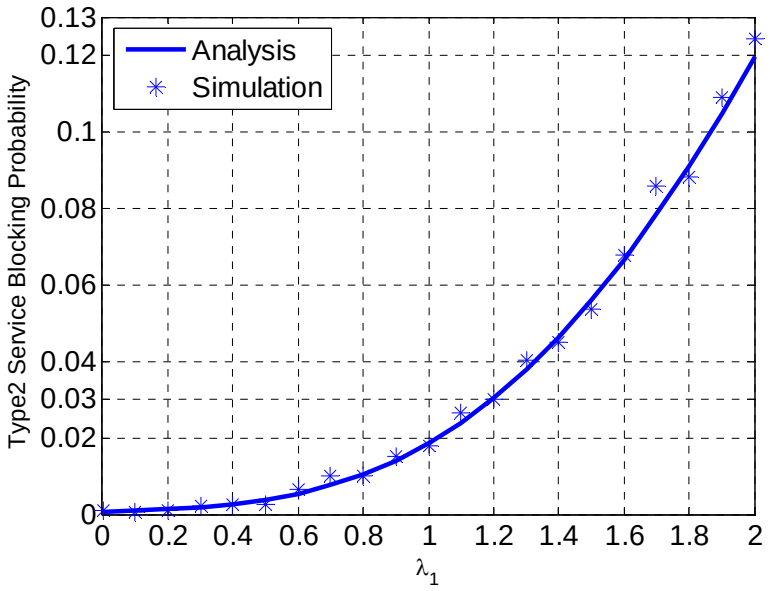

Fig. 4.3 Blocked Type 2 service probability for multi-radio network.

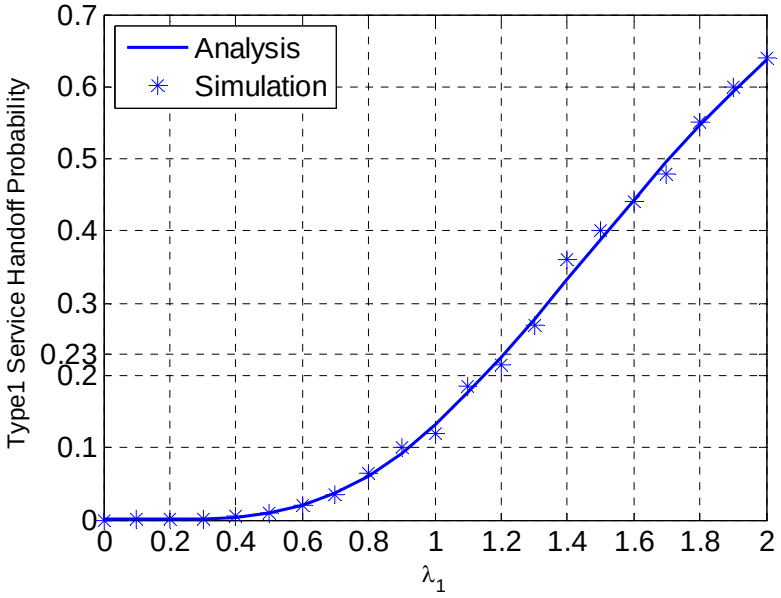

Fig. 4.4 Type 1 service vertical handoff probability.

From Fig. 4.2 and Fig. 4.3, the maximum Type 1 service arrival rate is about $\lambda_1 = 1.2$ for the multi-radio network. The increase in service capacity is about 60% (from 0.752 to 1.2) compared to when R_A and R_B operate independently. However, from Fig. 4.4, the enhancement in service capacity is at the expense of about 23%

vertical handoff probability. The Type 2 vertical handoff probability is trivial as the traffic demands for the service is held constant in this evaluation and already fulfills the prescribed GoS.

From the results, we showed that the multi-radio network can support significantly more traffic compared to when the systems operate separately. However, it is observed from Fig. 4.2 and Fig. 4.3 that the maximum allowed arrival rate of Type 1 service is constrained by the blocked service guarantee of Type 2 service. This is because at $\lambda_1 = 1.2$, the blocked Type 2 service probability is already at its prescribed GoS limit. Hence, the current service capacity can still be enhanced. This is because at this operation point, R_A is still below its prescribed GoS guarantee and hence there are still resources available to support more traffic. The significant difference in the blocked service probability for Type 1 and Type 2 services can be exploited to further increase the offered traffic through the implementation of appropriate SAC policies.

4.5 Analysis and Results for RES Policy

For this policy, we allow R_B (which is limiting the overall multi-radio network service capacity) to always reserve an integer multiple r units of resources for its exclusive use. The amount of resources shared by R_B is thus reduced to $(N_B - rU_A)$. For this scheme, $x_{\max} = (N_B - rU_A)/U_A$. Figure 4.5 shows an example of the Markov chain model for the RES policy with $N_A = 3$, $U_A = 1$, $N_B = 4$ and $U_B = 2$ at $w = 0$ with $r = 2$. In this case, R_B only admits two Type 1 vertical handoff services.

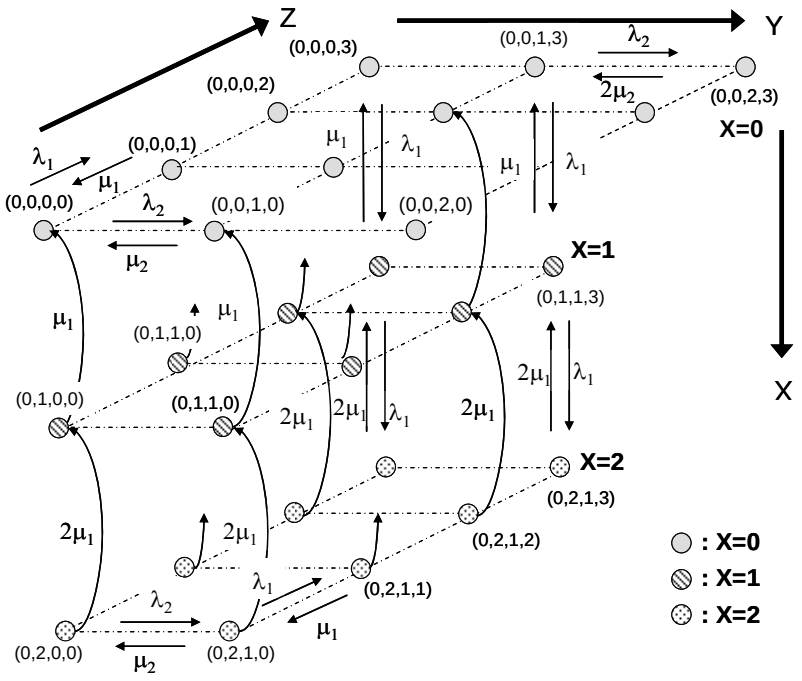

Fig. 4.5 Markov chain model for RES policy. $w = 0$ and $r = 2$.

The transition equations for the RES policy can be obtained from that presented in Section 4.2 with the following modifications:

Eq. (4.3) is replaced by:

- Increase in the number of Type 1 vertical handoff services, i.e. $(0, x, y, z_{\max}) \rightarrow (0, x+1, y, z_{\max})$ with rate λ_1 for $z = z_{\max}$ and $(x+1)U_A + yU_B \le N_B$ and $(x+1) \le (N_B - rU_A)/U_A$. (4.23)

Eq. (4.5) is replaced by:

- Increase in the number of Type 1 vertical handoff services, i.e. $(w, x, y, z) \rightarrow (w, x+1, y, z)$ with rate λ_1 for $(z+1)U_A + wU_B > N_A$, $(x+1)U_A + yU_B \le N_B$ and $(x+1) \le (N_B - rU_A)/U_A$. (4.24)

Eq. (4.6) is replaced by:

- Increase in the number of Type 1 services being served by R_A, i.e. $(w,x,y,z) \rightarrow (w,x,y,z+1)$ with rate λ_1 for $(z+1)U_A + wU_B \le N_A$, $xU_A + yU_B \le N_B$ and $(x+1) \le (N_B - rU_A)/U_A$. (4.25)

Eq. (4.11) is replaced by:

- Decrease in the number of Type 1 vertical handoff services i.e. $(0,x,y,z) \rightarrow (0,x-1,y,z)$ with rate $x\mu_1$ for $0 \le z \le z_{\max}$, $xU_A + yU_B \le N_B$ and $1 \le x \le (N_B - rU_A)/U_A$. (4.26)

Eq. (4.13) is replaced by:

- Decrease in the number of Type 1 vertical handoff services i.e. $(w,x,y,z) \rightarrow (w,x-1,y,z)$ with rate $x\mu_1$ for $zU_A + wU_B \le N_A$, $xU_A + yU_B \le N_B$ and $1 \le x \le (N_B - rU_A)/U_A$. (4.27)

Eq. (4.14) is replaced by:

- Decrease in the number of Type 2 vertical handoff services i.e. $(w,x,y,z) \rightarrow (w-1,x,y,z)$ with rate $w\mu_2$ for $xU_A + yU_B \le N_B$, $wU_B + zU_A \le N_A$, $w \ge 1$ and $x \le (N_B - rU_A)/U_A$. (4.28)

Eq. (4.15) is replaced by:

- Decrease in the number of Type 1 services being served by R_A i.e. $(w,x,y,z) \rightarrow (w,x,y,z-1)$ with rate $z\mu_1$ for $zU_A + wU_B \le N_A$, $xU_A + yU_B \le N_B$, $z \ge 1$ and $x \le (N_B - rU_A)/U_A$. (4.29)

Eq. (4.16) is replaced by:

- Decrease in the number of Type 2 services being served by R_B i.e. $(w,x,y,z) \rightarrow (w,x,y-1,z)$ with rate $y\mu_2$ for $yU_B + xU_A \le N_B$, $zU_A + wU_B \le N_A$, $y \ge 1$ and $x \le (N_B - rU_A)/U_A$. (4.30)

The blocked Type 1service probability is now given as:

$$P_{block^1} = P\left\{\left[\left(wU_B + (z+1)U_A > N_A\right) \cap \left(yU_B + (x+1)U_A > N_B\right)\right] \cup \left[\left(wU_B + (z+1)U_A > N_A\right) \cap \left((x+1) > (N_B - rU_B)/U_A\right)\right] \mid \lambda_1\right\}. \quad (4.31)$$

The blocked Type 2 service probability remains unchanged from Eq. 4.19. Type 1 service vertical handoff probability is given as:

$$P_{VHO^1} = P\left\{\left[\left(wU_B + (z+1)U_A > N_A\right) \cap \left(yU_B + (x+1)U_A \le N_B\right)\right] \mid \lambda_1, (x+1) \le x_{\max}\right\}. \quad (4.32)$$

The Type 2 service vertical handoff probability remains unchanged from Eq. 4.21.

The objective function of the RES policy is to determine the optimum value of *r* such that the total service capacity of the network is maximized given the GoS requirements of the respective radio systems. Mathematically, it is expressed as:

$$C_i = \max\left\{\left[\lambda_i^{(r)} \middle| P_{block^1} < p_{b^1}, \lambda_i^{(r)} \middle| P_{block^2} < p_{b^2}\right]_{r=0,1,\ldots N_B/U_B}\right\}, \quad (4.33)$$

where $i = 1,2$, and notation $\lambda_i^{(r)} \middle| P_{block^1} < p_{b^1}$ denotes the arrival rate of Type 1 service conditioned on the blocked Type 1service probability being satisfied given *r* amount of reserved resources.

For the results below, we keep constant the traffic demands of Type 2 service and investigate the blocked service probabilities corresponding to the optimum value of *r*. Similarly, we let $N_A = 5$, $U_A = 1$, $N_B = 6$ and $U_B = 2$. For comparison, the values of the traffic parameters used in Section 4.4 are also used in this evaluation.

The provisioned GoS is kept at 3% blocked service probability for both services. Figure 4.6 shows the blocked service probabilities for $r = 4$, and Figure 4.7 shows the vertical handoff probabilities. We plot the amount of supported Type 1 service traffic for different values of *r* in Figure 4.8.

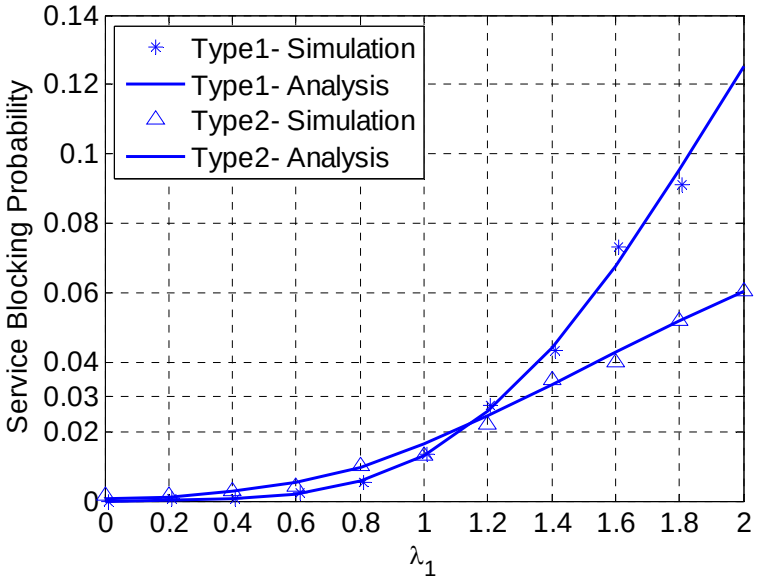

Fig. 4.6 Blocked service probabilities, $r = 4$.

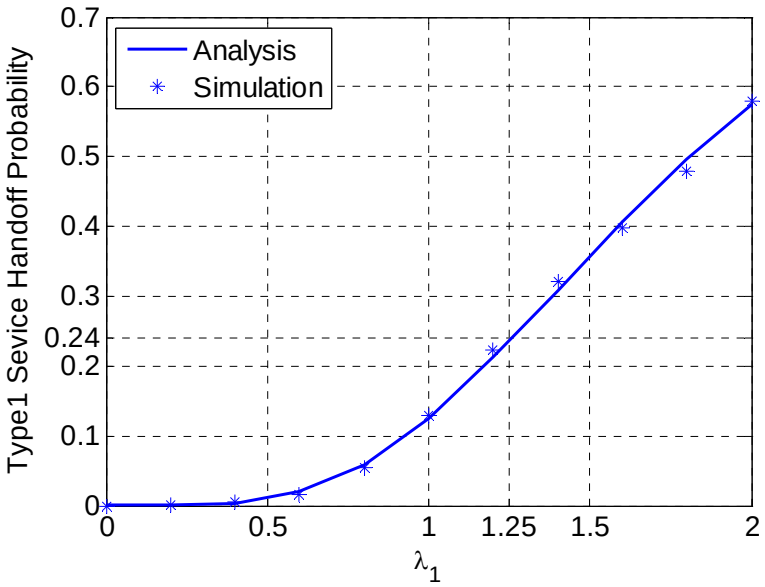

Fig. 4.7 Type 1 service vertical handoff probability.

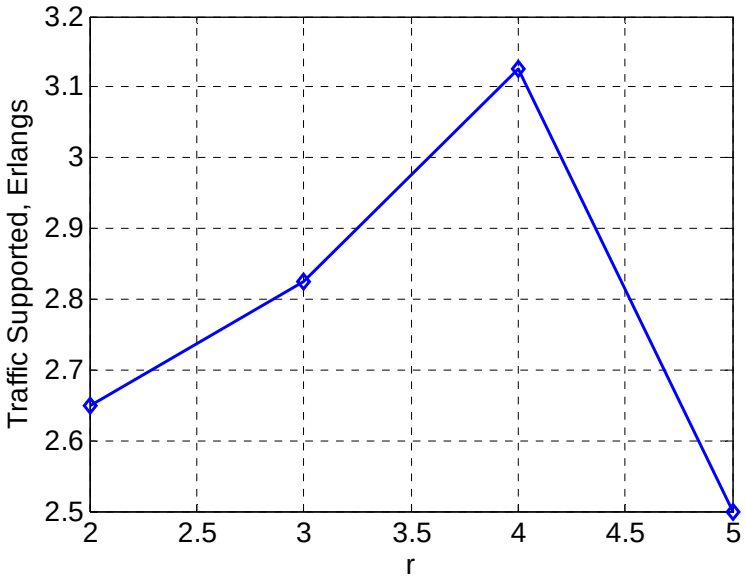

Fig. 4.8 Supported Type 1 service traffic for different values of *r*.

From Figs 4.6 and 4.7, the amount of supported Type 1 service traffic has increased by about 5% ($\lambda_1 = 1.26$), at the expense of about 1% increase in vertical handoff probability compared to the FCFS admission policy. From Fig. 4.8, maximum supported traffic for the multi-radio network is achieved when $r = 4$. This means that maximum amount of Type 1 service traffic is supported (for the given traffic parameters) by reserving about 67% of R_Bs' spectrum for exclusive access by Type 1 services. When $r = 5$, the amount of spectrum is over reserved and results in lower supported traffic.

4.6 Analysis and Results for RD Policy

In this policy, R_B regulates the admission of Type 1 vertical handoff services through an admission probability, ρ. The state transition equations are similar to the FCFS scheme except for the following modifications:

Eq. (4.3) is replaced by:

- Increase in the number of Type 1 vertical handoff services, i.e. $(0, x, y, z_{\max}) \rightarrow (0, x+1, y, z_{\max})$ with rate $\rho\lambda_1$ for $z = z_{\max}$ and $(x+1)U_A + yU_B \le N_B$. (4.34)

Eq. (4.5) is replaced by:

- Increase in the number of Type 1 vertical handoff services, i.e. $(w, x, y, z) \rightarrow (w, x+1, y, z)$ with rate $\rho\lambda_1$ for $(z+1)U_A + wU_B > N_A$ and $(x+1)U_A + yU_B \le N_B$. (4.35)

Figure 4.9 shows an example of the Markov chain model for the RD policy with $N_A = 3$, $U_A = 1$, $N_B = 4$ and $U_B = 2$ for $w = 0$.

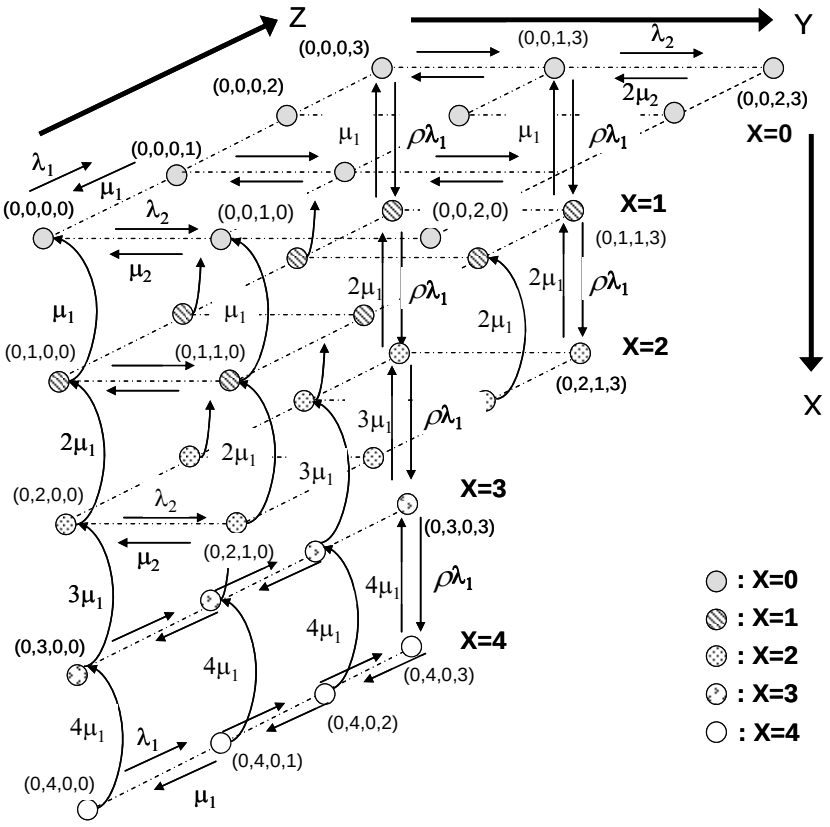

Fig. 4.9 Markov chain model for RD policy, $w = 0$.

The Type 1 blocked service probability is now given as:

$$P_{block^1} = P\left\{\left[\left(wU_B + (z+1)U_A > N_A\right) \cap \left(yU_B + (x+1)U_A > N_B\right)\right] | \lambda_1\right\} + (1-\rho)P\left\{\left[\left(wU_B + (z+1)U_A > N_A\right) \cap \left(yU_B + (x+1)U_A < N_B\right)\right] | \lambda_1\right\}. \quad (4.36)$$

However, the Type 2 blocked service probability is unchanged from (4.19). Type 1 vertical handoff probability is now given as:

$$P_{VHO^1} = P\left\{\left[\left(wU_B + (z+1)U_A > N_A\right) \cap \left(yU_B + (x+1)U_A \le N_B\right)\right] | \rho\lambda_1\right\}. \quad (4.37)$$

The Type 2 vertical handoff probability is given as (4.21).

The objective function of the RD policy is to determine the optimum value of ρ such that the GoS performance is maximized:

$$C_i = \max\left\{\left[\lambda_i^{(\rho)} \middle| P_{block^1} < p_{b^1}, \lambda_i^{(\rho)} \middle| P_{block^2} < p_{b^2}\right] \middle| \rho \in [0,1]\right\}, \quad (4.38)$$

where $i = 1,2$, and notation $\lambda_i^{(\rho)} \middle| P_{block^1} < p_{b^1}$ denotes the arrival rate of Type 1 service conditioned on the blocked Type 1 service probability being satisfied when given a value of ρ.

For comparison, the values of the parameters used in the following evaluation are kept the same as those in Section 4.4. Figure 4.10 shows the blocked service probabilities and Figure 4.11 shows the Type 1 service vertical handoff probability for the RD SAC policy.

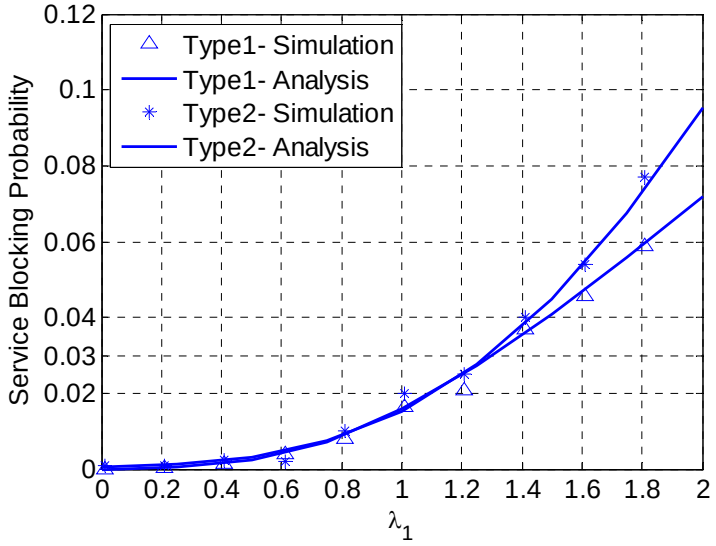

Fig. 4.10 Blocked service probabilities for RD scheme, $\rho = 0.825$.

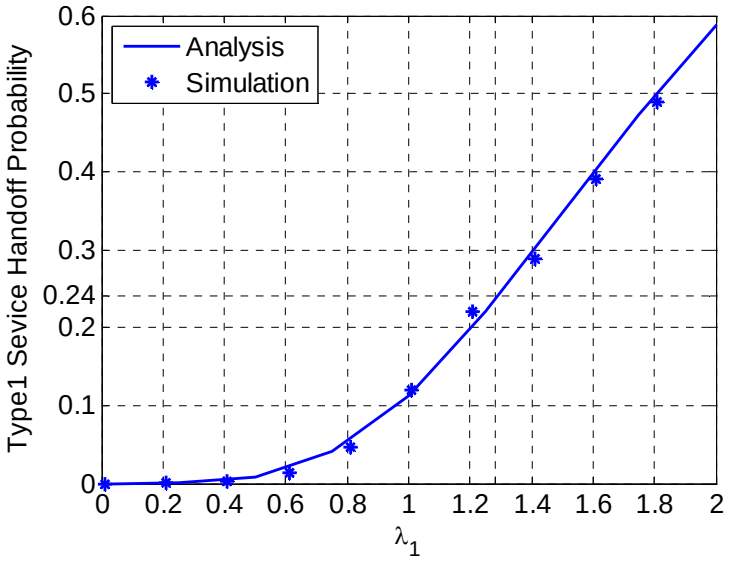

Fig. 4.11 Type 1 service vertical handoff probability.

From Fig. 4.10, it is observed that the RD policy achieves slightly higher service capacity than the RES policy, i.e. the Type 1 service arrival rate is $\lambda_1 = 1.28$ compared to $\lambda_1 = 1.26$ for the RES policy. In addition, the RD scheme is able to balance the traffic load of the two services so that the multi-radio network can operate at its maximum service capacity. This is shown by the convergence of the blocked service probabilities for the two services to their respective GoS guarantee at the

optimum value of ρ in Fig. 4.10. In the case of the RES policy, a slight difference between the respective blocked service probabilities still exist even at the optimum value of *r*. We summarize the results for Sections 4.4, 4.5 and 4.6 in Table 4.1 below.

TABLE 4.1 SUMMARY OF RESULTS FOR THREE ADMISSION POLICIES

Separate	**FCFS Policy**		**RES Policy**		**RD Policy**	
Max. λ_1	Max. λ_1	Vertical Handoff Probability	Max. λ_1	Vertical Handoff Probability	Max. λ_1	Vertical Handoff Probability
0.752	1.2	0.23	1.26	0.24	1.28	0.24

4.7 Performance Comparison and Further Results

In this section, the performances of the three SAC policies are compared further. The average service time of Type 1 and Type 2 services are $\mu_1 = 0.4$ and $\mu_2 = 0.5$, respectively. In the following evaluation, we let $N_A = 6$, $U_A = 1$, $N_B = 6,\ 8,\ 10,\ 12,\ 14$ and 16, and $U_B = 2$. The Type 2 service arrival rate is selected such that when the radio systems operate independently, R_B is at maximum service capacity for all values of N_B (i.e. blocked Type 2 service probability is 3%). The network service capacity is then maximized.

The average spectrum utilization at maximum network service capacity is shown in Figure 4.12. From the figure, the RD and RES policies result in higher average spectrum utilization compared to the FCFS policy.

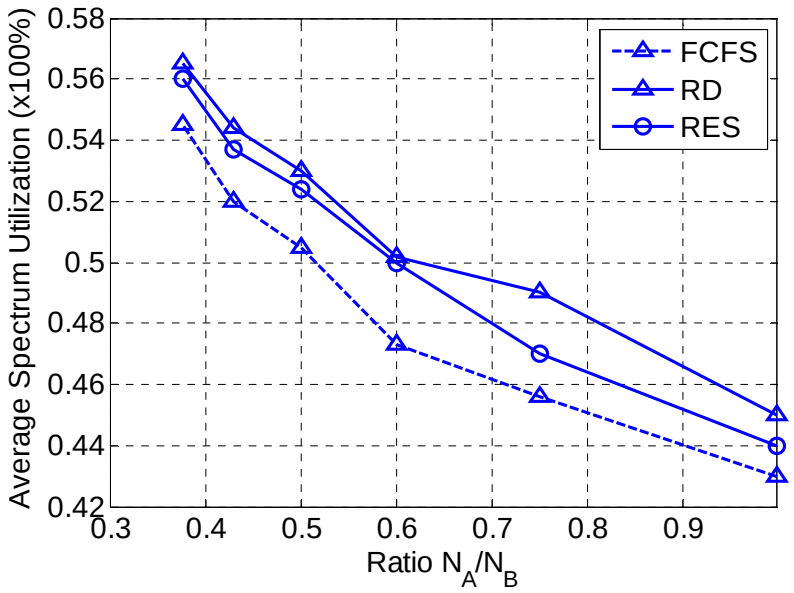

Fig. 4.12 Average spectrum utilization.

In Figure 4.13, the Type 1 service vertical handoff probability given by the three SAC policies are compared. The amount supported traffic in this evaluation is maintained the same and is equal to the maximum capacity given by the FCFS policy. From the figure, it is observed that both the RD and RES policies result in lower vertical handoff probability compared to the FCFS policy. The difference is about 5% between the RD and FCFS policies.

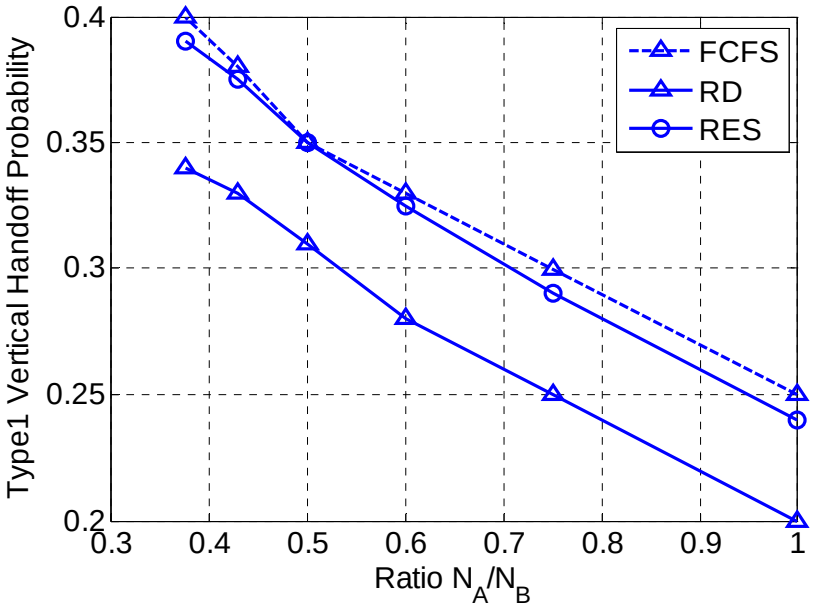

Fig. 4.13 Type 1 service vertical handoff probability.

4.8 Conclusion

In this chapter, with the aid of a novel four dimensional Markov chain model, we have developed an analytical platform for analyzing the blocked service and vertical handoff probabilities concurrently for the multi-radio network. From the results of a simple FCFS SAC policy, very significant increase in network service capacity is observed compared to the aggregated service capacity when the radio systems operate independently. The tradeoff for the increase in service capacity is the performance of vertical handoffs. However, it is observed that the service capacity can still be further enhanced. We then compare and analyze the performance and tradeoffs of a RES and a RD SAC policy. Both these policies result in higher average spectrum utilization compared to the FCFS policy, as the introduction of extra design parameters provides flexibility to meet the provisioned GoS guarantee of the respective radio systems concurrently.

Chapter 5

Complete Spectrum Sharing Multi-radio Network

In this chapter, we focus on complete spectrum sharing under the coordinated access policy. In contrast to the scenario analyzed in Chapter 4, the traffic demands from the radio systems are now aggregated at a centralized spectrum manager which coordinates their spectrum access as well as allocate spectrum resources in accordance to their traffic demands. The scenario in which a spectrum licensee performs short duration lease of spectrum to several operators could be a possible operation model under this framework.

Some similar works in the literature on coordinated dynamic spectrum sharing can be found in [24, 90, 110 - 115]. In this work, we consider two possible operation models adopted by the spectrum manager. For the first case, the objective of the spectrum manager is to maximize the supported traffic of the network so as to share the limited resources efficiently among the radio systems and still fulfill their respective GoS guarantee. For the second case, we assume the offered services incur different charges in accordance to the adopted transmission modulation scheme. In this case, their service pricing are incorporated in the objective function of the problem in which the objective of the spectrum manager is to maximize the average collectable revenue, subjected to the GoS constraints of the individual radio systems.

In Section 5.1, we present the system model. Introduction to the first operation model and the SAC policies are described in detail in Section 5.2. The RD policy is formulated in Section 5.3, and the RES policy is formulated in Section 5.4. The formulation of the CMDP based policy is presented in Section 5.5. The results and discussions on the performance of each policy are presented in Section 5.6. In Section

5.7, we present the second operation model and study the achievable gain in revenue. This chapter is concluded in Section 5.8.

5.1 System Model and Assumptions

The general functionality of the system model is already described in Section 1.3 and is illustrated in Fig. 1.7. It is assumed that a spectrum band is dynamically leased to two radio systems denoted by R_A and R_B which adopt the same RAT. We assume that each of the radio systems supports one service, and are denoted by S_A and S_B, respectively. Bandwidth is measured in terms of basic bandwidth units (bbu) and the shared spectrum band has a total capacity of *C* bbu. The bandwidth required for a S_A is denoted by b_A and that for S_B is denoted by b_B. As the services have unequal bandwidth demands, usage of the spectrum band may become fragmented. This can be easily overcome if the spectrum is managed using the OFDMA approach.

The arrivals of spectrum requests for S_A and S_B are assumed to obey the Poisson distribution with mean arrival rates denoted by λ_A and λ_B, respectively. The service time of S_A and S_B are described by a negative exponential distribution with mean $1/\mu_A$ and $1/\mu_B$, respectively. Although such a traffic model may not fully describe the traffic demands for all the radio systems, we assume that such a model is sufficient as an initial study since it is analytically manageable.

The prescribed GoS guarantee for S_A and S_B is respectively denoted by g_A and g_B, which represent the maximum acceptable blocked service probability. Without loss in generality, we arbitrarily set $g_B > g_A$. The average spectrum utilization, υ, can be expressed as

$$\mathcal{U} = \left[(1 - g_{\mathrm{A}}) b_{\mathrm{A}} T_{\mathrm{A}} + (1 - g_{\mathrm{B}}) b_{\mathrm{B}} T_{\mathrm{B}} \right] / C \,. \tag{5.1}$$

where $T_{\mathrm{A}} = \lambda_{\mathrm{A}} / \mu_{\mathrm{A}}$ and $T_{\mathrm{B}} = \lambda_{\mathrm{B}} / \mu_{\mathrm{B}}$ are respectively the traffic intensities for $\mathrm{R_A}$ and $\mathrm{R_B}$. The inclusion of $(1 - g_{\mathrm{A}})$ and $(1 - g_{\mathrm{B}})$ is to account for the requests which are blocked (within the GoS specification). The specifics of the system model and its functionalities are illustrated in Figure 5.1.

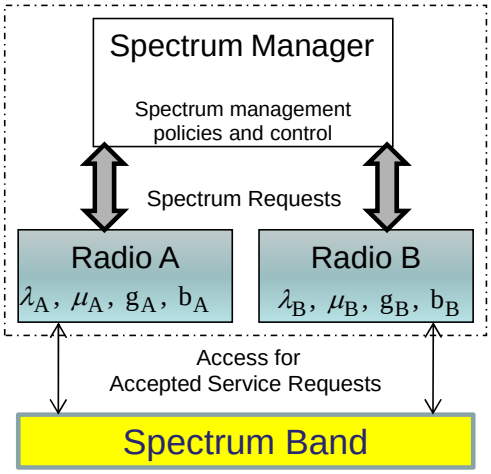

Fig. 5.1 Model of the complete spectrum sharing multi-radio network.

5.2 Spectrum Admission Control Policies

In the following, we describe the design of three SAC policies with the objective to maximize the traffic offered subjected to the respective radio systems' prescribed GoS guarantee. For some operating parameters, it is assumed that $\mathrm{R_A}$ is the performance limiting radio system. This means that $\mathrm{R_A}$ will exceed its GoS requirement before $\mathrm{R_B}$. Hence in the design of the SAC policies, we aim to obtain an operation point such that the blocked service probabilities for both $\mathrm{R_A}$ and $\mathrm{R_B}$ are as close to their prescribed guarantee as possible.

In the random discard (RD) policy, the spectrum manager admits a new $\mathrm{S_B}$

request with a probability which decreases with increasing number of S_B users $(= j)$ currently being served, even if resources are available at the instant of its request. This probability is described by the function $f(j)$, and is denoted as f_j. The purpose of doing so is to regulate the number of admitted S_B users, so that more resources can be allocated to serve S_A spectrum requests. The optimal operation point for different traffic conditions can then be controlled through $f(j)$.

In the reservation (RES) policy, the spectrum manager reserves a portion of the total resources (denoted by rb_B bbu) for exclusive distribution to S_A requests only. Thus S_B spectrum requests are limited to $(C - rb_B)$ resources only. In this case, the optimal operation point for the system can be controlled though varying r.

For the third policy, we model the SAC as a discrete time Markov decision process (MDP). In this case, the spectrum manager performs SAC periodically at the beginning of an admission control period (ACP). The interval between each ACP (decision epoch) is denoted as τ_{ACP}. Spectrum requests from each radio system are collected over the duration of an ACP and are queued in separate queues. The spectrum manager maintains a record of all the spectrum request arrivals, the number of active transmissions, the allocated and available bandwidth and ensures the prescribed GoS guarantee of each radio system is fulfilled.

Just before the start of the next ACP, the spectrum manager estimates the available bandwidth. At each decision epoch, it determines the number of requests that can be admitted given the available bandwidth, the admission policy and the GoS constraints of the respective radio systems. Requests from the same queue are served in order. However, requests from one queue may get rejected if the SAC is in favor of requests from another queue. Admitted requests are served at the beginning of each ACP, while all rejections are dropped and new requests are queued again until the

next ACP. The services leave the network once they have been served and the spectrum manager updates the network status accordingly.

5.3 Markov Chain Model for RD Policy

Figure 5.2 shows the Markov chain model of the RD policy. The states in the model are denoted as (i, j), where i and j represent the number of S_A users and S_B users currently being served, respectively. The transition rate from the current state to the next state when a S_B request is received and admitted is given by $f_j\lambda_B$, where $f_j\lambda_B < \lambda_B$. It indicates that the request will be blocked intentionally with probability $1-f_j$. However, the RD policy is not imposed on the R_A which is the performance limiting radio.

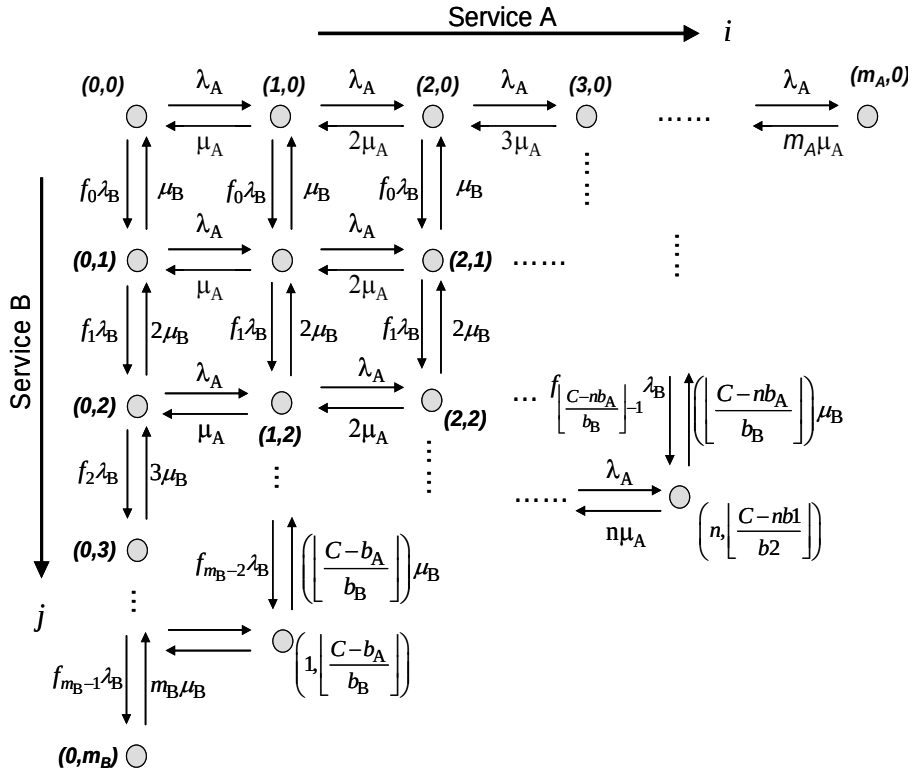

Fig. 5.2 Markov chain representation for RD policy.

Let $m_{\mathrm{A}} = \lfloor C / b_{\mathrm{A}} \rfloor$ represent the maximum number of S_A requests that can be served concurrently using all C bbu. The notation $\lfloor \theta \rfloor$ denotes the largest integer value less than or equals to θ. Similarly, let $m_{\mathrm{B}} = \lfloor C / b_{\mathrm{B}} \rfloor$ represent the maximum number of S_B requests that can be served concurrently using all the C bbu. It can be shown that the steady-state probability of a general state (i, j) may be expressed as:

$$P(i, j) = P(0,0)\left[{T_{\mathrm{A}}}^{i} {T_{\mathrm{B}}}^{j} \frac{1}{j!i!} \prod_{q=1}^{j} f_{q-1} \right], \; ib_{\mathrm{A}} + jb_{\mathrm{B}} \le C, \tag{5.2}$$

where $P(0,0)$ denote the steady state probability of $(0,0)$ and

$$P(0,0) = \left[\sum_{i=0}^{m_{\mathrm{A}}} \frac{{T_{\mathrm{A}}}^{i}}{i!} \sum_{j=0}^{\varphi_{\mathrm{B}}} \frac{{T_{\mathrm{B}}}^{j}}{j!} \prod_{q=1}^{j} f_{q-1} \right]^{-1}. \tag{5.3}$$

Further, let $\varphi_{\mathrm{A}} = \lfloor (C - jb_{\mathrm{B}}) / b_{\mathrm{A}} \rfloor$ and $\varphi_{\mathrm{B}} = \lfloor (C - ib_{\mathrm{A}}) / b_{\mathrm{B}} \rfloor$. The blocking probability for S_A is then given as:

$$P_{block,\mathrm{A}} = P(0,0)\left[\sum_{j=0}^{m_{\mathrm{B}}} \frac{{T_{\mathrm{B}}}^{j}}{j!} \frac{{T_{\mathrm{A}}}^{\varphi_{\mathrm{A}}}}{\varphi_{\mathrm{A}}!} \prod_{q=1}^{j} f_{q-1} \right]. \tag{5.4}$$

The blocking probability for S_B is expressed as:

$$\begin{aligned} P_{block,\mathrm{B}} = P(0,0)\Bigg[& \sum_{i=0}^{m_{\mathrm{A}}} \frac{{T_{\mathrm{A}}}^{i}}{i!} \frac{{T_{B}}^{\varphi_{\mathrm{B}}}}{\varphi_{\mathrm{B}}!} \prod_{q=1}^{\varphi_{\mathrm{B}}} f_{q-1} + \\ & \sum_{j=0}^{m_{\mathrm{B}}-1} \left(1 - f_j\right) \frac{{T_{\mathrm{B}}}^{j}}{j!} \prod_{q=1}^{j} f_{q-1} \sum_{i=0}^{\lfloor (C-(j+1)b_{\mathrm{B}})/b_{\mathrm{A}} \rfloor} \frac{{T_{\mathrm{A}}}^{i}}{i!} \Bigg]. \end{aligned} \tag{5.5}$$

The second term in (5.5) takes into consideration the intentional blocking of S_B spectrum requests introduced by the SAC function $f(j)$. The objective function for the RD policy can be expressed as:

$$\max_{T_{\mathrm{A}}, T_{\mathrm{B}}, f(j)} \Gamma \Big|_{P_{block,\mathrm{A}} < g_{\mathrm{A}}, P_{block,\mathrm{B}} < g_{\mathrm{B}}}, \tag{5.6}$$

where $\Gamma = T_A + T_B$ and $\big|(\bullet)$ means subjected to the condition given by $(\bullet)$.

5.4 RES Policy

Next we analyze the case for $f(j) = 1 - U(j - r)$, where

$$U(j-r) = \begin{cases} 1 & j \geq r \\ 0 & j < r \end{cases}. \tag{5.7}$$

This function represents a RES policy where the spectrum manager reserves rb_B bbu for allocation to S_A requests only. Hence the maximum amount of resources which can be assigned to R_B is limited to $(C - rb_B)$, and for this case, $m_B = \lfloor (C - rb_B)/b_B \rfloor$. The Markov chain representation for the RES policy can be easily obtained with some modifications to Fig. 5.2. The steady-state probability of a general state (i, j) can be expressed as:

$$P(i,j) = P(0,0)\left[{T_A}^i {T_B}^j \frac{1}{j!i!} \right], \; ib_A + jb_B \leq C, \tag{5.8}$$

where

$$P(0,0) = \left[\sum_{j=0}^{m_B} \frac{{T_B}^j}{j!} \sum_{i=0}^{\varphi_A} \frac{{T_A}^i}{i!} \right]^{-1}. \tag{5.9}$$

For this policy, the blocking probability for S_A is given as:

$$P_{block,A} = P(0,0)\left[\sum_{i=r}^{m_A} \frac{{T_A}^i}{i!} \frac{{T_B}^{\varphi_B}}{\varphi_B!} \right]. \tag{5.10}$$

The blocking probability for S_B is given as:

$$P_{block,B} = P(0,0)\left[\sum_{i=0}^{r-1} \frac{{T_A}^i}{i!} \frac{{T_B}^{(m_B - r)}}{(m_B - r)!} + \sum_{i=r}^{m_A} \frac{{T_A}^i}{i!} \frac{{T_B}^{\varphi_B}}{\varphi_B!} \right]. \tag{5.11}$$

The objective function for this policy is thus expressed as:

$$\max_{T_A,\, T_B,\, r} \Gamma \Big|_{P_{block,A} < g_A, P_{block,B} < g_B} . \tag{5.12}$$

Note that r is a positive integer.

5.5 Markov Decision SAC Policy

We next formulate the SAC as a discrete time constrained Markov decision process (CMDP). The CMDP can be described by the 4-tuple $(\mathcal{S}, \mathcal{A}, \mathcal{P}, \mathcal{R})$. $\mathcal{S}$ and $\mathcal{A}$ respectively denotes the set of possible states and actions. For each state $\underline{x} \in \mathcal{S}$, there is a corresponding non-empty subset of $\mathcal{A}$ whose elements are the feasible actions when the system is in state $\underline{x}$. $\mathcal{P}$ is the transition probability matrix, and $P_{\underline{x}\underline{y}}(\underline{a})$ denotes the transition probability from state $\underline{x}$ to state $\underline{y}$ when taking action $\underline{a}$ where $\underline{a} \in \mathcal{A}$. Each action is associated with a reward, and $\mathcal{R}$ denotes the expected reward matrix for the action taken at each valid state.

1) State space, $\mathcal{S}$

The vector $\underline{s}^t = \left(s_A^t, s_B^t\right)$ denotes the number of S_A and S_B users being served at time t, respectively. Let $\underline{e}^t = \left(e_A^t, e_B^t\right)$ respectively denote the number of new S_A and S_B requests at the beginning of the t^{th} ACP. The *state space* is specified by $\mathcal{S}$,

$$\mathcal{S} = \left\{ (\underline{s}, \underline{e}) \,\middle|\, 0 \le s_A b_A + s_B b_B \le C \right\}. \tag{5.13}$$

Note that a state $\underline{x}$ of the system is defined by the vector $(\underline{s}, \underline{e})$. To simplify the analysis, the maximum number of new request arrivals within an ACP is assumed to be finite. Let $\underline{d}^t = \left(d_A^t, d_B^t\right)$ respectively denote the number of completely served S_A and S_B users during the t^{th} ACP.

2) Action space, $\mathcal{A}$

The action taken at the t^{th} ACP is defined by the vector $\underline{a}^t = \left(a_{\text{A}}^t, a_{\text{B}}^t\right)$, where it respectively represents the number of S_A and S_B requests to be admitted. The policy, $\underline{\pi}$, is a vector whose elements denote the selected action for each state. As the number of new requests is assumed to be finite, hence the possible actions for any state are also finite. Note that the number of admissions cannot exceed the number of new spectrum requests for the service in the queue, i.e. $0 \le a_{\text{A}}^t \le e_{\text{A}}^t$ and $0 \le a_{\text{B}}^t \le e_{\text{B}}^t$ for all *t.*

3) State transitions and transition probability matrix, $\mathcal{P}$

The number of users being served evolves at discrete time intervals given by $\mathcal{T}_{\text{ACP}}$ according to the following equation:

$$\underline{s}^{t+1} = \underline{s}^t + \underline{a}^t - \underline{d}^t , \tag{5.14}$$

where $s_{\text{A}}^{t+1}, s_{\text{B}}^{t+1} \ge 0$. From (6.14), it can be deduced that numerous requests may be admitted or completely served in $\mathcal{T}_{\text{ACP}}$. Hence in this case, the SAC is modeled as a batch admission and departure process.

Assuming that the radios are independent and new requests arrive independently of the ACP and the action taken in the previous ACP, the state transition probabilities can be evaluated as follows. If the system at the t^{th} decision epoch (ACP) is at state $\underline{x} = \left(\underline{k}, \underline{u}\right)$ and action $\underline{a}$ is taken, then the system will transit to state $\underline{y} = \left(\underline{l}, \underline{v}\right)$ at the $(t+1)^{\text{th}}$ decision epoch with probability $P_{\underline{x}\underline{y}}\left(\underline{a}\right)$ given by:

$$
\begin{aligned}
P_{\underline{x}\underline{y}}(\underline{a}) &= P\left(\underline{y}=\left(\underline{s}^{t+1},\underline{e}^{t+1}\right)\middle|\underline{x}=\left(\underline{s}^{t},\underline{e}^{t}\right)\right) \\
&= P\left(\underline{s}^{t+1}=\underline{l}\,|\,\underline{s}^{t}=\underline{k},\underline{a}\right)P\left(\underline{e}^{t+1}=\underline{v}\,|\,\underline{e}^{t}=\underline{u},\underline{a}\right) \\
&= P\left(\underline{s}^{t+1}=\underline{l}\,|\,\underline{s}^{t}=\underline{k},\underline{a}\right)P\left(\underline{e}^{t+1}=\underline{v}\right) \\
&= \mathcal{B}\left(k_{\mathrm{A}}+a_{\mathrm{A}},k_{\mathrm{A}}+a_{\mathrm{A}}-l_{\mathrm{A}},p_d^{\mathrm{A}}\right)\times\mathcal{B}\left(k_{\mathrm{B}}+a_{\mathrm{B}},k_{\mathrm{B}}+a_{\mathrm{B}}-l_{\mathrm{B}},p_d^{\mathrm{B}}\right)\times \\
&\quad P\left(e_{\mathrm{A}}=u_{\mathrm{A}}\right)\times P\left(e_{\mathrm{B}}=u_{\mathrm{B}}\right), \qquad (5.15)
\end{aligned}
$$

where $P\left(e_{\mathrm{A}}=u_{\mathrm{A}}\right)$ and $P\left(e_{\mathrm{B}}=u_{\mathrm{B}}\right)$ respectively denote the probability that u_{A} new $\mathrm{S_A}$ requests and u_{B} new $\mathrm{S_B}$ requests are queued during the t^{th} ACP. $\mathcal{B}(n,m,p)$ denotes the Binomial probability distribution and

$$
\mathcal{B}(n,m,p)=\begin{cases}\binom{n}{m}p^{m}(1-p)^{n-m} & \text{if } 0\le m\le n,\\ 0 & \text{otherwise.}\end{cases} \qquad (5.16)
$$

Note that $\mathcal{B}(0,0,p)=1$, and p_d^{A} and p_d^{B} are respectively the probabilities that a $\mathrm{S_A}$ and a $\mathrm{S_B}$ transmission is completely served and departs the system in the duration $\mathcal{T}_{\mathrm{ACP}}$. They are expressed respectively as:

$$
p_d^{\mathrm{A}}=1-e^{-\mu_{\mathrm{A}}\mathcal{T}_{\mathrm{ACP}}} \text{ and } p_d^{\mathrm{B}}=1-e^{-\mu_{\mathrm{B}}\mathcal{T}_{\mathrm{ACP}}}. \qquad (5.17)
$$

4) Rewards, $\mathcal{R}$

Fixed revenue is collected for each admitted request and the revenues are denoted as:

i. r_{A} : for admitting a spectrum request for $\mathrm{S_A}$,
ii. r_{B} : for admitting a spectrum request for $\mathrm{S_B}$.

If the action $\underline{a}=\left(a_{\mathrm{A}},a_{\mathrm{B}}\right)$ is taken at the current state $\underline{x}$, then the expected revenue incurred until the next decision epoch is expressed as:

$$
r\left(\underline{x},\underline{a}\right)=a_{\mathrm{A}}r_{\mathrm{A}}+a_{\mathrm{B}}r_{\mathrm{B}}. \qquad (5.18)
$$

The cost, in terms of number of blocked requests, of taking action $\underline{a}$ at the current state $\underline{x}$ until the next decision epoch is given by:

$$\left.\begin{aligned} c_{\mathrm{A}}\left(\underline{x},\underline{a}\right) &= \left(u_{\mathrm{A}} - a_{\mathrm{A}}\right) \\ c_{\mathrm{B}}\left(\underline{x},\underline{a}\right) &= \left(u_{\mathrm{B}} - a_{\mathrm{B}}\right) \end{aligned}\right\}. \tag{5.19}$$

Note that u_{A} and u_{B} are the number of new requests from the respective radio systems at state $\underline{x}$. From the above expression, the expected cost for that service is essentially the average number of blocked spectrum requests per stage.

We formulate the MDP such that its performance is evaluated based on the expected average reward criterion. The long-run average reward for the policy $\underline{\pi}$, which is denoted by $h_{\underline{\pi}}$, can be expressed as:

$$h_{\underline{\pi}} = \lim_{N\to\infty} \frac{1}{N} \mathcal{E}_{\underline{\pi}} \left[\sum_{n=1}^{N} r\left(\underline{x}^n, \underline{a}_{\underline{\pi}}^{\underline{x}^n} \right) \right], \tag{5.20}$$

where $\underline{x}^n$ is the system state at the n^{th} decision epoch, and $\underline{a}_{\underline{\pi}}^{\underline{x}^n}$ is the selected action at the n^{th} decision epoch. The expectation, $\mathcal{E}_{\underline{\pi}}$, is taken over the probability distribution of policy $\underline{\pi}$. At the same time, the blocking probabilities for the offered services must abide to their respective system GoS guarantee. For the policy $\underline{\pi}$, the long-run average number of blocked requests is given respectively by:

$$\left.\begin{aligned} c_{\mathrm{A}}\left(\underline{\pi}\right) &= \lim_{N\to\infty} \frac{1}{N} \mathcal{E}_{\underline{\pi}} \left[\sum_{n=1}^{N} c_{\mathrm{A}}\left(\underline{x}^n, \underline{a}_{\underline{\pi}}^{\underline{x}^n} \right) \right] \\ c_{\mathrm{B}}\left(\underline{\pi}\right) &= \lim_{N\to\infty} \frac{1}{N} \mathcal{E}_{\underline{\pi}} \left[\sum_{n=1}^{N} c_{\mathrm{B}}\left(\underline{x}^n, \underline{a}_{\underline{\pi}}^{\underline{x}^n} \right) \right] \end{aligned}\right\}. \tag{5.21}$$

The problem is therefore mathematically expressed as:

$$\max_{\underline{\pi},\ \underline{x}\in\mathcal{S},\ \underline{a}\in\mathcal{A}} h_{\underline{\pi}}$$

subject to

$$c_{\mathrm{A}}\left(\underline{\pi}\right) \le g_{\mathrm{A}}\lambda_{\mathrm{A}}\mathcal{T}_{\mathrm{ACP}}\ ,$$

and

$$c_{\mathrm{B}}\left(\underline{\pi}\right) \le g_{\mathrm{B}}\lambda_{\mathrm{B}}\mathcal{T}_{\mathrm{ACP}}\,. \tag{5.22}$$

Note that $g_{\mathrm{A}}\lambda_{\mathrm{A}}\mathcal{T}_{\mathrm{ACP}}$ and $g_{\mathrm{B}}\lambda_{\mathrm{B}}\mathcal{T}_{\mathrm{ACP}}$ respectively denotes the maximum acceptable average number of blocked requests for S_A and S_B.

The Lagrangian method is used to identify stationary points of the optimization problem and the Lagrange function for policy $\underline{\pi}$, $\mathcal{L}_{\underline{\pi}}$, is expressed as:

$$\mathcal{L}_{\underline{\pi}} = h_{\pi} - m_1\left(c_{\mathrm{A}}\left(\underline{\pi}\right) - \overline{c_{\mathrm{A}}}\right) - m_2\left(c_{\mathrm{B}}\left(\underline{\pi}\right) - \overline{c_{\mathrm{B}}}\right), \tag{5.23}$$

where m_1 and m_2 are the Largange multipliers, and $\overline{c_{\mathrm{A}}} = g_{\mathrm{A}}\lambda_{\mathrm{A}}\mathcal{T}_{\mathrm{ACP}}$, $\overline{c_{\mathrm{B}}} = g_{\mathrm{B}}\lambda_{\mathrm{B}}\mathcal{T}_{\mathrm{ACP}}$ represent the GoS constrains in (6.22). The maximization problem can be re-written as:

$$\max_{\underline{\pi},\ m_1\ge 0,\ m_2\ge 0} \mathcal{L}_{\underline{\pi}} \tag{5.24}$$

The above problem is solved using a combination of the subgradient method [116] and the relative value iteration (RVI) algorithm [117]. The subgradient method iteratively searches for the Lagrange multipliers and is proven to converge to the optimal solution [116]. The RVI algorithm is an inner-loop of the subgradient iteration, and given known values of the Lagrange multipliers, it provides an efficient means to solve CMDP. Details of the subgradient method and the RVI algorithm are explicitly presented in Appendix E and F, respectively.

The RVI solution is ε-optimal, i.e. its average-reward differs from the optimal by at most ε. We assume $\varepsilon \le 1\%$ is acceptable. Note also that the optimal solution

for constrained MDPs is a stochastic policy with randomizations in at most *K* states, where *K* is the number of constraints [118]. On the other hand, the RVI algorithm returns a deterministic policy. We assume the performance difference is negligible in this problem as the number of states far exceeds the number of constraints.

5.6 Results and Discussion

In this section, we first present some preliminary results before comparing the performance of the three proposed policies at two different traffic conditions. The evaluation parameters are summarized in Table 5.1. In addition, we arbitrarily set $C = 12$, and $\tau_{\text{ACP}} = 1$.

TABLE 5.1 EVALUATION PARAMETERS

Parameter	μ_{A}	μ_{B}	b_{A}	b_{B}	g_{A}	g_{B}
Value	0.4	0.4	2	2.4	3	10

The parameters r_{A} and r_{B} in (5.18) are both set to unity, such that the expected reward is essentially the average number of admitted requests per stage. Therefore, the three SAC policies given in (5.6), (5.12) and (5.18) have a common basis for comparison.

We assume that a cumulated Poisson arrival probability (within a τ_{ACP}) of at least 0.999 is sufficiently accurate for the analysis. Given the largest value of T_{A} and T_{B}, this probability is found to be satisfied when the minimum number of new requests within a τ_{ACP} is greater than five, i.e. $\sum_{i=0}^{5} P(u_{\omega} = i) \geq 0.999$, where ω denotes either R_{A} or R_{B}. Hence in the subsequent evaluations, we let $e_{\text{A}} = e_{\text{B}} = 5$.

5.6.1 Preliminary results (FCFS Policy)

The performance for the FCFS policy is first analyzed by setting $f(j)=1 \; \forall \, j$ such that Eq. (5.6) is fulfilled. In Figure 5.3, we plot the blocked service probabilities when the multi-radio network is operating at maximum offered traffic against T_{A}. From Fig. 5.3, it is evident that the blocked service probability for R_A is the at its prescribed GoS guarantee of 3% throughout these traffic conditions, while the blocked service probability for R_B is still below its GoS limit. Hence for the FCFS policy, R_A is the performance limiting radio system. The corresponding supported traffic for the multi-radio network based on the FCFS policy is plotted in Figure 5.4.

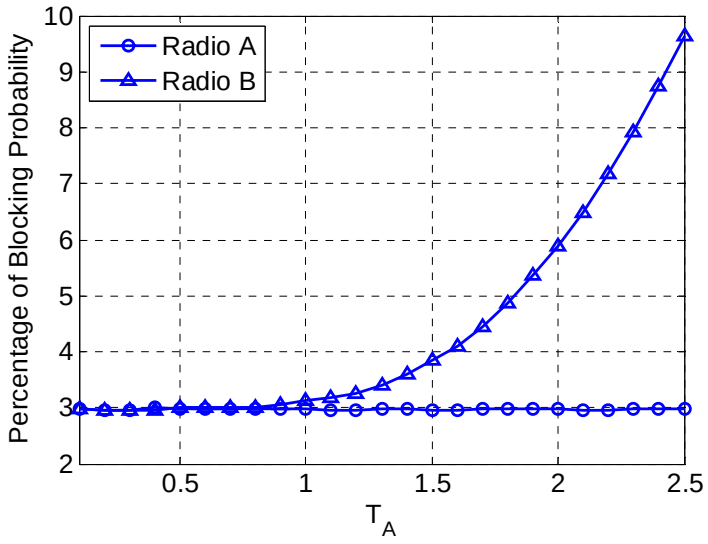

Fig. 5.3 Blocking probabilities at maximum offered traffic for FCFS policy.

5.6.2 Results for RD Policy

We arbitrarily select the function $f(j)=\alpha^{j}$, where $\alpha<1$. For a given α, the maximum offered traffic while satisfying both radio systems' GoS requirements are

obtained. Figure 5.4 shows the maximum offered traffic for different values of α. For this policy, $m_A = 6$ and $m_B = 5$. Note that $\alpha = 1$ is equivalent to the FCFS policy.

With the RD policy and for $\alpha < 1$, more S_B requests will be denied and hence more resources are available to serve S_A requests. The blocking probability for S_B increases, but it is still maintained within the specified GoS guarantee. In this way, more traffic can actually be offered. This also results in higher spectrum utilization efficiency. It is also observed from Fig. 5.4 that for $\alpha \leq 0.94$, if the S_A traffic is below a certain threshold, then there is no advantage by limiting the admission of S_B requests. This is explained by the fact that the traffic for S_A is low. However, the SAC still deny the admission of S_B requests even though there are available resources. In this case, R_B becomes the performance limiting radio system.

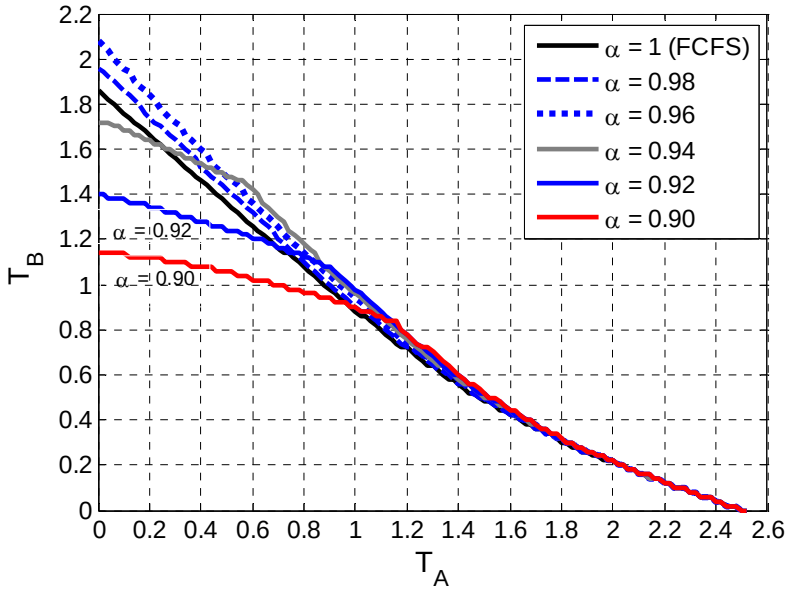

Fig. 5.4 Region of maximum offered traffic for different values of α.

5.6.3 Results for RES Policy

In this case, $m_A = 6$ and $m_B = \lfloor (C - rb_B)/b_B \rfloor$. Figure 5.5 shows the performance given by the RES policy. When $r = 0$, we have the FCFS policy. For a given $r > 0$, there exists a threshold such that if T_A is reduced further, T_B cannot be increased further due to unnecessary reservation of bbu.

From the two results shown in Fig. 5.4 and Fig. 5.5, the total offered traffic can be higher than when no regulation is employed ($r = 0$ or $\alpha = 1$). Therefore, the average spectrum utilization can be increased with the selection of the appropriate α or r. For example, in Fig. 5.5, for $T_A = 0.4$, we obtain $T_B \approx 1.5$ if no resources are reserved ($r = 0$). But if $r = 1$, we obtained $T_B = 1.8$, which is about 20% increase.

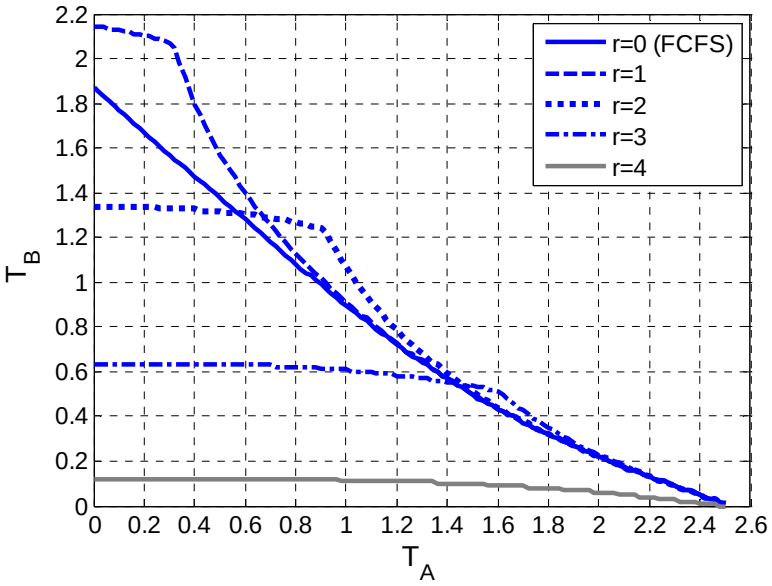

Fig. 5.5 Region of maximum offered traffic for different values of *r*.

5.6.4 Comparison of Results

In this sub-section, we investigate and compare the performance of all three policies for two ranges of traffic conditions: $0.1 \le T_A \le 0.35$ and $1.5 \le T_A \le 1.8$. These two ranges respectively correspond to between 4% and 14%, and between 60% and 72% of the maximum offered traffic for S_A. The optimal design parameters for the RD and RES policies are obtained using an exhaustive search algorithm. Note that the MDP based policy does not require any assumption on the performance limiting radio; however, both the RD and RES policies are developed based on R_A being the performance limiting radio.

1) For $0.1 \le T_A \le 0.35$

For these values of T_A, we investigate the maximum offered T_B such that the GoS requirements remain satisfied. Figure 5.6 shows the results for all three admission policies, and the percentage increase in offered traffic for the MDP based admission policy compared to the other two policies. For this range of values, $\alpha = 0.96$ is found to maximize the offered traffic for the RD policy. On the other hand, maximum offered traffic is achieved when $r = 1$ for the RES policy.

From the results, the SAC policy using CMDP is able to admit more traffic compared to both the RD and RES policies. The increase over the RD policy is on the average about 30% across the evaluated range while that for the RES policy is about 18%. The CMDP based SAC policy enables the spectrum manager to estimate the future rewards (average number of admissions) and costs incurred (average number of rejections) in taking a particular action at each state. With such 'prediction', the spectrum manager can better balance the difference (from their GoS limit) in the blocking probabilities of the radios and hence support more traffic compared to the

other policies. On the other hand, both the RD and RES policies just admit spectrum requests without costs considerations. The average spectrum utilization is computed using (5.1) and is plotted in Figure 5.7. The results show that the offered traffic and average spectrum utilization is increased (compared to the FCFS policy) through the use of the three SAC policies to regulate the admission of spectrum requests.

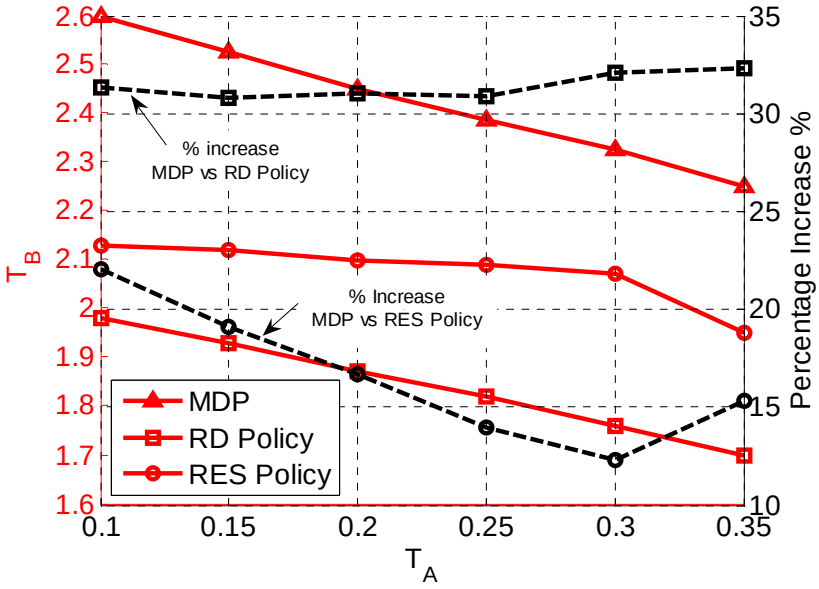

Fig. 5.6 Maximum S_B traffic for $0.1 \le T_A \le 0.35$.

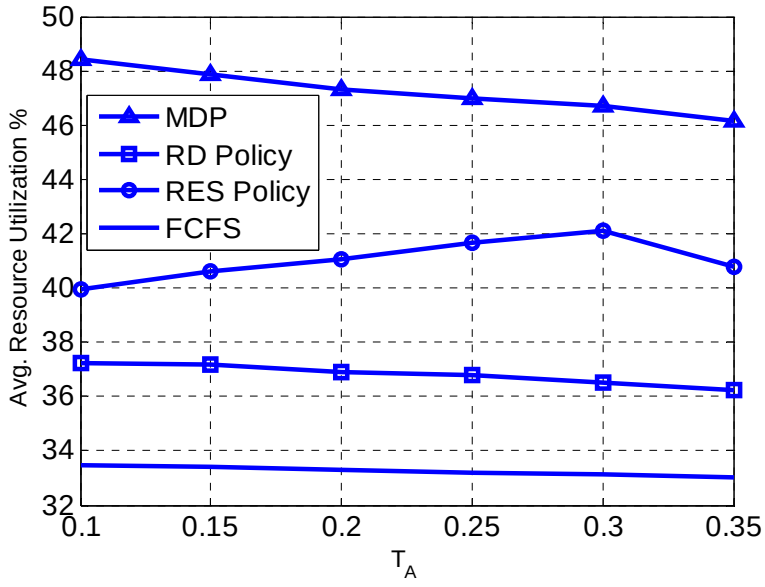

Fig. 5.7 Average spectrum utilization for $0.1 \le T_A \le 0.35$.

2) For $1.5 \le T_A \le 1.8$

Figure 6.8 shows the results for all three admission policies for $1.5 \le T_A \le 1.8$. For this range of values, maximum offered traffic is achieved when $\alpha = 0.864$ for the RD policy and when $r = 3$ for the RES policy. Again for this range of traffic, the MDP based policy achieves the highest offered traffic. The increase is about 8% across the range compared to the RD policy and about 4% compared to the RES policy. The average resource utilization for this range is plotted in Figure 5.9.

The results show that the increase in offered traffic by the MDP based policy over the other policies is lower in this case. This is because at this range of traffic, both the RD and RES policies are already performing quite efficiently. Moreover, both radio systems are operating very close to their GoS limit. Hence, the advantage of the CMDP algorithm is less significant at this range of traffic. On the other hand, if the GoS requirements were relaxed then more traffic can be supported.

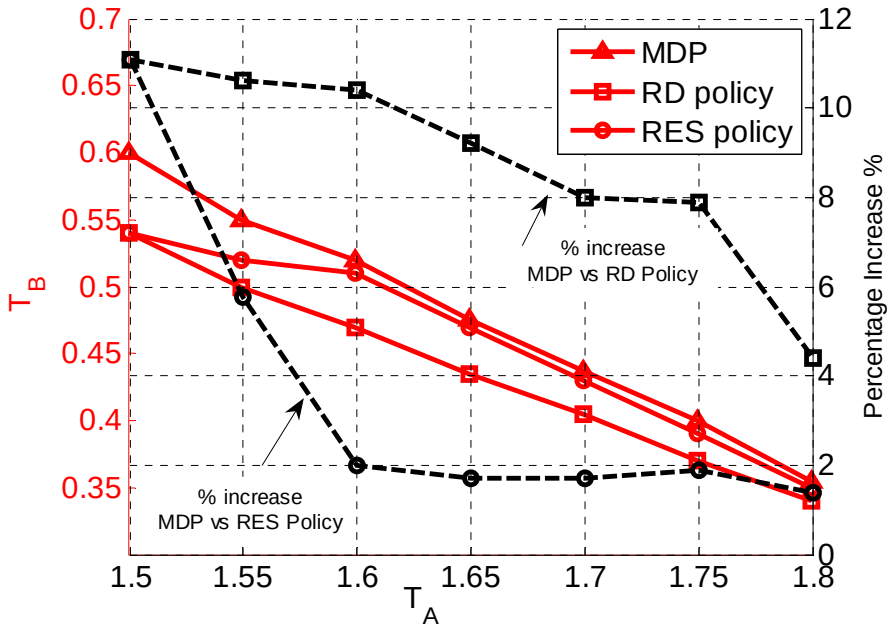

Fig. 5.8 Maximum S_B traffic for $1.5 \le T_A \le 1.8$.

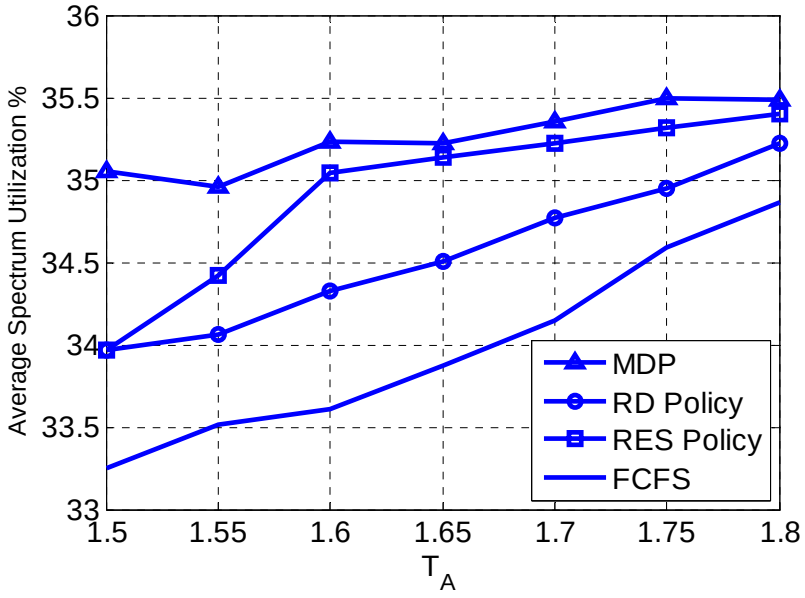

Fig. 5.9 Average resource utilization for $1.5 \le T_{\mathrm{A}} \le 1.8$.

5.7 Maximizing Average Revenue

In this section, it is assumed that through the use of reconfigurable technologies in the future, the radio systems are capable of supporting variable transmission bandwidth for each service. The transmission bandwidth requirements for $\mathrm{S_A}$ are denoted by b_{A}^1 and b_{A}^2 where $b_{\mathrm{A}}^1 > b_{\mathrm{A}}^2$; and that for $\mathrm{S_B}$ are denoted by b_{B}^1 and b_{B}^2, where $b_{\mathrm{B}}^1 > b_{\mathrm{B}}^2$.

When smaller transmission bandwidth (or higher order constellation) is used, a service will generally suffer from more impairments under a given transmission power constraint. Hence, the service charge is lesser. This provides an incentive for the operators to provide better quality transmission particularly when the overall network traffic is low so as to increase their overall revenues. These tradeoffs are modelled in the proposed SAC algorithm, and the objective of this section is to study

the increase in average revenue when compared to the case where only a single transmission bandwidth is used.

For comparison, it is assumed that another multi-radio network only support a single transmission bandwidth for each service. This network is referred to as System 1 and it is assumed it offers high order modulation transmission only, i.e. require b_{A}^{2} and b_{B}^{2} bbu, respectively. On the other hand, System 2 which supports multiple modulation schemes for each service is assumed to offer both high and low order modulation. The advantage of System 2 over one which only offers low order modulation for each service is trivial; hence its performance is not compared.

The traffic arrival for S_A and S_B is given by λ_{A} and λ_{B}, respectively. The mean service duration for S_A using b_{A}^{1} is denoted by $1/\mu_{\mathrm{A1}}$ and that for b_{A}^{2} is denoted by $1/\mu_{\mathrm{A2}}$. The mean service duration for S_B using b_{B}^{1} is denoted by $1/\mu_{\mathrm{B1}}$ and that for b_{B}^{2} is denoted by $1/\mu_{\mathrm{B2}}$.

5.7.1 SAC Formulation

The SAC in this problem is also formulated as a discrete-time MDP:

1) State space, $\mathcal{S}'$

The state space is now specified by $\mathcal{S}'$ which is expressed as:

$$\mathcal{S}' = \left\{ (\underline{s}', \underline{e}') \middle| 0 \le s_{\mathrm{A1}} b_{\mathrm{A}}^{1} + s_{\mathrm{A2}} b_{\mathrm{A}}^{2} + s_{\mathrm{B1}} b_{\mathrm{B}}^{1} + s_{\mathrm{B2}} b_{\mathrm{B}}^{2} \le C \right\}, \tag{5.25}$$

where the vector $\underline{s}_t' = (s_{\mathrm{A1}}^{t}, s_{\mathrm{A2}}^{t}, s_{\mathrm{B1}}^{t}, s_{\mathrm{B2}}^{t})$ now denote the number of S_A users with bandwidth requirements b_{A}^{1} and b_{A}^{2}, the number of S_B users with bandwidth requirements b_{B}^{1} and b_{B}^{2} being served, respectively; and $\underline{e}_t' = (e_{\mathrm{A}}^{t}, e_{\mathrm{B}}^{t})$ now denote the

number of new S_A and S_B requests at the beginning of the t^{th} ACP.

2) Action space, $\mathcal{A}'$

The action taken at the t^{th} ACP is now denoted by the vector $\underline{a}'_t = (a^t_{A1}, a^t_{A2}, a^t_{B1}, a^t_{B2})$, where it respectively represents the number of admitted S_A with bandwidth requirements b^1_A and b^2_A, and S_B with bandwidth requirements b^1_B and b^2_B. Note that in this case, $0 \le a^t_{A1} + a^t_{A2} \le e^t_A$ and $0 \le a^t_{B1} + a^t_{B2} \le e^t_B$ for all *t*.

3) State transitions and transition probability matrix, $\mathcal{P}'$

If the network at the t^{th} decision epoch (ACP) is at state $\underline{x} = (\underline{i}, \underline{m})$ and action $\underline{a}'$ is taken, then the network will transit to state $\underline{y} = (\underline{j}, \underline{n})$ at the $(t+1)^{th}$ decision epoch with probability $P_{\underline{x}\underline{y}}(\underline{a}')$ given by:

$$
\begin{aligned}
P_{\underline{x}\underline{y}}(\underline{a}') &= P\left(\underline{y} = \left(\underline{s}'_{t+1}, \underline{e}'_{t+1}\right) \middle| \underline{x} = \left(\underline{s}'_t, \underline{e}'_t\right)\right) \\
&= P\left(\underline{s}'_{t+1} = \underline{j} \mid \underline{s}'_t = \underline{i}, \underline{a}'\right) P\left(\underline{e}'_{t+1} = \underline{n} \mid \underline{e}'_t = \underline{m}, \underline{a}'\right) \\
&= P\left(\underline{s}'_{t+1} = \underline{j} \mid \underline{s}'_t = \underline{i}, \underline{a}'\right) P\left(\underline{e}'_{t+1} = \underline{n}\right) \\
&= \mathcal{B}\left(i_{A1} + a_{A1}, i_{A1} + a_{A1} - j_{A1}, p_d^{A1}\right) \times \mathcal{B}\left(i_{A2} + a_{A2}, i_{A2} + a_{A2} - j_{A2}, p_d^{A2}\right) \times \\
&\quad \mathcal{B}\left(i_{B1} + a_{B1}, i_{B1} + a_{B1} - j_{B1}, p_d^{B1}\right) \times \mathcal{B}\left(i_{B2} + a_{B2}, i_{B2} + a_{B2} - j_{B2}, p_d^{B2}\right) \times \\
&\quad P\left(e_A = n_A\right) \times P\left(e_B = n_B\right), \qquad (5.26)
\end{aligned}
$$

where $P(e_A = n_A)$ and $P(e_B = n_B)$ respectively denote the probability that n_A new S_A requests and n_B new S_B requests are queued during the t^{th} ACP. In addition, p_d^{A1}, p_d^{A2}, p_d^{B1} and p_d^{B2} are the probabilities that an admitted request using the respective transmission bandwidth departs the system in $\mathcal{T}_{ACP}$. $\mathcal{B}(n, m, p)$ is the Binomial probability distribution as defined in (5.16).

4) Rewards, $\mathcal{R}'$

In this section, the revenues are denoted as:

i. r'_{A1}: for admitting a S_A request with bandwidth b_A^1,
ii. r'_{A2}: for admitting a S_A request with bandwidth b_A^2,
iii. r'_{B1}: for admitting a S_B request with bandwidth b_B^1,
iv. r'_{B2}: for admitting a S_B request with bandwidth b_B^2.

To model the tradeoffs as described previously, we let $r'_{A1} > r'_{A2}$ and $r'_{B1} > r'_{B2}$.

If the action $\underline{a}' = (a_{A1}, a_{A2}, a_{B1}, a_{B2})$ is taken at the current state $\underline{x}$, the immediate expected revenue incurred until the next decision epoch is expressed as:

$$r(\underline{x}, \underline{a}') = a_{A1} r'_{A1} + a_{A2} r'_{A2} + a_{B1} r'_{B1} + a_{B2} r'_{B2}. \tag{5.27}$$

The new cost (in terms of number of blocked service requests) of taking action $\underline{a}'$ at the current state $\underline{x}$ until the next decision epoch is given by:

$$\left.\begin{aligned} c'_A(\underline{x}, \underline{a}') &= \left(m_A - a_{A1} - a_{A2}\right) \\ c'_B(\underline{x}, \underline{a}') &= \left(m_B - a_{B1} - a_{B2}\right) \end{aligned}\right\}. \tag{5.28}$$

Note that m_A and m_B are the number of new requests for the respective radio system. In this problem, the long-run average reward for the policy $\underline{\pi}'$ is:

$$h'_{\underline{\pi}'} = \lim_{N\to\infty} \frac{1}{N} \mathcal{E}_{\underline{\pi}'} \left[\sum_{n=1}^{N} r\left(\underline{x}^n, \underline{a}'_{\underline{\pi}'}{}^{\underline{x}^n} \right) \right]. \tag{5.29}$$

Likewise the long-run average number of blocked requests for R_A and R_B is given respectively by:

$$\left.\begin{aligned} c'_A(\underline{\pi}') &= \lim_{N\to\infty} \frac{1}{N} \mathcal{E}_{\underline{\pi}'} \left[\sum_{n=1}^{N} c'_A\left(\underline{x}^n, \underline{a}'_{\underline{\pi}'}{}^{\underline{x}^n} \right) \right] \\ c'_B(\underline{\pi}') &= \lim_{N\to\infty} \frac{1}{N} \mathcal{E}_{\underline{\pi}'} \left[\sum_{n=1}^{N} c'_B\left(\underline{x}^n, \underline{a}'_{\underline{\pi}'}{}^{\underline{x}^n} \right) \right] \end{aligned}\right\}. \tag{5.30}$$

The CMDP in section is therefore mathematically expressed as:

$$\max_{\underline{\pi}', \underline{x} \in \mathcal{S}', \underline{a}' \in \mathcal{A}'} h'_{\underline{\pi}'}$$

subject to

$$c'_{\mathrm{A}}(\underline{\pi}') \le g_{\mathrm{A}} \lambda_{\mathrm{A}} \tau_{\mathrm{ACP}} ,$$

and

$$c'_{\mathrm{B}}(\underline{\pi}') \le g_{\mathrm{B}} \lambda_{\mathrm{B}} \tau_{\mathrm{ACP}} . \qquad (5.31)$$

With the above formulations, the optimization problem is solved similarly using a combination of the subgradient method and RVI algorithm.

5.7.2 Results and Discussion

In this section, we assume $g_{\mathrm{A}} = g_{\mathrm{B}} = 3\%$ are acceptable GoS guarantees. In addition, we arbitrarily let $C = 10$, $\tau_{\mathrm{ACP}} = 1$, $b_{\mathrm{A}}^{1} = 10/3$, $b_{\mathrm{A}}^{2} = 2$, $b_{\mathrm{B}}^{1} = 5$ and $b_{\mathrm{B}}^{2} = 2.5$. Table 5.2 summarizes the values of the remaining parameters. The blocked service probabilities and average revenue are analyzed when the systems' traffic are reasonably light and also when the systems experience high traffic.

TABLE 5.2 ANALYSIS PARAMETERS

Parameter	μ_{A1}	μ_{A2}	μ_{B1}	μ_{B2}	r_{A1}	r_{A2}	r_{B1}	r_{B2}
System 1	-	0.6	-	0.7	-	0.4	-	0.55
System 2	0.4	0.6	0.45	0.7	0.65	0.4	0.75	0.55

1) *For* $0.1 \le \lambda_{\mathrm{B}} \le 0.2$

We study the revenue and blocked service probabilities for the two systems during reasonably light traffic. We assume $\lambda_{\mathrm{A}} = 0.1$ and λ_{B} is varied from 0.1 to 0.2.

Figure 5.10 shows the maximum average collectable revenue for both systems in the multi-radio network. Figure 5.11 shows the average blocking probabilities of the services.

From Fig. 5.10, the received revenue for System 2 is higher than that for System 1. This is because when the traffic is reasonably low, the spectrum manager can assign some users to transmit using low order modulation so as to collect higher revenue, while still able to satisfy the GoS requirement of the radio systems. The increase in revenue is about 10% across the range of values investigated. The use of lower order modulation will mean longer average holding time in order to complete the same transmission. Hence, the blocked service probability is expected to be higher for System 2 since some services are transmitted using lower order modulation, and this can be verified from Fig. 5.11.

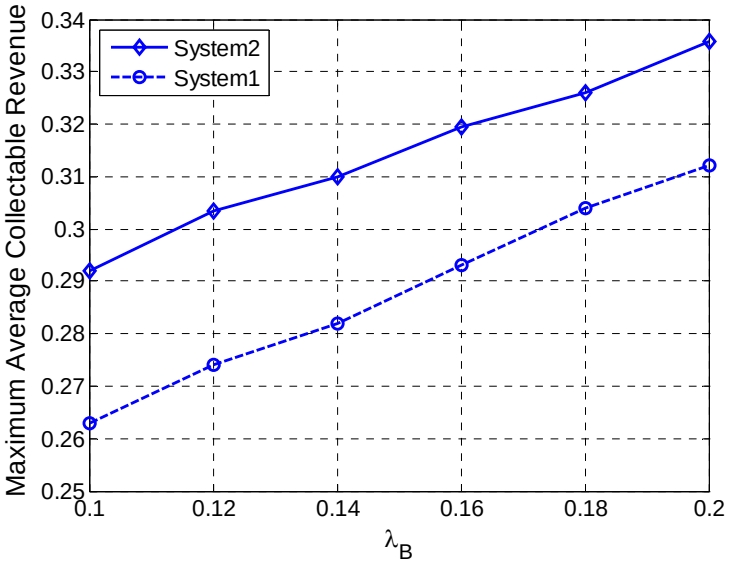

Fig. 5.10 Maximum average collectable revenue for reasonably light traffic.

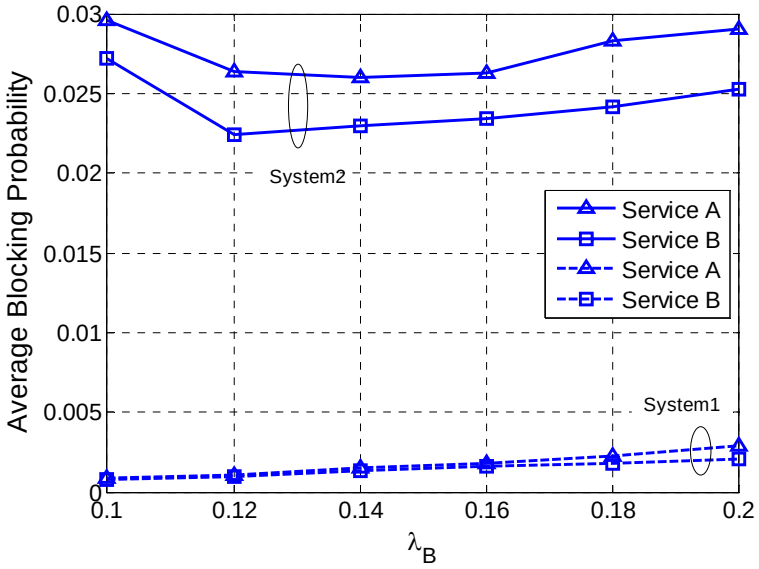

Fig. 5.11 Average blocking probabilities for $0.1 \le \lambda_B \le 0.2$.

2) *For* $0.3 \le \lambda_B \le 0.38$

We now investigate the average revenue and blocked service performance for the two systems in the multi-radio network during heavy traffic. For these results, $\lambda_A = 0.4$ and λ_B is varied from 0.3 to 0.38. Figure 5.12 shows the maximum average revenue for both systems. Figure 5.13 shows the average blocking probabilities.

From Fig. 5.12, for $\lambda_B = 0.3$ to 0.36, the received revenue for System 2 is still larger than that for System 1. However, the increase in revenue has decreased to about 1%. This is because with more traffic, the spectrum manager must assign fewer services to transmit on low order modulation if the GoS constraints are to be satisfied. For $\lambda_B = 0.36$ and 0.38, the admission policy is found to coincide for both systems and average revenue is thus identical. At these points, the spectrum manager cannot assign any services to transmit on low order modulation without exceeding the GoS constraints. Hence, all admitted requests are assigned to transmit using high order modulation which require less transmission bandwidth and have shorter average service holding time.

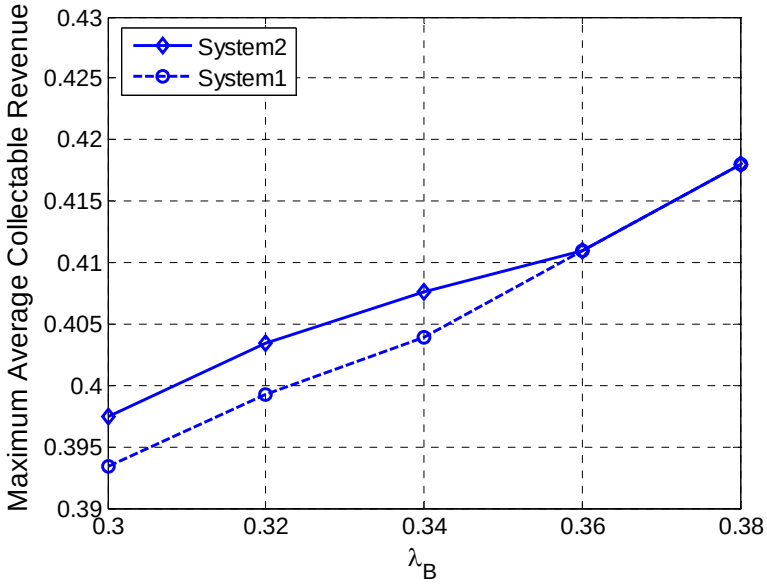

Fig. 5.12 Maximum average revenue.

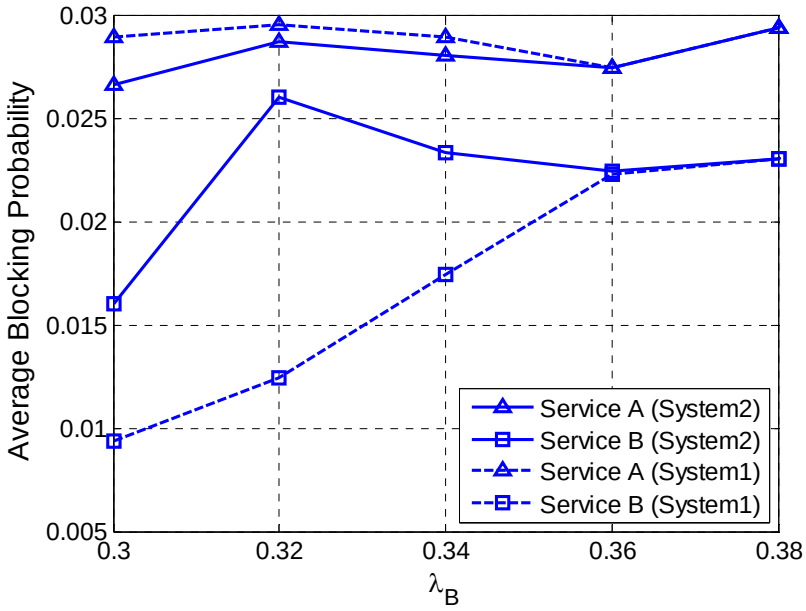

Fig. 5.13 Average blocking probabilities for $0.3 \le \lambda_B \le 0.38$.

5.8 Conclusion

In this chapter, the complete spectrum sharing model in a heterogeneous multi-radio network is studied. We examined two possible operation models adopted by the spectrum manager. In the first case, the objective is to maximize the total

supported traffic of the network, subjected to the respective GoS requirements of the radio systems. The results of a FCFS policy show that R_A is the performance limiting radio while R_B is still operating below its GoS limit. Three SAC policies are designed and compared. The introduction of the extra design parameters in the respective policies provide greater flexibility to meet the GoS requirements concurrently, and hence result in higher offered traffic and average spectrum utilization compared to the FCFS policy. However, the MDP based policy shows the best adaptability to different traffic conditions compared to the RD and RES policies.

For the second operation model, the spectrum manager adopts a SAC policy to maximize the average collectable revenue. We studied the revenue gained when the services are support by variable transmission bandwidth and incur different charges in accordance to the modulation scheme used. Our analysis shows significant gain in revenue especially when the network experiences light traffic. However, the gain diminishes as the traffic demands become higher.

Chapter 6

Conclusion

6.1 Thesis Contributions

In opportunistic spectrum access (OSA), SRs make use of the available spectrum holes in time and frequency domains for transmission. In Chapter 3, we studied the PR activities impact on the secondary transmission opportunity time and the duration of the 'black spaces'. We considered the cases whereby the statistics of the PR activities in the *N* frequency bins are pair-wise distinct and also when they are similar. Our system model assumes that the PR activities in each frequency bin follow an exponential on/ off process. A continuous time Markov chain (CTMC) model with 2^N dimensions was developed to model the PR activities. Theoretical derivations using this model would be extremely complex and tedious especially for large number of frequency bins. To resolve the problem, an irreducible lumped Markov chain model was derived (based on the CTMC model) which significantly reduces the complexity of the analysis. Using this model, the theoretical p.d.f. of the opportunity time was derived for small number of frequency bins. The analytical approach (which can be performed systematically with a computer) was then generalized to *N* frequency bins. The theoretical p.d.f. of the 'black spaces' is also derived.

Our results show the theoretical p.d.f. of the opportunity time for *N* frequency bins follows a hyper-exponential distribution with $(2^N - 1)$ terms when the PR on/off activities in the frequency bins are pair-wise distinct, while having *N* terms if the activities are statistically identical. Extensive computer simulations were performed to verify the correctness of the derived theoretical expressions. In addition, based on

extensive simulation and theoretical data, we used commercial software and further show through statistical distribution fitting methods that the theoretical expression of the distribution may be closely approximated using only three exponential terms.

The study provides insights on the relationship between the statistics of the PR activities, the opportunity time and the duration of the 'black spaces'. In addition, from the theoretical p.d.f. of the opportunity time, we can obtain its cumulative density function (c.d.f.). From the c.d.f, given a probability of occurrence, say α, the duration of the SR access opportunities can be determined. If there is only one secondary request, the probability of it being completely served without being forced to drop is 1-α if its service time is within the stipulated duration. In addition, from the theoretical p.d.f. for the 'black spaces', we can obtain a measure of the duration in which SR transmissions are not possible due to no available spectrum hole.

In Chapter 4, we studied virtual spectrum partitioning (Fig. 1.6) for the coordinated spectrum access model. We developed analytical platforms which enable the study of both the enhancement in service capacity as well as the incurred tradeoffs when two proprietary radio systems with different system parameters share their excess spectrum resources to support each others' traffic demands.

A four dimensional Markov chain model based on a simple FCFS SAC policy is developed and analyzed. From the steady-state solution, it is shown that the service capacity of the radio systems is significantly improved compared to when they operate independently. The increase in service capacity is at the expense of performance of vertical handoffs. It is also found that the blocked service guarantee of a radio system is first exceeded and the service capacity of the multi-radio network is thus limited by the GoS constraint of this radio system (referred to as the performance limiting radio).

Two other SAC policies, namely, a RES policy and a random discard (RD) policy were proposed. In the RES policy, we let the performance limiting radio to always reserve an integer multiple, *r*, units of resources for its exclusive access only. In the RD policy, the performance limiting radio regulates the admission of vertical handoff services by an admission probability, ρ. The objective of the RES and RD policies is to optimize the parameters *r* and ρ, respectively, so as to maximize the supported traffic of the network. The optimization of these parameters to adapt to different traffic demands is also presented.

Both policies show significant improvement in the network service capacity (over the FCFS policy) as the introduction of the extra design parameter provides the flexibility to meet the GoS of the respective radio systems concurrently. In particular, the RD policy shows greater flexibility in adapting to variable traffic demands and also averages lower vertical handoff probability than the RES policy. The vertical handoff probability was found to be highest in the FCFS policy. A simulation model is developed and extensive computer simulations were performed which verified the correctness of the developed models and its analysis. The developed analytical platforms which enable evaluation of the multi-radio network service capacity in relation to a particular level of incurred tradeoff and vice versa.

In Chapter 5, we studied the complete spectrum sharing model described in Fig. 1.7 and examined two possible objective functions. For the first case, the objective of the spectrum manager is to maximize the amount of supported traffic, subjected to the GoS guarantees of the respective radio systems. We compared the maximum service capacities of the multi-radio network given by three SAC policies. Two of these policies, namely a RES and a RD policy, are based on CTMC models.

The third policy is developed upon discrete time constrained Markov decision process (CMDP) framework.

We derived and presented the respective closed-form steady-state solutions to the Markov chain models for the RD and RES policies. In addition, the optimization of the RES and RD policies so as to maximize the supported network traffic are also shown. For our CMDP, the GoS constraints are formulated as Lagrange functions and our analytical solution to the constrained problem uses an iterative subgradient method. Convergence to the optimal solution based on this method is more efficient compared to generic linear programming approaches. From the results, the SAC policy using CMDP is able to support greater amount of traffic compared to both the RD and RES policies.

For the second case, the objective of the spectrum manager is to maximize the average revenue, subjected to the GoS constraints of the individual radio systems. The radio systems can use different modulation schemes for the services, and revenue received from transmissions using smaller bandwidth is lesser, as it is reasonably assumed that user satisfaction is lower when the higher order modulation suffers more impairment under the same transmission power. The tradeoffs between service admission and maximum collectable revenue are modelled in the SAC which is formulated and analyzed as a discrete time CMDP. We showed the analytical solution of the problem using a combination of the subgradient method and the relative value iteration (RVI) algorithm. Our results showed the advantage of having variable transmission bandwidth as it enables the spectrum manager to collect higher revenue when the traffic demands are relatively low. The average increase in revenue is about 10% for the evaluation range and parameters. However, this is at the expense of

higher blocked service probabilities (but is still kept within the GoS guarantee). When the traffic load of the system is high, the gain in revenue diminishes.

6.2 Future Work

The modeling of SAC policies in Chapters 5 and 6 are based on Poission distributed arrival and negative exponentially distributed service time model. While such a model is necessary to facilitate system modeling using Markov chains, there are also alternative traffic models in the literature. For example, Markov modulated Poisson process has been shown to model a mixture of voice and data traffic [119]. On the other hand, the service times of cellular digital packet services may be modeled using a Lognormal distribution [120]. The investigation and comparison of the performances of the SAC policies under different traffic models is an interesting future work.

It is shown in Fig. 1.5 that the SR could also be distributed. For example, in the case of PANs/BANs which have small wireless coverage, many distributed SRs may be deployed within the bigger coverage of a PR base station. In general, distributed SR systems are more suited for ad-hoc deployment scenarios despite imposing a more challenging design problem. Under such circumstances, there is a tradeoff between the amount of information to be exchanged between distributed SRs and the system effective throughput, which is always an important design consideration for secondary radios using distributed MAC. It is therefore required to study efficient distributed MAC schemes which can provide reasonable throughput and at the same time resolve the access contention for spectrum resources in the absence of a centralized controller.

Recently, there are increasing interests to apply wideband sensing to OSA. When applying wideband spectrum sensing and detection, there should be only one sensing rate for all the frequency bins. Under this circumstance, the optimal sensing rate seems to be a result of the distribution of the opportunity time and the “black space”, so as to maximize the secondary usage of spectrum under given energy, false alarm and missed detection probability constraints. Intuitively, if the average duration of the ‘black space’ is long, then a faster wideband sensing rate may incur unnecessary sensing as there is a higher probability of encountering ‘black space’. On the other hand, slower wideband sensing rate may result in increased proportion of missed opportunities i.e. shorter opportunity time and higher collision probability. These are design tradeoffs are illustrated in Fig. 2.5. Although modeling the false alarm and missed detection probabilities remain a challenging problem for wideband sensing, we believe that the derived distribution of the opportunity time can be useful.

For our study on the complete spectrum sharing model in which the SAC is based on revenue maximization, a static revenue function for the spectrum manager and an infinite willingness-to-pay function (willing to pay at whatever stipulated price) was adopted for the radio systems. An interesting and challenging possible future work involve studying and comparing the performances of dynamic revenue functions for SAC. From the spectrum managers’ perspective, a dynamic revenue function should reflect a higher service charge for a unit of spectrum resource when the traffic demands are high. The service charge should then decrease when the demand for spectrum is low so as to encourage higher usage. On the other hand, from the radio systems’ perspective, a more realistic willingness-to-pay function is required to indicate the price the user is willing to pay for a unit of spectrum. The objective of the spectrum manager is to maximize its collectable revenue, whereas the users wish

to complete its transmission at minimum costs. The design of SAC policies through the use of dynamic cost and revenue functions better reflect the economics of demand and supply of spectrum resources in a secondary spectrum market. A well-designed and well-implemented SAC policy will assign spectrum resources to the radio system which values it most highly. However, in addition to the GoS guarantees, spectrum access fairness among the radio systems in the multi-radio network has to be ensured too. The analysis of such a problem is technically challenging and game theoretic methods may be a useful tool for this study.

Bibliography

[1] NTIA, "U.S. frequency allocations", [Online]. Available at: http://www.nita.doc.gov/osmhome/allochrt.pdf.

[2] H. H. Chen, M. Guizani, "Next Generation Wireless Systems and Networks", Wiley, 2006.

[3] SPTF, "Spectrum Policy Task Force Report of the Spectrum Efficiency Working Group, November 15 2002", [Online]. Available at: http://www.fcc.gov/sptf/files/SEWGFinalReport_1.doc

[4] Mark A. McHenry, D. McCloskey, "Spectrum Occupancy Measurements: Chicago, Illinois, November 16-18, 2005", Shared Spectrum Company Report, 2005. [Online]. Available at: http://www.sharedspectrum.com/measurements/download/NSF_Chicago_2005_ 11_measurements_v12.pdf

[5] T. Erpek, K. Steadman, D. Jones, "Spectrum Occupancy Measurements: Dublin, Ireland, April 16-18, 2007", Shared Spectrum Company Report, 2007. [Online]. Available at: http://www.sharedspectrum.com/measurements/download/Ireland_Spectrum_Occupancy_ Measurements_v2.pdf

[6] M. H. Islam, C. L. Koh, S. W. Oh,; X. Qing; Y. Y. Lai, Cavin Wang; Y. C. Liang; B. E. Toh, F. Chin, G. L. Tan, W. Toh, "Spectrum Survey in Singapore: Occupancy Measurements and Analyses", *IEEE CrownCom*, pp. 1-7, 2008.

[7] S. Pollin, I. Tan, B. Hodge, C. Chun, A. Bahai, "Harmful Coexistence Between 802.15.4 and 802.11: A Measurement-based Study", *IEEE CrownCom*, pp. 1-6, 2008.

[8] Y. Zhang; X. Zhang; D. Yang; "Performance Analysis of Channel-Aware Multichannel CSMA in Wireless Networks", *IEEE VTC*, pp. 1657-1660, 2008.

[9] IEEE 802.11h, Part 11: Wireless Lan Medium Access Control (MAC) and Physical Layer (PHY) specifications, Amendment 5: Spectrum and Transit Power Management Extensions in the 5 GHz band in Europe, 14 October 2003.

[10] S. M. Mishra, S. T. Brink, R. Mahadevappa, R. W. Brodersen, "Cognitive Technology for Ultra-Wideband/WiMax Coexistence", *IEEE DySPAN*, pp. 179-186, 2007.

[11] S. Geirhofer, Lang Tong, B. M. Sadler, "Cognitive Medium Access: Constraining Interference Based on Experimental Models", *IEEE J. Sel. Areas Commun.*, vol. 26, Issue 1, pp.95-105, Jan. 2008.

[12] G. Giancola, D. Domenicali, M. G. di Benedetto, "Cognitive UWB: interference mitigation by spectral control", *IEEE CrownCom*, pp. 1-6, 2006.

[13] H. G. Zhang; X. F. Zhou; K. Y. Yazdandoost, I. Chlamtac, "Multiple signal waveforms adaptation in cognitive ultra-wideband radio evolution", *IEEE J. Sel. Areas Commun.*, vol. 24, Issue 4, pp. 878-884, 2006.

[14] S. Haykin, "Cognitive radio: brain-empowered wireless communications", *IEEE J. Sel. Areas Commun.*, vol. 23, Issue 2, pp. 201-220, Feb. 2005.

[15] S. N. Shankar C. T. Chou, K. Challapali, S. Mangold, "Spectrum agile radio: capacity and QoS implications of dynamic spectrum assignment", *IEEE Globecom*, 2005.

[16] C. T. Chou, S. N. Shankar, H. Kim, K. G. Shin, "What and how much to gain by spectrum agility?", *IEEE J. Sel. Areas Commun.*, vol. 25, Issue 3, pp. 576-588, 2007.

[17] P. K. Tang, Y. H. Chew, L. C. Ong, "On the Time Distribution of White Space Access Opportunities", *IEEE WCNC*, pp. 729-734, 2008.

[18] J. M. Chapin, W. H. Lehr, "Time-limited leases in radio systems", *IEEE Commun. Mag.*, vol. 45, Issue 6, pp. 76-82, 2007.

[19] M. McHenry, E. Livsics, T. Nguyen, N. Majumdar, "XG Dynamic Spectrum Sharing Field Test Results", *IEEE DySPAN*, pp. 676-684, 2007.

[20] IEEE 802.22 working group on wireless regional area networks, [Online]. Available at: http://www.ieee802.org/22/.

[21] S. Mangold, A. Jarosch, C. Monney, "Operator Assisted Cognitive Radio and Dynamic Spectrum Assignment with Dual Beacons - Detailed Evaluation", *IEEE Comsware*, pp. 1-6, 2006.

[22] Z. Han, H. Jiang, "Replacement of Spectrum Sensing and Avoidance of Hidden Terminal for Cognitive Radio", *IEEE WCNC*, pp. 1448-1452, 2008.

[23] IEEE P1900.4, [Online]. Available at: http://www.scc41.org/

[24] M. M. Buddhikot, P. Kolodzy, S. Miller, K. Ryan, J. Evans, "DIMSUMnet: new directions in wireless networking using coordinated dynamic spectrum", *IEEE WoWMoM*, pp. 78-85, 2005.

[25] A. Hac, A. Armstrong, "Resource allocation scheme for QoS provisioning in microcellular networks carrying multimedia traffic", *International Journal of Network Management*, vol. 11, Issue 5, pp.277-307, September 2001.

[26] S. Geirhofer, L. Tong, B. M. Sadler, "Cognitive radios for dynamic spectrum access - dynamic spectrum access in the time domain: modeling and exploiting white space", *IEEE Commun. Mag.*, vol. 25, No. 5, pp. 66-72, 2007.

[27] Motamedi Ali, Bahai Ahmad, "MAC protocol design for spectrum-agile wireless networks: stochastic control approach", *IEEE DySPAN*, pp. 448-451, 2007.

[28] M. K. Pereirasamy, J. Luo, M. Dillinger, C. Hartmann, "Inter-Operator Spectrum Sharing for UMTS FDD", *Proc. 5th World Wireless Congress*, May 2004.

[29] M. K. Pereirasamy, J. Luo, M. Dillinger, C. Hartmann, "An Approach for Inter-Operator Spectrum Sharing for 3G Systems and Beyond", *IEEE PIMRC*, 2004.

[30] Federal Communications Commission, "Notice of proposed rulemaking and order, Rep. ET Docket no. 03-322, Dec. 2003", [Online]. Available at: http://hraunfoss.fcc.gov/edocs_public/attachmatch/FCC-03-22A1.pdf.

[31] P. Ramsdale, "Trading and liberalization of spectrum", The IEE Seminar on Broadcasting Spectrum: The Issues, pp. 12, Jun., 2005.

[32] O. Sallent, J. Perez-Romero, R. Agusti, L. Giupponi, C. Kloeck, I. Martoyo, S. Klett, J. Luo, "Resource auctioning mechanisms in heterogeneous wireless access networks", *IEEE VTC.*, vol.1, pp. 52-56, 2006.

[33] D. Niyato, E. Hossain, "Competitive Pricing for Spectrum Sharing in Cognitive Radio Networks: Dynamic Game, Inefficiency of Nash Equilibrium, and Collusion", *IEEE J. Sel. Areas Commun.*, vol. 26, Issue 1, pp. 192-202, 2008.

[34] Walter H.W. Tuttlebee, "Software Defined Radio- Enabling Technologies", John Wiley & Sons, Ltd, 2004.

[35] A. Hüseyin, "Cognitive Radio, Software Defined Radio, and Adaptive Wireless Systems", Springer, 2007.

[36] F. K. Jondral, "Software-defined radio: basics and evolution to cognitive radio", *EURASIP Journal on Wireless Communications and Networking*, vol. 5, Issue 3, pp. 275-283, 2005.

[37] Blaze Mobile, [Online]. Available at: http://www.blazemobile.com/

[38] J. Mitola III, "Software radio architecture: a mathematical perspective", *IEEE J. Select Areas Commun.*, vol. 17, Issue 4, pp. 514-538, 1999.

[39] SDR Forum, [Online]. Available at: http://www.sdrforum.org/

[40] W. H. W. Tuttlebee, "Software Defined Radio: Facets of a Developing Technology", *IEEE Pers. Commun.*, vol. 6, Issue 2, pp.38- 44, April 1999.

[41] G. Hueber, L. Maurer,G. Strasser, R. Stuhlberger, K. Chabrak, R. Hagelauer, "On the Design of a Multi-Mode Receive Digital-Front-End for Cellular Terminal RFICs", *European Microwave Conference*, vol. 3, pp.1679- 1682, 2005.

[42] N. Cohen, R. Hohlfeld, D. Moschella, P. Salkind, "Fractal wideband antennas for software defined radio, UWB, and multiple platform applications", Proceedings Radio and Wireless Conference, pp.99- 102, 2003.

[43] J. Mar, Y. R. Lin, G. C. Chen, C. H. Chou, Y. L. Su, "Implementation of the SDR beamformer system on a digital signal processor", *IEEE VTC*, pp.3895- 3899, 2004.

[44] R.H.M van Veldhoven, "A triple-mode continuous-time Sigma Delta modulator with switched-capacitor feedback DAC for a GSM-EDGE/CDMA2000/UMTS receiver", *IEEE J. Solid-State Circuits*, vol. 38, Issue 12, pp.2069- 2076, December 2003.

[45] J. Mitola III., "Cognitive Radio An Integrated Agent Architecture for Software Defined Radio", PhD thesis, KTH Royal Institute of Technology, Stockholm, Sweden, 2000.

[46] J. Mitola III, "Cognitive radio: Making software radios more personal," *IEEE Pers. Commun.*, vol. 6, Issue. 4, pp. 13-18, August 1999.

[47] J. Mitola III, "Cognitive radio for flexible mobile multimedia communications", *IEEE MoMuC*, pp. 3-10, 1999.

[48] T. A. Weiss, F. K. Jondral, "Spectrum pooling: an innovative strategy for the enhancement of spectrum efficiency", *IEEE Commun. Mag.*, vol.42, No. 3, pp. 8-14, 2004.

[49] The Next Generation Program, [Online]. Available at: http://www.darpa.mil/sto/smallunitops/xg.html

[50] D. Wilkins, G. Denker, M-O Stehr, D. Elenius, R. Senanayake, C. Talcott, "Policy-Based Cognitive Radios", *IEEE Pers. Commun.*, vol. 14, Issue 4, pp. 41-46, August 2007.

[51] R. Brodersen, A. Wolisz, D. Cabric, S. Mishra, D. Willkomm, "Corvus: A cognitive radio approach for usage of virtual unlicensed spectrum.", [Online]. Available at: http://bwrc.eecs.berkeley.edu/Publications/2005/PRESENTATIONS/d.cabric/IST_paper_final_411.pdf.

[52] Cognitive Radio Oriented Wireless Networks and Communications, [Online]. Available at: http://www.crowncom2009.org/

[53] K. Hyoil, K. G. Shin, "Efficient Discovery of Spectrum Opportunities with MAC-Layer Sensing in Cognitive Radio Networks", *IEEE Trans. Mobile Comput.*, vol. 7, Issue 5, pp. 533-545, May 2008.

[54] Q. Zhao, L. Tong, A. Swami, Y. Chen, "Decentralized cognitive MAC for opportunistic spectrum access in ad hoc networks: A POMDP framework", *IEEE J. Select Areas Commun*., vol. 25, Issue 3, pp. 289-600, April 2007.

[55] Q. Zhao, S. Geirhofer, L. Tong, B. M. Sadler, "Optimal Dynamic Spectrum Access via Periodic Channel Sensing", *IEEE WCNC*, pp. 33-37, 2007.

[56] Y. Hur, J. Park, W. Woo, J. S. Lee, K. Lim, G. H. Lee, H. S. Kim, J. Laskar, " A Cognitive Radio (CR) System Employing A Dual-Stage Spectrum Sensing Technique : A Multi-Resolution Spectrum Sensing (MRSS) and A Temporal Signature Detection (TSD) Technique", *IEEE Globecom*, pp. 1-5, 2006.

[57] A. Taherpour, S. Gazor, M. Nasiri-Kenari, "Wideband spectrum sensing in unknown white Gaussian noise", *IET Commun.*, vol. 2, Issue 6, pp. 763-771, July 2008.

[58] N. M. Neihart, S. Roy, D. J. Allstot, "A Parallel, Multi-Resolution Sensing Technique for Multiple Antenna Cognitive Radios", *IEEE ISCAS*, pp. 2530-2533, 2007.

[59] Z. Tian, B. Giannakis Georgios, "A Wavelet Approach to Wideband Spectrum Sensing for Cognitive Radios", *IEEE CrownCom*, pp. 1- 5, 2006.

[60] Y. Hur, J. Park, W. Woo, K. Lim, C.H. Lee, H. S. Kim, J. Laskar, "A wideband analog multi-resolution spectrum sensing technique for cognitive radio systems," *IEEE ISCAS*, pp. 4090-4093, 2006.

[61] S. M. Mishra, R. Tandra, A. Sahai, "Wideband Sensing", [Online]. Available: http://www.ieee802.org/22/Meeting_documents/2007_July/index.html.

[62] S. Kyperountas, N. Correal, Q. Shi, Z. Ye, "Performance Analysis of Cooperative Spectrum Sensing in Suzuki Fading Channels", *IEEE CrownCom*, pp. 428-432, 2007.

[63] Y. Liu, D. Yuan, Q. Lin, Q. Liang, Q. Jin, "New Insights to Cooperative Spectrum Sensing for Cognitive radios", *IEEE CrownCom*, pp. 414-419, 2007.

[64] G. Ganesan, L. Ye, "Cooperative Spectrum Sensing in Cognitive Radio, Part I: Two User Networks", *IEEE Trans. Wireless Commun.*, vol. 6, Issue 6, pp. 2204-2213, June 2007.

[65] G. Ganesan, L. Ye, "Cooperative Spectrum Sensing in Cognitive Radio, Part II: Two User Networks", *IEEE Trans. Wireless Commun.*, vol. 6, Issue 6, pp. 2214-2222.

[66] S. M. Mishra, A. Sahai, R. W. Brodersen, "Cooperative Sensing among Cognitive Radios", *IEEE ICC*, pp. 1658-1663, 2006.

[67] A. Ghasemi, E. S. Sousa, "Spectrum sensing in cognitive radio networks: requirements, challenges and design trade-offs", *IEEE Commun. Mag.*, vol. 46, Issue 4, pp. 32-39, April 2008.

[68] M. Ghozzi, M. Dohler, F. Marx, and J. Palicot, "Cognitive radio: methods for the detection of free band", Comptes Rendus Physique, Elsevier, vol. 7 pp. 794-804, September 2006.

[69] C. Danijela, R. W. Robert, "Physical Layer Design Issues Unique to Cognitive Radio Systems", *IEEE PIMRC*, pp. 759-763, 2005.

[70] S. N. Shankar, C. Cordeiro, K. Challapali, "Spectrum agile radios: utilization and sensing architectures", *IEEE DySPAN*, pp.160- 169, 2005.

[71] P. Pawelczak, F. Hoeksema, R. V. Prasad, R. Hekmat, "Dynamic spectrum access: an emergency network case study", [Online]. Available at: http://www.wmc.ewi.tudelft.nl/~przemyslawp/files/aaf_ dsa.pdf

[72] M. R. Musku, A. T. Chronopoulos, S. Penmatsa, D. C. Popescu, "A Game Theoretic Approach for Medium Access of Open Spectrum in Cognitive Radios", *IEEE CrownCom*, pp. 336-341, 2007.

[73] D. Willkomm, J. Gross, A. Wolisz, "Reliable link maintenance in cognitive radio systems", *IEEE DySPAN*, pp. 371-378, 2005.

[74] L. Berlemann, S. Mangold, B. H. Walke, "Policy-based reasoning for spectrum sharing in radio networks", *IEEE DySPAN*, pp. 1-10, 2005.

[75] R. Menon, A. B. MacKenzie, R. M. Buehrer, J. H. Reed, "A Game-Theoretic Framework for Interference Avoidance in Ad hoc Networks", *IEEE Globecom*, pp. 1-6, 2006.

[76] Y. Chen; Q. Zhao, A. Swami, "Distributed Cognitive MAC for Energy-Constrained Opportunistic Spectrum Access", *IEEE MILCOM*, pp. 1-7, 2006.

[77] L. Long, E. Hossain, "OSA-MAC: A MAC Protocol for Opportunistic Spectrum Access in Cognitive Radio Networks", *IEEE WCNC*, pp. 1426-1430, 2008.

[78] S. Hang, Z. Xi, "Cross-Layer Based Opportunistic MAC Protocols for QoS Provisionings Over Cognitive Radio Wireless Networks", *IEEE J. Select Areas Commun.*, vol. 26, Issue 1, pp. 118-129, January 2008.

[79] M. Roberts, "Initial acquisition performance of a transform domain communication system: Modeling and simulation results," *IEEE MILCOM*, pp. 1119-1123, 2000.

[80] I. F. Akyildiz, W. Y. Lee, M. C. Vuran, S. Mohanty, "A survey on spectrum management in cognitive radio networks", *IEEE Commun. Mag.*, vol. 46, Issue 4, pp. 40-48, April 2008.

[81] J. Bater, H. P. Tan, K. Brown, L. Doyle, "Maximising Access to a Spectrum Commons using Interference Temperature Constraints", *IEEE CrownCom*, pp. 441-447, 2007.

[82] FCC, ET Docket No 03-237, "Notice of inquiry of proposed Rulemaking", November 2003.

[83] T. Farnham, G. Clemo, R. Haines, E. Seidel, A. Benamar, S. Billington, N. Greco, N. Drew, T. H. Le, B. Arram, P. Mangold, "IST-TRUST: a perspective on the reconfiguration of future mobile terminals using software download", *IEEE PIMRC*, pp. 1054-1059, 2000.

[84] L. Xu, R. Tonjes, T. Paila, W. Hansmann, M. Frank, M. Albrecht, "DRiVE-ing to the Internet: Dynamic Radio for IP services in Vehicular Environments", *IEEE Conference on Local Computer Networks*, pp. 281-289, 2000.

[85] WINNER- Wireless World Initiative New Radio, [Online]. Available at: http://www.ist-winner.org/

[86] End-to-End Reconfigurability (E^2R), [Online]. Available at: http://e2r2.motlabs.com/

[87] P. Leaves, S. Ghaheri-Niri, R. Tafazolli, L. Christodoulides, T. Sammut, W. Staht, J. Huschke, "Dynamic spectrum allocation in a multi-radio environment: concept and algorithm", *International Conference on 3G Mobile Communication Technologies*, pp. 53-57, 2001.

[88] S. Kumar, G. Costa, S. Kant, F. B. Frederiksen, N. Marchetti, P. Mogensen, "Spectrum sharing for next generation wireless communication networks", *IEEE CogART*, pp. 1-5, 2008.

[89] S. Filin, K. Ishizu, H. Murakami, H. Harada, G. Miyamoto,T. H. Nguyen, S. Kato, M. Hasegawa, "Dynamic Spectrum Assignment and Access Scenarios, System Architecture, Functional Architecture and Procedures for IEEE P1900.4 Management System", *IEEE CrownCom*, pp. 1-7, 2008.

[90] V. Brik, E. Rozner, S. Banerjee, P. Bahl, "DSAP: a protocol for coordinated spectrum access", *IEEE DySPAN*, pp. 611-614, 2005.

[91] H. Kim; Y. Lee; S. Yun, "A dynamic spectrum allocation between network operators with priority-based sharing and negotiation", *IEEE PIMRC*, pp. 1004-1008, 2005.

[92] O. Sallent, J. Perez-Romero, R. Agusti, L. Giupponi, C. Kloeck, I. Martoyo, S. Klett, J. Luo, "Resource Auctioning Mechanisms in Heterogeneous Wireless Access Networks", *IEEE VT*C, pp. 52-56, 2006.

[93] J. Huang, R. A. Berry, M. L. Honig, "Auction-Based Spectrum Sharing", Mobile Networks and Applications, SpringerLink, vol. 11, No. 3, pp. 405-408, 2006.

[94] N. S. Shankar, "Pricing for spectrum usage in cognitive radios", *IEEE CCNC*, pp. 579-582, 2006.

[95] C. Kloeck, H. Jaekel, F. K. Jondral, "Dynamic and local combined pricing, allocation and billing system with cognitive radios", *IEEE DySPAN*, pp. 73-81, 2005.

[96] F. Granelli, H. Zhang, "Cognitive ultra wide band radio: a research vision and its open challenges", International Workshop on Networking with Ultra Wide Band for Sensor Networks, pp. 55-59, 2005.

[97] A. Giorgetti, M. Chiani, D. Dardari, "Coexistence Issues in Cognitive Radios Based on Ultra-Wide Bandwidth Systems", *IEEE CrownCom*, pp. 1-5, 2006.

[98] M. Sablatash, "Mitigation of Interference by Ultra Wide Band Radio into Other Communication Services: Evolution to Cognitive Ultra Wide Band Radio", Canadian Conference on Electrical and Computer Engineering, pp. 1345-1348, 2007.

[99] M. Sablatash, "Adaptive and Cognitive UWB Radio and a Vision for Flexible Future Spectrum Management", Canadian Workshop on Information Theory, pp. 41-44, 2007.

[100] V. D. Chakravarthy, A. K. Shaw, M. A. Temple, J. P. Stephens, "Cognitive radio - an adaptive waveform with spectral sharing capability", *IEEE WCNC*, pp. 724-729, 2005.

[101] W. Zhang, H. Shen, Z. Bai, K. S. Kwak, "A Novel Modulation Waveform on Ultra-Wideband Based Cognitive Radio Systems", *IEEE CrownCom*, pp. 306-311, 2007.

[102] A. Batra, S. Lingam, J. Balakrishnan, "Multi-band OFDM: a cognitive radio for UWB", *IEEE ISCAS*, 2006.

[103] J. Lansford, "UWB coexistence and cognitive radio", *IEEE* Joint *UWBST* and *IWUWBS*, pp. 35-39, 2004.

[104] R. Mahapatra, "Cosine Modulated Filterbank Technique for Cognitive UWB", *IEEE WOCN*, pp. 1-4, 2007.

[105] X. Zhou, K. Y. Yazdandoost, H. Zhang, I. Chlamtac, "Cognospectrum: spectrum adaptation and evolution in cognitive ultra-wideband radio", *IEEE IcUWB*, pp. 713-718, 2005.

[106] M. D. Perez-Guirao, K. Jobmann, "Cognitive Resource Access Scheme for IR-UWB Autonomous Networks", *IEEE WPNC*, pp. 267-271, 2007.

[107] M. Vose, "Modeling simple genetic algorithms", *Evolutionary Computation*, Vol. 3, No. 4, 453-472, 1995.

[108] J. P. Tignol, "Galois' Theory of Algebraic Equations", World Scientific, 2001, pp. 115.

[109] M. K. Pereirasamy, J. Luo, M. Dillinger, C. Hartmann, "Dynamic inter-operator spectrum sharing for UMTS FDD with displaced cellular networks", *IEEE WCNC*, pp.1720-1725, 2005.

[110] P. Houze, D. Ruiz, S. Ben Jemaa, P. Cordier, "Dynamic Spectrum Allocation Algorithm for Cognitive Networks", *IEEE ICWMC*, 2007.

[111] M. M. Buddhikot, K. Ryan, "Spectrum management in coordinated dynamic spectrum access based cellular networks", *IEEE DySPAN*, pp. 299-307, 2005.

[112] Y. Bai, L. Chen, "Flexible Spectrum Allocation Methods for Wireless Network Providers", *IEEE PIMRC*, pp.1-5, 2006.

[113] J. Acharya, R. D. Yates, "A price based dynamic spectrum allocation scheme", *ACSSC*, pp.797-801, 2007.

[114] O. Yu, E. Saric, A. Li "Dynamic Control of Open Spectrum Management", *IEEE WCNC*, pp.127-132, 2007.

[115] Q. Wang, T. X. Brown, "Public safety and commercial spectrum sharing via network pricing and admission control", *IEEE J. Sel. Areas Commun.*, vol. 25, Issue 3, pp. 622-632, April 2007.

[116] N. Z. Shor, "Monimization Methods for Non-Differentiable Functions", Springer, 1985.

[117] M. L. Puterman, "Markov Decision Process: Discrete Stochastic Dynamic Programming", New York; Wiley, 1994.

[118] E. Altman, "Constrained Markov Decision Processes", Chapman & Hall/CRC, 1999.

[119] A. Adas, "Traffic models in broadband networks", *IEEE Commun. Mag.*, Vol. 35, Issue 7, July 1997, pp. 82-89.

[120] C. Jedrzycki, V. C. Leung, "Probability distribution of channel holding time in cellular telephony systems", *IEEE VTC*, 1996, pp. 247-251.

Appendix A

We present the approach to derive the sojourn time of $a_2^{\mathcal{A}_1} = (1,0)$ which can be generalized to *N* frequency bins. As the radio activities among frequency bins are independent,

$$P(T_{1,0} > t) = P(T_{1,\text{on}} > t)P(T_{2,\text{off}} > t),$$

where $P(T_{1,\text{on}} > t)$ denotes the probability that frequency bin 1 is in the on state for a duration longer than *t*, and $P(T_{2,\text{off}} > t)$ denotes the probability that frequency bin 2 is in the off state for a duration longer than *t*. We can also express $P(T_{1,0} > t)$ as

$$P\left(T_{1,0} > t\right) = \int_t^\infty \mu_{\text{on},1} e^{-t\mu_{\text{on},1}} dt \int_t^\infty \mu_{\text{off},2} e^{-t\mu_{\text{off},2}} dt = e^{-t\left(\mu_{\text{on},1}+\mu_{\text{off},2}\right)},\ t \geq 0.$$

Since $P\left(T_{1,0} \leq t\right) = 1 - P\left(T_{1,0} > t\right)$, the p.d.f. of the sojourn time for $a_2^{\mathcal{A}_1}$ is given as

$$f_{a_2^{\mathcal{A}_1}}(t) = \frac{d}{dt} P\left(T_{1,0} \leq t\right) = \left(\mu_{\text{on},1} + \mu_{\text{off},2}\right) e^{-t\left(\mu_{\text{on},1}+\mu_{\text{off},2}\right)},\ t \geq 0.$$

Generalizing the approach to *N* frequency bins, we arrive at (3.2).

Appendix B

Supposing there are *p* indistinguishable black balls (B) and *q* indistinguishable white balls (W) to be placed in (*p*+*q*) boxes with one ball in each box. The boxes are to be arranged clockwise in a circular manner. Given that one of the boxes is unique, so as to represent the starting position and a black ball has to be placed in this box, how many distinct permutations are possible with respect to this box? The total number of ways is given by $\frac{(p+q-1)!}{p!(q-1)!} = C_q^{p+q-1}$. Note that $p \geq 1$ for the problem to be valid. For example, given two black balls and two white balls, the number of distinct circular permutation is given to be $C_2^3 = 3$. The possible arrangements with respect to the unique box, are given in a clockwise direction as BWBWB, BWWBB, BBWWB, where the first and last 'B' indicate the same black ball. The possible permutations are illustrated in the figure below.

Arrangement		
BWBWB 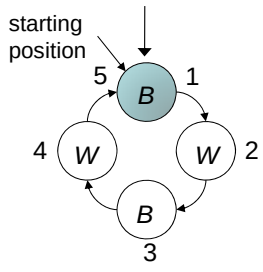 	*BWWBB* 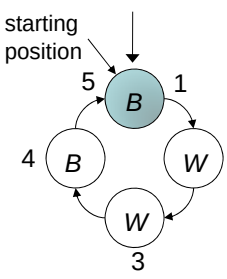 	*BBWWB* 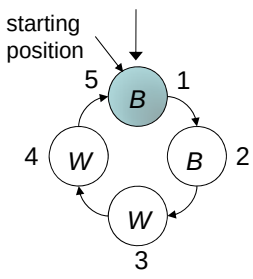
$\mathcal{A}_m \to \mathcal{A}_{(m+1)} \to \mathcal{A}_m$ $\to \mathcal{A}_{(m+1)} \to \mathcal{A}_{(m+2)} \to \mathcal{A}_{(m+1)}$ $\to \mathcal{A}_{(m+2)} \to \mathcal{A}_{(m+1)} \to \mathcal{A}_m$	$\mathcal{A}_m \to \mathcal{A}_{(m+1)} \to \mathcal{A}_{(m+2)}$ $\to \mathcal{A}_{(m+1)} \to \mathcal{A}_{(m+2)} \to \mathcal{A}_{(m+1)}$ $\to \mathcal{A}_m \to \mathcal{A}_{(m+1)} \to \mathcal{A}_m$	$\mathcal{A}_m \to \mathcal{A}_{(m+1)} \to \mathcal{A}_m$ $\to \mathcal{A}_{(m+1)} \to \mathcal{A}_{(m+2)} \to \mathcal{A}_{(m+1)}$ $\to \mathcal{A}_{(m+2)} \to \mathcal{A}_{(m+1)} \to \mathcal{A}_m$

Possible distinct permutations.

Now, referring to Fig. 3.3 and consider any two pairs of adjacent states, i.e. $\mathcal{A}_m$ and $\mathcal{A}_{(m+1)}$, $\mathcal{A}_{(m+1)}$ and $\mathcal{A}_{(m+2)}$, where $1 \le m \le (N-2)$. We can draw a parallel with the arrangement model by letting the order of arranging a black ball be analogous to the order of performing a loop between the states $\mathcal{A}_m$ and $\mathcal{A}_{(m+1)}$, and the order of arranging a white ball be analogous to the order of performing a loop between the states $\mathcal{A}_{(m+1)}$ and $\mathcal{A}_{(m+2)}$. For example, for the arrangement, BBWWB, the first black ball indicates the system begins at the state $\mathcal{A}_m$ and transits to state $\mathcal{A}_{(m+1)}$. The second black ball indicates that the system transits from state $\mathcal{A}_{(m+1)}$ to state $\mathcal{A}_m$ and returns back to $\mathcal{A}_{(m+1)}$, in which one complete loop is performed between the states $\mathcal{A}_m$ and $\mathcal{A}_{(m+1)}$. The following two white balls indicate the performance of two consecutive loops between the states $\mathcal{A}_{(m+1)}$ and $\mathcal{A}_{(m+2)}$. The last black ball is used to indicate the system returns back to the starting state $\mathcal{A}_m$. The path given by this arrangement is $\mathcal{A}_m \to \mathcal{A}_{(m+1)} \to \mathcal{A}_m \to \mathcal{A}_{(m+1)} \to \mathcal{A}_{(m+2)} \to \mathcal{A}_{(m+1)} \to \mathcal{A}_{(m+2)} \to \mathcal{A}_{(m+1)} \to \mathcal{A}_m$.

We let l_m and $l_{(m+1)}$ denote the number of loops to be performed between the lumped states $\mathcal{A}_m$ and $\mathcal{A}_{(m+1)}$, and $\mathcal{A}_{(m+1)}$ and $\mathcal{A}_{(m+2)}$, respectively. As a result of visiting the states in different order, there can be multiple ways to complete these l_m and $l_{(m+1)}$ loops. Using the result discussed before, there are altogether $C_{l_{(m+1)}}^{l_m + l_{(m+1)} - 1}$ distinct ways to perform these l_m and $l_{(m+1)}$ loops.

Appendix C

The negative binomial expansion of $(1-\zeta)^{-n}$ is given as:

$$(1-\zeta)^{-n} = \sum_{k=0}^{\infty}\left(C_k^{-n}(-\zeta)^k\right) = \sum_{k=0}^{\infty}\left((-1)^k C_k^{n+k-1}(-\zeta)^k\right) = \sum_{k=0}^{\infty}\left(C_k^{n+k-1}(\zeta)^k\right), \quad \zeta < 1$$

The proof for the identity in (3.19) is thus complete.

Appendix D

From (3.14), for $N = 4$, we have

$$\begin{aligned}\mathcal{G}_\tau(s) = P_{\mathcal{A}_0\to\mathcal{A}_1}P_{\mathcal{A}_1\to\mathcal{A}_0}\frac{\lambda_1}{\lambda_1 - s}\sum_{l_1=0}^{\infty}\left\{\left(P_{\mathcal{A}_1\to\mathcal{A}_2}P_{\mathcal{A}_2\to\mathcal{A}_1}\lambda_1\lambda_2/\left[(\lambda_1 - s)(\lambda_2 - s)\right]\right)^{l_1}\right\}\\ \times\sum_{l_2=0}^{\infty}\left\{C_{l_2}^{l_1+l_2-1}\left(P_{\mathcal{A}_2\to\mathcal{A}_3}P_{\mathcal{A}_3\to\mathcal{A}_2}\lambda_2\lambda_3/\left[(\lambda_2 - s)(\lambda_3 - s)\right]\right)^{l_2}\right\}\\ \times\sum_{l_3=0}^{\infty}\left\{C_{l_3}^{l_2+l_3-1}\left(P_{\mathcal{A}_3\to\mathcal{A}_4}P_{\mathcal{A}_4\to\mathcal{A}_3}\lambda_3\lambda_4/\left[(\lambda_3 - s)(\lambda_4 - s)\right]\right)^{l_3}\right\}.\end{aligned}$$

Substituting the expressions for X_0, X_1, X_2 and X_3 by applying (3.19), we have:

$$\begin{aligned}\mathcal{G}_\tau(s) &= X_0\sum_{l_1=0}^{\infty}\left\{(X_1)^{l_1}\sum_{l_2=0}^{\infty}\left\{C_{l_2}^{l_1+l_2-1}(X_2)^{l_2}\sum_{l_3=0}^{\infty}\left\{C_{l_3}^{l_2+l_3-1}(X_3)^{l_3}\right\}\right\}\right\}\\ &= X_0\sum_{l_1=0}^{\infty}\left\{(X_1)^{l_1}\sum_{l_2=0}^{\infty}\left\{C_{l_2}^{l_1+l_2-1}\left[X_2/(1-X_3)\right]^{l_2}\right\}\right\}\\ &= X_0\sum_{l_1=0}^{\infty}\left\{\left[X_1(1-X_3)/(1-X_2-X_3)\right]^{l_1}\right\}\\ &= X_0(1-X_2-X_3)/(1-X_1-X_2-X_3+X_1X_3).\end{aligned}$$

Appendix E

Convergence to the stationary points are evaluated using the subgradient method [116], where m_1 and m_2 are updated in the opposite direction to the subgradients $\partial \mathcal{L}_\pi / \partial m_1$ and $\partial \mathcal{L}_\pi / \partial m_2$:

$$\left.\begin{aligned} m_1^{k+1} &= \left[m_1^k + \delta_1 \left(\overline{c_{\mathrm{A}}} - c_{\mathrm{A}}(\pi) \right) \right]^+ \\ m_2^{k+1} &= \left[m_2^k + \delta_2 \left(\overline{c_{\mathrm{B}}} - c_{\mathrm{B}}(\pi) \right) \right]^+ \end{aligned} \right\}, \tag{E.1}$$

where δ_1 and δ_2 are positive scalar step sizes less than one, and '+' denotes the projection onto the set $\Re^+$ of non-negative real numbers. The super-script '*k*' represents the k^{th} update step. The proof for convergence to optimality using the subgradient method can be found in [133].

Appendix F

The value iteration and RVI algorithms [118] may be used to evaluate Markov decision problems. However, to avoid computational overflow, the RVI algorithm is adopted. The Bellman optimality equation [118] for the *unconstrained* average reward MDP is given as:

$$J^*(\underline{x}) = \max_{\underline{a}\in\mathcal{A}(\underline{x})}\left[r(\underline{x},\underline{a}) - h^* + \sum_{\underline{y}} P_{\underline{x}\underline{y}}(\underline{a}) J^*(\underline{y})\right], \tag{F.1}$$

where $\mathcal{A}(\underline{x})$ is the set of possible actions in state $\underline{x}$; $J^*(\underline{x})$ are the elements of the optimal value function $\underline{J}^*$; h^* is the average reward associated with the optimal policy. In this algorithm, we select any arbitrary state in the state space $\mathcal{S}$ to be a distinguished state. The value of h^* in (4.26) is replaced by the value of the distinguished state. The RVI algorithm is evaluated as follows:

1. *Select an arbitrary state,* $\underline{x}^*$*, from the state space* $\mathcal{S}$*. Set the run counter* $q=1$*. Select an arbitrary value for* $J^1(\underline{x}^*)$*. Specify the error bounds* ε *and set* $m_1=0$*,* $m_2=0$ *and* $k=0$*. Select values for* δ_1 and δ_2*.*

2. *Compute:*

   i) $J^{q+1}(\underline{x}^*) = \max_{\underline{a}\in\mathcal{A}(\underline{x}^*)}\left[r(\underline{x}^*,\underline{a}) - m_1 c_{\mathrm{A}}(\underline{x}^*,\underline{a}) - m_2 c_{\mathrm{B}}(\underline{x}^*,\underline{a}) + \sum_{\underline{y}} P_{\underline{x}^*\underline{y}}(\underline{a}) J^q(\underline{y})\right].$

   and select:

   $$\underline{a}' = \arg\max_{\underline{a}\in\mathcal{A}(\underline{x}^*)}\left[r(\underline{x}^*,\underline{a}) - m_1 c_{\mathrm{A}}(\underline{x}^*,\underline{a}) - m_2 c_{\mathrm{B}}(\underline{x}^*,\underline{a}) + \sum_{\underline{y}} P_{\underline{x}^*\underline{y}}(\underline{a}) J^q(\underline{y})\right].$$

   Then compute:

   ii) $C_1^{q+1}(\underline{x}^*) = c_{\mathrm{A}}(\underline{x}^*,\underline{a}') + \sum_{\underline{y}} P_{\underline{x}^*\underline{y}}(\underline{a}') C_1^q(\underline{y})$*, and*

   iii) $C_2^{q+1}(\underline{x}^*) = c_{\mathrm{B}}(\underline{x}^*,\underline{a}') + \sum_{\underline{y}} P_{\underline{x}^*\underline{y}}(\underline{a}') C_2^q(\underline{y})$*.*

3. *For each* $\underline{x} \in \mathcal{S}$ *, compute:*

   i) $J^{q+1}(\underline{x}) = \max_{\underline{a} \in \mathcal{A}(\underline{x})} \left[r(\underline{x},\underline{a}) - m_1 c_{\mathrm{A}}(\underline{x},\underline{a}) - m_2 c_{\mathrm{B}}(\underline{x},\underline{a}) + \sum_{\underline{y}} P_{\underline{x}\underline{y}}(\underline{a}) J^q(\underline{y}) \right] - J^{q+1}(\underline{x}^*).$

   and for each $\underline{x} \in \mathcal{S}$ *select:*

   $$\underline{a}'' = \arg \max_{\underline{a} \in \mathcal{A}(\underline{x})} \left[r(\underline{x},\underline{a}) - m_1 c_{\mathrm{A}}(\underline{x},\underline{a}) - m_2 c_{\mathrm{B}}(\underline{x},\underline{a}) + \sum_{\underline{y}} P_{\underline{x}\underline{y}}(\underline{a}) J^q(\underline{y}) \right] - J^{q+1}(\underline{x}^*).$$

   Using $\underline{a}''$ *for each* $\underline{x} \in \mathcal{S}$ *, compute:*

   ii) $C_1^{q+1}(\underline{x}) = c_{\mathrm{A}}(\underline{x},\underline{a}'') + \sum_{\underline{y}} P_{\underline{x}\underline{y}}(\underline{a}'') C_1^q(\underline{y}) - C_1^{q+1}(\underline{x}^*)$,

   iii) $C_2^{q+1}(\underline{x}) = c_{\mathrm{B}}(\underline{x},\underline{a}'') + \sum_{\underline{y}} P_{\underline{x}\underline{y}}(\underline{a}'') C_2^q(\underline{y}) - C_2^{q+1}(\underline{x}^*)$.

4. *Proceed to Step 5 if* $sp\left(\underline{J}^{q+1} - \underline{J}^q\right) < \varepsilon$ *and* $sp\left(\underline{C}_1^{q+1} - \underline{C}_1^q\right) < \varepsilon$ *and* $sp\left(\underline{C}_2^{q+1} - \underline{C}_2^q\right) < \varepsilon$ *. Otherwise, increment run counter, q, by one and return to Step 2.*

5. *Check if* $C_1^{q+1}(\underline{x}^*) \le \overline{c_{\mathrm{A}}}$ *and* $C_2^{q+1}(\underline{x}^*) \le \overline{c_{\mathrm{B}}}$ *. If the constraints are satisfied,* $J^{q+1}(\underline{x}^*)$*,* $C_1^{q+1}(\underline{x}^*)$ *and* $C_2^{q+1}(\underline{x}^*)$ *gives respectively the optimal long-run average reward and the average blocking probabilities for* S_A *and* S_B*. Otherwise, proceed to Step 6.*

6. *Increment, k, by one and update the Lagrange multipliers according to (25) and return to Step 2.*

The notation $sp(\underline{Z}(l))$ in Step 4 denotes the span semi-norm function which is defined as: $sp(\underline{Z}(l)) = \max_l(\underline{Z}(l)) - \min_l(\underline{Z}(l))$.

Publications

1) Pak Kay Tang, Yong Huat Chew, Ling Chuen Ong, Francois Chin, “On the Grade-of-Services in the Sharing of Radio Spectrum”, *IEEE CrownCom*, pp. 85-89, 2007.

2) Pak Kay Tang, Yong Huat Chew, Ling Chuen Ong, “Improvement in the grade-of-service in a cooperative overlay heterogeneous network”, *IEEE ICICS*, pp. 1-5, 2007.

3) Pak Kay Tang, Yong Huat Chew, Ling Chuen Ong, “On the distribution of white space access opportunities for secondary radios”, *IEEE WCNC*, pp. 729-734, 2008.

4) Pak Kay Tang, Yong Huat Chew, Ling Chuen Ong, “Comparison of two resource sharing schemes in an overlay heterogeneous network”, *IEEE PIMRC*, 2008.

5) Pak Kay Tang, Yong Huat Chew, Ling Chuen Ong, “Performance analysis of coordinated dynamic spectrum sharing multi-radio networks supporting variable transmission bandwidth”, *submitted*.

6) Pak Kay Tang, Yong Huat Chew, Ling Chuen Ong, “On the distribution of opportunity time for secondary usage of spectrum”, *IEEE Trans. Veh. Technol.* (Accepted, to appear May 2009).

7) Pak Kay Tang, Yong Huat Chew, Wai-Leong Yeow, Ling Chuen Ong, “Performance Comparison of Three Spectrum Admission Control Policies in Coordinated Dynamic Spectrum Sharing Systems”, *IEEE Trans. Veh. Technol.* (Accepted, to appear).